IEEE Access
Multidisciplinary ⋮ Rapid Review ⋮ Open Access Journal

Received March 20, 2022, accepted April 2, 2022, date of publication April 12, 2022, date of current version April 20, 2022.

Digital Object Identifier 10.1109/ACCESS.2022.3166935

A Comprehensive Review of Power Converter Topologies and Control Methods for Electric Vehicle Fast Charging Applications

MD SAFAYATULLAH, (Graduate Student Member, IEEE), MOHAMED TAMASAS ELRAIS, (Graduate Student Member, IEEE), SUMANA GHOSH, (Graduate Student Member, IEEE), REZA REZAII, (Graduate Student Member, IEEE), AND ISSA BATARSEH, (Fellow, IEEE)
Department of Electrical and Computer Engineering, University of Central Florida, Orlando, FL 32816, USA

Corresponding author: Md Safayatullah (safayatullah@knights.ucf.edu)

This work was supported in part by NSF-Electrical, Communications and Cyber Systems (ECCS) under Grant 2103442, and in part by the University of Central Florida (UCF) College of Graduate Studies Open Access Publishing Fund.

ABSTRACT Wide-scale adoption and projected growth of electric vehicles (EVs) necessitate research and development of power electronic converters to achieve high power, low-cost, and reliable charging solutions for the EV battery. This paper presents a comprehensive review of EV off-board chargers that consist of ac-dc and dc-dc power stages from the power network to the EV battery. Although EV chargers are categorized into two types, namely, on-board and off-board chargers, it is essential to utilize off-board chargers for dc fast and ultra-fast charging so that volume and weight of EV can be reduced significantly. Here, we discuss the state-of-the-art topologies and control methods of both ac-dc and dc-dc power stages for off-board chargers, focusing on technical details, ongoing progress, and challenges. In addition, most of the recent multiport EV chargers integrating PV, energy storage, EV, and grid are presented. Moreover, comparative analysis has been carried out for the topologies and the control schemes of ac-dc rectifiers, dc-dc converters, and multiport converters in terms of architecture, power and voltage levels, efficiency, bidirectionality, control variables, advantages, and disadvantages which can be used as a guideline for future research directions in EV charging solutions.

INDEX TERMS Charging stations, converter control, converter topologies, DC fast chargers, electric vehicle (EV), EV fast chargers, multilevel AC-DC converter, multiport converter, off-board charger.

I. INTRODUCTION

Amid increasing concerns of the harmful impacts on environment due to our daily transportation, which is responsible for 29% of greenhouse gas emissions in the US, government, industry, and academia are working together to develop electric vehicle (EV) based transportation system connected to the grid that will reduce the consumption of fossil fuel significantly [1], [2]. In 2020, the total number of global EV stock has exceeded the ten million mark with a 43% increase compared to 2019 and despite the COVID-19 pandemic, EV registrations are being increased in major markets of the world [3]. In addition, EV sales are forecasted to increase swiftly in the upcoming few years, growing from 3.1 million in 2020 to 14 million in 2025 [4]. With the development of dc fast and ultra-fast charging infrastructure, EV driving range can be matched with the internal combustion (IC) engine-based vehicle, and plugging to the power grid facilitates to achieve reactive power support, ancillary services, peak load shaving, load balance, and integration of renewable energy resources [5].

Battery technology is the keystone of advancement in EV adoption, as the battery cost alone can account for up to one-third of the overall EV cost and EV's weight is substantially increased with battery pack deployment. Li-ion, the most prolific battery technology at present, has a gravimetric energy density between 200Wh/kg and 300Wh/kg [6]. According to the BloombergNEF, Li-ion battery price has plummeted to $137/kWh in 2020 from $1100/kWh in 2010 [7]; however, IC engine vehicles are still cheaper than EVs. It is predicted that the price difference between them will be only 9% by 2030 owing to the declining nature of battery price [8], [9].

The associate editor coordinating the review of this manuscript and approving it for publication was Emanuele Crisostomi.

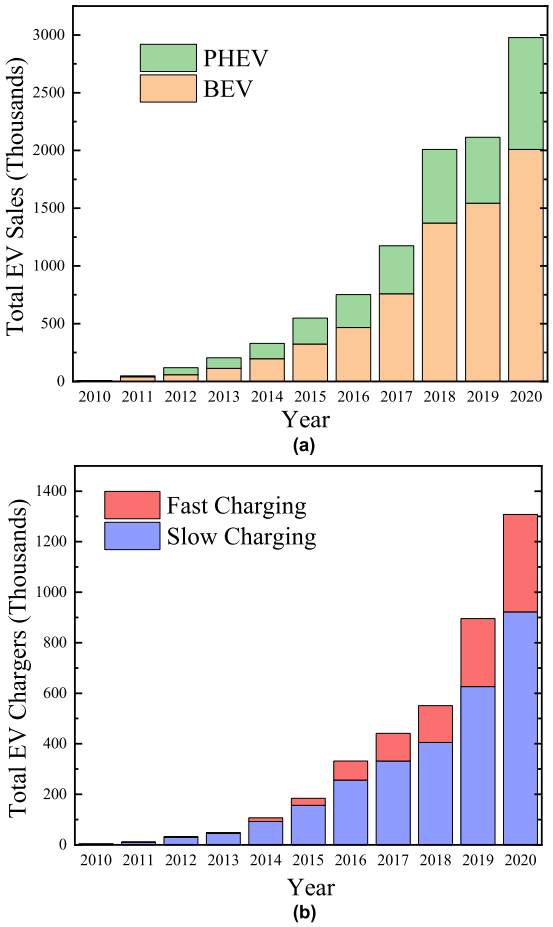

FIGURE 1. (a) Total EV (plug-in-hybrid electric vehicles and battery electric vehicle) sales in the whole world. (b) Total publicly available EV chargers including fast chargers (>22kW) and slow chargers (<22kW) in the whole world [3].

Over the past several years, there is an exponential increase in the number of total EV sales and publicly available EV chargers worldwide for slow and fast charging as shown in Fig. 1 [3]. Still, widespread acceptance of EV is not possible owing to technical, economic, and policy barriers. High battery cost, short battery lifetime, reliability issues, lower driving range, long charging time, and complex charging infrastructure pose major challenges to flourish EV technology [10], [11]. In addition, design of suitable power converter topology and implementation of advanced control methods are essential to achieve reliable and low-cost operation while delivering high power with increased efficiency. Normally, EV adoption does not give rise to substantial problems for the distribution, transmission, and generation of the electrical grid; however, if EV charging is left unmanaged, utilities may be forced to alter the existing infrastructure prior to their planned cycle due to sharp increase of load [12]. Besides, EV chargers can produce harmful harmonics that degrade power quality [13]. The ac-dc power stage of the charger including harmonic compensation technique can mitigate this issue [14], [15].

As the EVs currently have higher battery capacities and driving ranges compared to their earlier versions, there is a growing need for energy-efficient charging stations to facilitate dc fast and ultra-fast charging [16]. Charging specifications and infrastructure of top-selling EVs on the market are shown in Table 1. Battey lifetime and charging time are related to the EV chargers and therefore, design, development, and control of the EV chargers are very important factors to consider while establishing dc fast charging infrastructure. High efficiency, high power density, high reliability, low cost, low weight, and small volume are the desired features of an EV charger. In addition, total harmonic distortion (THD) must be very low (<5%) to mitigate power quality issues and grid current should be drawn at high power factor so that maximum availability of real power is ensured. EV chargers can be categorized into on-board and off-board types with unidirectional and bidirectional power flow. The power module of an off-board charger is usually designed for high power flow between the grid and the EV supporting dc fast and ultra-fast charging, whereas, on-board charger allows low ac power-based Level-1 and Level-2 charging. In this article, we will mainly discuss appropriate power converter topologies and their associated control methods related to off-board dc fast chargers which are located outside the EV.

Various features related to EV charging technology have been reviewed in the open literature [17]–[25]. In [17] and [18], the state-of-the-art EV technologies and their impacts on the grid have been discussed. Optimization methods regarding EV charging infrastructures have been studied in [19]. Authors have reviewed EV charging standards and infrastructure including EV market analysis in [20], [21]. However, power converter topologies and control algorithms are missing in the aforementioned references. In [22]–[24], details on the power electronic circuits for on-board EV chargers are provided considering electrical machines. In [25], an overview of the energy storage devices, low-level control for energy management, and high-level supervisory control inside EVs has been discussed. Studies in [22]–[25] are not appropriate for dc fast charging, as they support low power EV chargers. The work reported in [14] describes three-phase ac-dc converters which are used to reduce THD, correct power factor, and regulate stable dc link voltage. A thorough discussion regarding EV charger topologies, charging power levels, and infrastructure is presented in [5] that is well-suited for on-board and off-board chargers including unidirectional and bidirectional power flow. The studies described in [5], [26], [27], have provided very insightful details of circuit topologies for both ac-dc and dc-dc power stages. In addition, a good review of medium voltage ultra-fast EV chargers based on solid-state transformers is presented in [28]. However, control methods are not discussed in [5], [14], [26]–[28]. Although the above-stated review articles cover a wide spectrum of topics related to EV charging, they lack in-depth technical details and comparison of the power converter topologies as

TABLE 1. Charging specifications of the manufactured EVs in current market.

EV Model	Battery Capacity (kWh)	Battery Voltage (V)	Energy Consumption (Wh/mile)	Distance Range (miles)	Charging Time for 50kW (minutes)	Connector Type	Charging Power: AC 1-Phase (kW) / AC 3-phase(kW) / DC Fast(kW)
Honda e 2020	35.5	-	275	138	40	CCS, Type 2	6.6 / 6.6 / 56
Volkswagen e- Golf	35.8	323	245	144	60	CCS, Type 2	6.6 / 6.6 / 100
Nissan Leaf	40	350	330	168	60	CHAdeMO, Type 2	3.6 / 3.6 / 50
BMW I3	42.2	352	245	191	50	CCS, Type 2	7.4 / 11 / 155
Renault Zoe R110 ZE50	52	400	280	245	50	CCS, Type 2	7.4 / 22 / 46
Lexus UX 300e	54.3	-	270	196	40	CHAdeMO, Type 2	6.6 / 6.6 / 50
Tesla Model 3	55-82	350	225-265	278-360	40-60	Supercharger	7.4 / 11 / 250
SKODA Enyaq iV	62	-	252	256	50	CCS, Type 2	7.2 / 11 / 100
Kia Niro EV	64	327	255	283	75	CCS, Type 2	7.2 / 7.2 / 77
Nissan Leaf Plus	64	350	285	239	45	CHAdeMO, Type 2	6.6 / 6.6 / 100
Mercedes EQA	66.5	405	355	263	50	CCS, Type 2	7.4 / 11 / 100
Tesla Model S	75-100	350	305-310	283-388	60	Supercharger	7.4 / 16.5 / 100-200
Ford Mustang Mach-E	75.7	450	275	273	60	CCS, Type 2	7.4 / 11 / 115
Volvo XC40 Recharger	78	-	380	257	60	CCS, Type 2	7.4 / 11 / 150
Polestar 2	78	400	305	292	60	CCS, Type 2	7.4 / 11 / 150
Porsche Taycan	79.2	800	335	254	60	CCS, Type 2	7.4 / 11 / 225
Volkswagen ID.4	82	365	290	310	60	CCS, Type 2	7.2 / 11 / 125
Jaguar I-PACE	90	390	354	292	55	CCS, Type 2	7.4 / 11 / 100
Audi E-Tron	95	400	426	249	60	CCS, Type 2	7.4 / 11 / 155
Tesla Model X	100	350	360-365	233-315	60	Supercharger	7.4 / 16.5 / 100-200

well as the review of the control methods used for dc fast chargers. In addition, there is no review article found in the literature about multiport EV charger which integrates PV, energy storage, grid, and EV.

In this work, we review the state-of-the-art EV charging infrastructure, suitable power converter topologies for ac-dc and dc-dc power stages of off-board dc fast charger, multiport EV charger, and their associated control strategies. The current status of the EV charging, power level, and connector types is provided in Section II. The architectures of ac and dc connected EV charging stations are discussed in Section III. Further, power converter topologies of ac-dc front-end rectifiers and dc-dc back-end converters are comprehensively reviewed in Sections IV and V respectively. Furthermore, we discuss the recently reported multiport EV chargers in Section VI. Moreover, details of the control methods of the topologies for both dc-dc and ac-dc stages are explained in Sections VII and VIII respectively. Then, impacts on the grid due to the operation of the fast charging station have been described in Section IX. An overall synthesis regarding the structures and topologies of EV dc fast chargers is provided in Section X. Finally, future trends of EV charging are introduced in Section XI and concluding remarks are drawn in the last section.

II. STATE-OF-THE-ART EV CHARGING

An EV charging station is a portion of electrical grid situated in a residential garage, commercial building street, or public parking spaces. Charging can be of both types-ac and dc charging; ac charging generally specifies Level-1 and

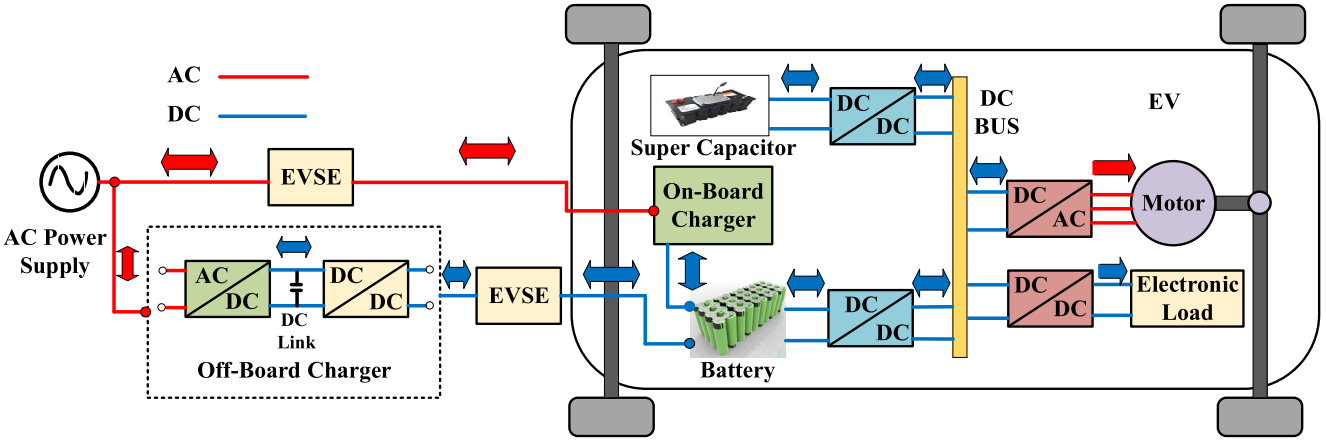

FIGURE 2. Electric vehicle (EV) charging system including off-board and on-board charger.

TABLE 2. Charging station classification based on charging power level.

Charging Station Type	Charger Location	Power Supply	Charger Power Level	Protection Type	Charging Time
Level-1 (AC)	On-board (Residential charging)	120/230V_{ac}; 12A to 16A (Single Phase)	From 1.44kW to 1.92kW	Breaker in cable	11-36 hours for EVs (16-50kWh)
Level-2 (AC)	On-board (Charging at home or workplace)	208/240V_{ac}; 15A to 80A (Single/split phase)	From 3.1kW to 19.2kW	Pilot function and breaker in cable	2-6 hours for EVs (16-30kWh)
Level-3 (DC Fast)	Off-board (Charging at public places similar to gas stations)	300-600V_{dc} (Maximum current 400 A) (Three phase)	From 50kW to 350kW	Monitoring and communication between charging station and EV	Less than 30 minutes for EVs (20-50kWh)
Next generation: DC Ultra-Fast Charging	Off-board (Charging at public places similar to gas stations)	800V_{dc} and higher; 400A and higher (Polyphase)	400kW and higher	Monitoring and communication between charging station and EV, liquid cooling	Approximately 10 minutes for EVs (20-50kWh)

Level-2 charging for on-board chargers, while dc charging is considered as Level-3 charging that requires off-board chargers. Level-1 charging is the slowest of all, as it supports the lowest power level. It is usually installed in residential buildings and the charging is done during the night. Level-1 ac charger takes $120V_{ac}/230V_{ac}$ as the input voltage and delivers 1.92kW power approximately. The connection may use a standard J1772 connector into the EV ac port [29]. Level-2 ac chargers provide power up to 20kW and are mostly used in commercial sites such as malls, offices, and so on. Present-day Level-2 charging facilities take input voltage of $208V_{ac}$ or $240V_{ac}$. In US, the Level-2 charging connector is SAEJ1772 Type-1 or proprietary Tesla plug, while in Europe, IEC62196-2 Type-2 plug is considered for Level-2 ac charging [29]–[31]. The limited power rating and longer charging time of on-board Level -1 and Level-2 ac chargers have stimulated the growth of Level-3 dc fast chargers that can handle power in the range between 50kW and 300kW. They can provide dc voltage around 300V or higher up to 800V and charge the existing EV batteries within 30 minutes. Due to high power flow, chargers are placed outside so that the weight and volume of the vehicle can be reduced. Generally, EVs have their own on-board charger located inside the vehicle. Off-board dc fast chargers are directly connected to EV battery, bypassing the on-board charger as shown in Fig. 2. In US, CCS combo 1, CHAdeMo, and the Tesla supercharger are considered for Level-3 dc charger connector while in Europe, they use CCS combo 3, CHAdeMo, and the Tesla supercharger [29]–[31]. To reduce the range anxiety of EV drivers even more and to be really competitive to the IC engine based refueling process, dc ultra-fast charging has emerged as a potential solution in which EV batteries are fully charged within 10 minutes rated at power 400kW or higher [32]. However, a substantial amount of power flow between the grid and EV raises challenges and research needs in EV battery, charging cable, charging infrastructure, and reliability. The charging stations categorized based on the power levels are summarized in Table 2 and specifications of the existing dc fast and ultra-fast chargers have been demonstrated in Table 3.

TABLE 3. Technical specifications of currently available dc fast and ultra-fast chargers.

Manufacturer Model	Power (kW)	Input Voltage	Output Voltage (V)	Output Current (A)	Peak Efficiency	Supported Protocols	Weight (lbs)	Cable Length (m)	Operating Temperature
AeroVironment EV50-PS	50	480V_{ac} (3 phase)	100-500	120	>90%	CHAdeMO	-	-	-30°C to 50°C
ABB Terra 54	50	480V_{ac} ± 10% (3 phase)	200-500	125	95%	CCS, CHAdeMO	775	3.65	-35°C to 55°C
TurboEVC	60	480V_{ac} (3 phase)	150-950	120	>94%	CCS1, CHAdeMO V1.2	518	3.96	-30°C to 50°C
Blink	75	480V_{ac} ± 10% (3 phase)	920 (Max)	188 (Max)	95%	CCS1/2, CHAdeMO	587	6	-35°C to 50°C
EVBox Troniq 100	100	480V_{ac} ± 10% (3 phase)	500	200	95%	CCS1, CHAdeMO	2535	3.96	-30°C to 50°C
BTC Power L3R-100	100	480V_{ac} (3 phase)	50-920	200	>92%	CCS1, CHAdeMO	1350	-	-30°C to 50°C
TurboEVC	120	480V_{ac} (3 phase)	150-950	120	>94%	CCS1, CHAdeMO V1.2	<926	3.96	-30°C to 50°C
Wallbox Supernova	130	400-480V_{ac}	150-920	325	97%	CCS1/2, CHAdeMO	551.2	3	-35°C to 50°C
Tesla Supercharger	135	380-480V_{ac}	50-410	330	91%	Supercharger	1323	2.5 - 5.5	-30°C to 50°C
EVTEC espresso&charge	150	400V_{ac} ± 10% (3 phase)	170-940	50-400	93%	SAE Combo-1, CHAdeMO 1.	881	-	-20°C to 45°C
Siemens Versicharge Ultra	175	480V_{ac} ± 10% (3 phase)	200-920	200	96%	CHAdeMO	573	4.1	-30°C to 50°C
Blink RT 175-S	175	480V_{ac} ± 10% (3 phase)	200-920	200-350	98.5%	CCS1, CHAdeMO	573	4.1	-10°C to 50°C
Delta	200	400V_{ac} ± 10% (3 phase)	200-1000	250-500	94%	CCS, CHAdeMO	992	2.2-5	-25°C to 50°C
ABB Terra HP	350	400V_{ac} ± 10% (3 phase)	150-920	500	95%	SAE Combo-1, CHAdeMO 1.2	2954	-	-35°C to 55°C
Tritium PK 350	350	480V_{ac} (3 phase)	920	200-500	98.5%	CCS2, CHAdeMO	1308	4.1	-35°C to 50°C
Signet DC350K-CC	350	480V_{ac} ± 10% (3 phase)	150-920	200-500	95%	CCS1/2 , CHAdeMO	418	-	-35°C to 55°C
PHIHONG (DO 360 Series)	360	480V_{ac} ± 10% (3 phase)	150-950	380-500	>94%	CCS1/2, GBT, , CHAdeMO	771	4	-30°C to 50°C
Ingeteam INGEREV RAPID ST400	400	400V_{ac} (3 phase)	50-1000	400-500	-	CCS2, CHAdeMO	1168	4.8	-20°C to 60°C

The power conversion system (PCS) in dc fast charging stations comprises ac-dc rectifier and dc-dc power converter which are located outside and connected to EV via electric vehicle supply equipment (EVSE). The fundamental requirement of PCS is that it must possess the capability to supply regulated dc output voltage in the range between 100-800V, according to the design of the battery packs of the EVs. Additionally, state of charge (SoC) of the battery must reach up to 80% in less than 30 minutes for a battery capacity of 20kWh-40kWh by the PCS and to do so, modular converters are preferrable that can be stacked together to deliver high power. Bidirectional power converters are attractive due to

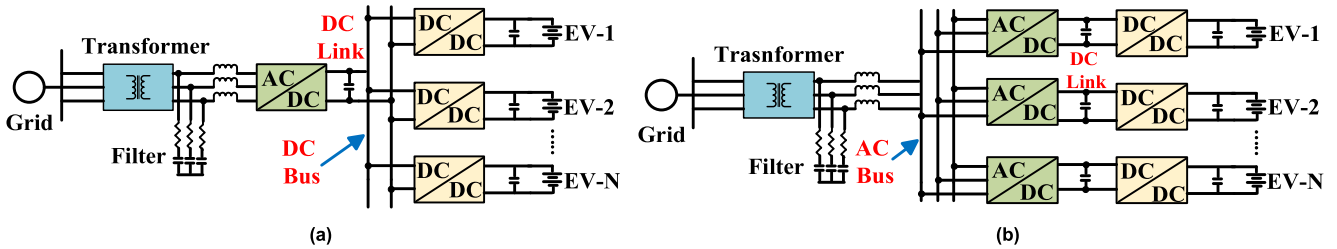

FIGURE 3. Architecture of an EV off-board charging station: (a) DC connected system. (b) AC connected system.

TABLE 4. Comparison between DC and AC connected EV charging architecture.

Criteria	DC Bus Architecture	AC Bus Architecture
Integration of Energy Sources	Easier	Complex
Number of Conversion stages	Lower	Higher
Efficiency	Higher	Lower
Impacts from utility side	Less	High
Rating of AC-DC rectifier	High	Medium
Protection devices	Sophisticated	Unsophisticated
Control	Simple	Complex
Cost	Less expensive	More expensive

emerging Vehicle to Grid (V2G) technology in which power is injected to the grid from the EV. Moreover, output voltage ripple of the dc-dc power stage should be less than 5% of maximum output voltage and current ripple at the battery pack is specified to be smaller than 1% of the minimal value of the current profile to secure the durability of the battery. Furthermore, galvanic isolation is necessary between the grid and the EV battery to meet up the safety standards. There are two types of galvanic isolation based on its location; the first one is the low-frequency transformer connected to the grid in front of input filter while the second type is the high-frequency transformer associated with the dc-dc converter [33]. The first type contains large magnetic components which make the system bulky and designing high-frequency transformer integrated to the dc-dc converter is recommended to attain high power density when the charging power goes up.

III. ARCHITECTURE OF EV CHARGING STATION

EVs are usually classified into three types: battery electric vehicle (BEV), plug-in-hybrid electric vehicle (PHEV), and hybrid electric vehicle (HEV) [34]. In this paper, we will focus only on BEVs which take only electrical power as a source of energy and require charging facility at a station. Charging methods can be conductive, inductive, and wireless; however, wireless and inductive charging are still at an early stage for large-scale implementation [35], [36]. Both on-board and off-board charger developments are centered on conductive charging process that maintain power flow to EV with wire connection. As we mentioned earlier, our review of converter topologies and control methods will focus on off-board chargers mainly. Generally, there are two configurations of an EV fast charging station based on the ac bus and dc bus structure as shown in Fig. 3. For an ac-connected system, three-phase ac bus operates around 250V-480V line to line voltage. Each charger unit consists of ac-dc rectifier and dc-dc converter and hence, the number of power stages is higher, increasing cost and complexity. However, most of the fast and ultra-fast charging stations adopt ac-connected system owing to the well-equipped and matured power electronics and ac power distribution system. In dc bus configurations, there is a central ac-dc rectifier that is connected to the low-frequency transformer on the input side; PV sources, energy storage devices, and EVs are connected to the dc bus through the dc-dc converter. This structure brings out more flexibility in the system and any abnormality from the grid side is easily avoided. As the number of ac-dc rectifiers becomes less, efficiency is higher in dc bus structure and control method implementation becomes simpler. However, there are still no well-established protection guidelines for dc bus EV charging stations and during V2G operation, this issue becomes more critical [37]. Comparison between ac and dc connected EV charging station is exhibited in Table 4. International standards such as IEC 62955:2018, IEC 61851-1:2017 require that the leakage current between the chassis of the charger and the earth should be less than 30mA to prevent electric shock in the human body [38]–[40]. Galvanic isolation provides a large common-mode impedance and thus, leakage current is significantly minimized [41]. Isolation provided by a low-frequency transformer necessitates huge conductors and large protection devices [42] and so, charging station installation cost is increased. This is a clear disadvantage for the EV charging infrastructure in urban areas where the cost of the land is high. However, with this configuration, non-isolated converters can be utilized for the dc-dc stages that feature simple architecture and control. Further, bidirectional power flow control is not complicated similar to isolated dc-dc converters. The second type of isolation which is achieved by a high-frequency transformer in the dc-dc power stage is preferable due to reduced installation cost and improved reliability. The transformer is operated with a high frequency (∼50kHz-300kHz) instead of line frequency (50Hz or 60Hz) which increases the power density. However, switching

modulation and control for isolated dc-dc converter can be complicated and bidirectional operation requires extra effort.

The ac-dc rectifier is the first power stage in an EV charging station that takes ac voltage of 250-480V_{ac} from the grid and delivers stable dc link voltage of approximately 800V. The rectifiers are connected to the utility grid and so, they can inject harmonics which degrades power quality. Power factor correction (PFC) techniques are employed to address this concern. Utilization of these PFC strategies ensures that input currents are sinusoidal and are in phase with the sinusoidal voltages. Low THD (<5%), sinusoidal input current, high power factor, bidirectional power flow capability, high efficiency and power density, simple modulation and control, reactive power compensation, and stable output dc voltage are the expected features of an ac-dc rectifier.

The dc-dc back-end converter is the second power conversion stage of an off-board charger that takes rectified input voltage from the first power stage and then, adjusts it according to the EV battery. Input voltage of the dc-dc stage is the dc link voltage and output voltage can vary between 100V and 1000V. The task of constant current (CC) and constant voltage (CV) charging of the battery is accomplished by the dc-dc converter. High efficiency, high frequency operation, high power density, bidirectionality, low output voltage ripple, soft switching capabilities, stable voltage regulation, and wide range of output voltage are the key characteristics of the dc-dc converter.

IV. TOPOLOGIES FOR AC–DC CONVERSION STAGE

In this section, we discuss the technical details of several topologies for the front-end ac-dc rectifiers. The topologies presented here are well-suited for dc fast charging. With a modular approach and proper design, the power rating of the rectifiers can be raised to meet the requirement of dc fast charging. Also, a technical comparison among the experimentally validated ac-dc rectifiers is presented in Table 5.

A. THREE-PHASE BUCK TYPE RECTIFIER

Achieving power factor correction (PFC), low THD, high efficiency, and high-power density are the key prerequisites for an ac-dc rectifier in the EV charging station. Three-phase buck type rectifier (TPBR) is a proper choice for the ac-dc power stage since it can deliver these features [43]–[46]. Moreover, TPBR provides inherent inrush current free startup, wider output voltage control range, phase leg shoot through protection, and overcurrent protection circuit during short circuit in comparison with boost type three-phase rectifier [47], [48]. Besides, input current can be controlled without closed-loop configurations. Conventional six switch TPBR consisting of three legs and one freewheeling diode has been depicted in Fig. 4(a). Additionally, details of three-switch TPBRs can be found in the literature [49]–[51]. The article in [48] presents an eight-switch 3-phase buck rectifier that suffers from the lowest semiconductor losses during the freewheeling state compared to conventional six-switch TPBR and three-switch TPBR. Since voltage stress on the switches in EV charging is very high, the study in [52], highlights slight modifications in the circuit structure which includes splitting the freewheeling diode into two diodes of series connection and connecting the input neutral point to the common node of the two diodes. Considering this adjustment, switches are currently required to withstand input phase voltage instead of line-to-line voltage. Further, a leg of two diodes is inserted in traditional TPBR including connecting a capacitor between input filter and middle of diode leg [53]. Along with the reconstruction of the circuit, corresponding space vector pulse width modulation (SVPWM) strategy results in lower voltage stress than the input phase voltage on the switches. Furthermore, a transfer matrix-based digital controller has been designed that reduces the input current THD and output voltage ripple under unbalanced ac input condition without any sophisticated calculation or phase-locked loop (PLL) [54]. Another issue for TPBR while operating in high frequency is caused by distributed parasitic capacitances between the dc link output and the ground, leading to input current distortion especially at light load condition. In study [55], authors have introduced a novel structure to suppress the high frequency input current and thereby, the input THD is reduced. In general, high step-down voltage gain is preferred, if multiple EVs available in the road are considered including their variation in terms of battery range. In this case, matrix-based TPBR is a good choice because regular TPBR modulation index is less than 0.5 when output voltage is lower than three-fourth of input phase voltage magnitude which increases losses and damages power quality [56], [57].

B. SWISS RECTIFIER

Swiss rectifier (SR) -another type of TPBR with eight switches shown in Fig. 4(b), has higher efficiency, lower common-mode noise, lower conduction, and switching loss of the switches compared to six-switch TPBR [58]. Control methods of dc-dc converter can be implemented on SR due to its circuit structure. Moreover, SVPWM can be avoided for SR and hence, control becomes simple. Interleaving of SRs offers smaller current and voltage ripple, lower filter requirement, high power, high bandwidth, and high reliability [59]. The work in [60], presents SR with interleaved dc-dc output stage that can achieve 99.3% efficiency with a rated power of 8 kW. High power operation can also be ensured using multilevel three-phase SR [61], but the circuit becomes too complex to control. In [62], full-bridge SR has been demonstrated that considers electrical isolation and ZVS switching intended for improving reliability and efficiency significantly with improved grid power quality. One key demerit of SR is that it allows only unidirectional power flow [58], [63]. However, bidirectional SR can be developed with the compromise of extra electrical components and intricated structure so that V2G operation can be possible [61], [64].

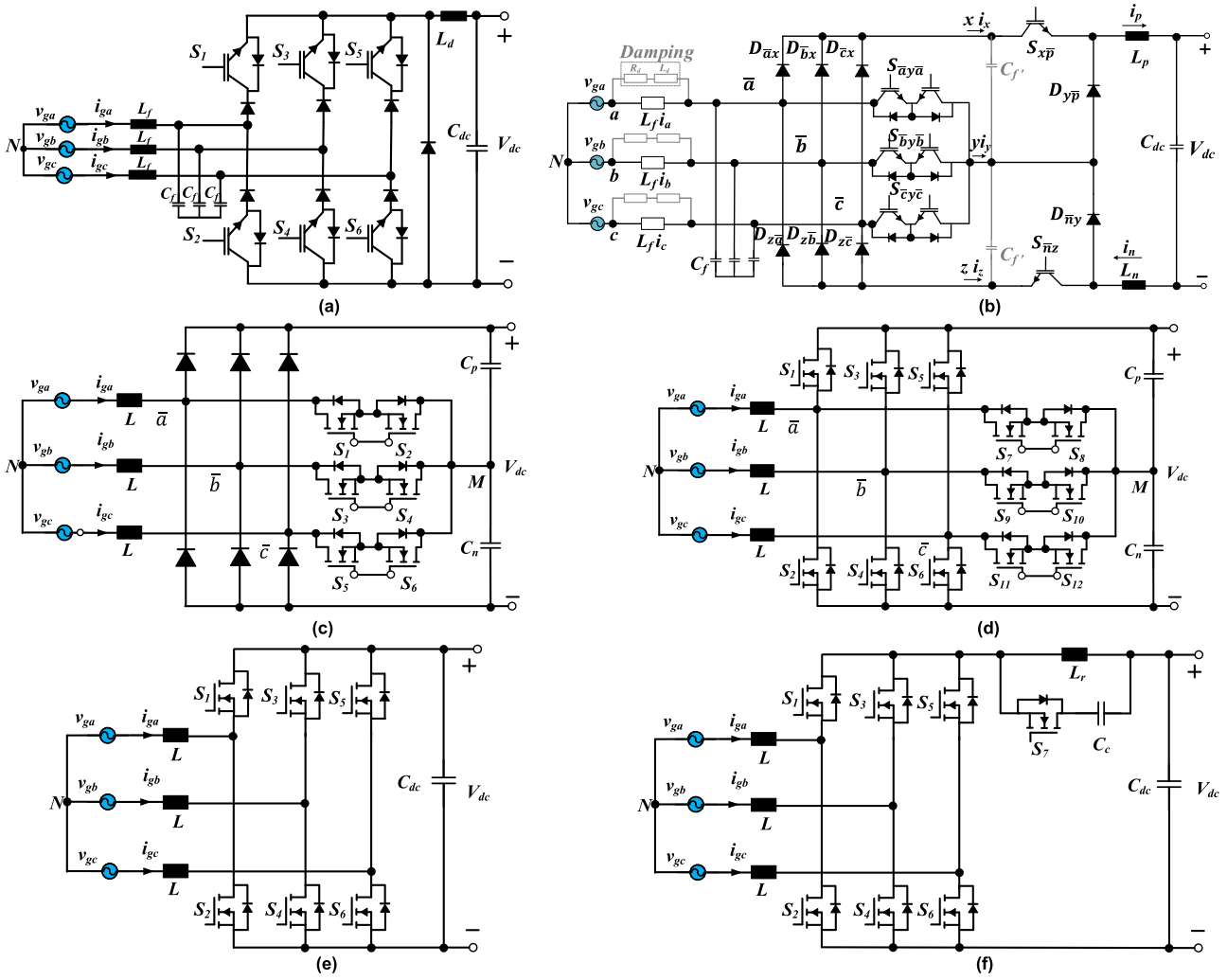

FIGURE 4. Circuit schematics of AC-DC power stage: (a) Three-phase six switch buck type rectifier. (b) Swiss rectifier. (c) Three-phase Vienna rectifier. (d) Three-phase bidirectional Vienna rectifier. (e) Three-phase six switch boost rectifier. (f) ZVS enabled three-phase boost rectifier.

C. VIENNA RECTIFIER

The three-phase Vienna rectifier (VR) shown in Fig. 4(c), exhibits similarity in operation if compared with a three-phase boost PFC rectifier; however, the power flow is unidirectional [63]. Though it retains the benefits of three-level converters, common drawbacks of three-level converters including the requirement of dc-link capacitors are also shared by VR. VR is widely used in high power applications because of its simple control method, high power density, high power efficiency, reduced number of switches, unity power factor, very low THD, and neutral connection-free structure [65]–[68]. On top of that, voltage stress on the switches is half of the dc link voltage and no dead zone switching drive is required [66]. A smaller volume of the VR can be accomplished, as its requirement of the boost inductance is nearly half compared to the two-level rectifiers. The three-phase VR comprises three boost inductors at the input, six fast rectifiers diodes, six switches (2 switches per leg), and two split capacitors at the output. In addition, VR is compatible with bipolar dc bus structure that allows better power flow capability while maintaining the step-down ratio of dc-dc power stage low. However, voltage imbalance in the bipolar dc bus structure needs to be fixed to prevent input current distortion [69]. In [70], authors have compared the power losses of various configurations of VR based on the utilization of diodes and switches, and from the analysis, it has been found that the structure presented in Fig. 4(c) incurs the lowest amount of losses. Also, a three-phase interleaved VR has been designed in [70] that provides 99.28% efficiency with improved thermal management. Circulating current generated due to interleaving can be minimized by the proper design of coupling inductors. A 15kW bidirectional VR has been presented in [71] that supports V2G operation. The diodes are replaced by the switches to ensure bidirectional power flow as shown in Fig. 4(d). This topology is also referred as a three-phase three-level T-type rectifier.

The modulation methods for three-phase VR are categorized as carrier-based PWM [72], SVPWM [73], and

discontinuous PWM [74]. Further, hybrid SVPWM is used for interleaved VR, as conventional SVPWM causes input current distortion near zero crossing, and both carrier-based PWM and discontinuous PWM generate large ripples [75]. For a better compromise between high-power density and efficiency using standard PCB technology, the frequency of VR is limited to approximately 250kHz [63]. Violation of this limit may lead to input current distortion, degrading grid power quality.

D. THREE-PHASE BOOST TYPE RECTIFIER

Three-phase boost rectifier is well-suited for the ac-dc power stage of the EV charger due to its simplified structure, continuous input current, bidirectional operation, high output dc voltage, low current stress, less number of switches, simple control scheme, low THD, and high efficiency [63], [76], [77]. The circuit schematic of a three-phase six switch boost rectifier (TPSSBR) has been demonstrated in Fig. 4(e) that comprises three inductors in series with three-phase input ac source and total six switches in the three legs. The inductors are utilized to boost the voltage and reduce the harmonic contents of the input current. Switching of the top and bottom switches is executed in a complimentary way. In [78], authors have demonstrated a parallel TPSSBR system where each rectifier is connected to the input and output side without any additional passive component. This configuration facilitates high power operation and modular design. The circulating current generated by this system can be suppressed by implementing zero-sequence current control method. Generally, the advantages of TPSSBR are justified under the assumption of a balanced input ac system. When the ac input voltage is not balanced, harmonics appear at the dc-link voltage [79]. This issue can be mitigated by utilizing a bulky capacitor which increases the size of the rectifier and deteriorates dynamic response [80]. Another approach is to develop an active control method so that the harmonic components of the dc-link voltage can be reduced [81], [82].

The antiparallel diodes in TPSSBR suffer from reverse recovery loss which worsens the switching loss of the MOSFETs. In [83], an ultra-fast dc rail diode has been integrated at the dc-link side to alleviate the reverse recovery loss of the anti-parallel diodes. Additionally, this structure ensures automatic step-up operation, avoids bridge short through problem, and maintains soft switching. Soft switching can also be achieved by employing zero voltage transition (ZVT) TPSSBRs and zero current transition (ZCT) TPSSBRs. An auxiliary network comprising a resonant inductor, a diode, and a switch is added at the dc-link side for ZVT TPSSBR. The bridge switches are turned on under zero voltage condition and hence, switching loss is reduced. For ZCT TPSSBR, an auxiliary network consisting of a resonant inductor, a capacitor, a switch, and a diode is inserted. Due to the resonance condition, the bridge switches are turned off under zero current condition in this case. However, above mentioned soft switched TPSSBRs are unidirectional and auxiliary switches suffer from hard switching. In study [84], authors have proposed a ZVS enabled TPSSBR which includes a clamp branch consisting of an active switch, a resonant inductor, and a clamping capacitor as shown in Fig. 4(f). In this architecture, the bridge switches and the auxiliary switch are turned on under zero voltage condition. Further, the reverse recovery losses of the anti-parallel diodes are minimized, and bidirectional operation is maintained.

E. MULTILEVEL AC–DC CONVERTER

Multilevel converter (MLC) is a popular topology among researchers that provides alternating voltage levels from several lower levels of dc voltages [85]. In EV fast and ultra-fast charging applications, MLC is a preferable choice over other topologies as an ac-dc power stage due to its capability of delivering high power with increased efficiency and power density. Considering various architectures found in the literature, MLC can be categorized into three types: 1) Cascaded H-Bridge (CHB), 2) Flying Capacitor (FC), and 3) Neutral Point Clamped (NPC) MLC. The basic working principle of a MLC converter lies in generating staircase waveform at the output using switches, capacitors, and voltage sources. The unique characteristics of a MLC include staircase multilevel PWM waveform to attain low THD, smaller dv/dt and minimization of magnetic components to allow superior performance, less voltage stress on the switches in high voltage application (e.g. 100V rated switch in 400V input voltage), low EMI, and reduced voltage transition between levels [86]–[95].

1) CASCADED H-BRIDGE MULTILEVEL AC–DC CONVERTER

In [86], [87], a three-phase EV charging station architecture using modular CHB multilevel ac-dc converter has been proposed. A large number of switching states is generated owing to modularity as well as high number of series and parallel connections of unit cell, which results in taking the advantage of voltage balancing of cell capacitors and isolation of faulty cells without any impediment in operations [86]. The study in [88] and [89], discuss single-phase CHB as an ac-dc rectifier. As nonlinearities like turn on/turn off delays and saturation voltage of active switch cause distortion in unit cells resulting in variations in the output voltage of CHB, a compensation technique including predictive current control has been employed to improve the harmonic content of grid current within a single fundamental period [88]. In [90], a modular MLC-based EV charging station is proposed where each submodule of the modular configuration is shown in Fig. 5(a). Multiple submodules connected in series enable adaptation to the charging requirement of high power and high voltage for EV fast charging. Among various modulation techniques developed for MLC, sinusoidal pulse width modulation (SPWM) and SVPWM are the most popular [91]. SPWM method makes use of different triangular signals, which are phase-shifted or level-shifted, and then, compared with sine wave leading

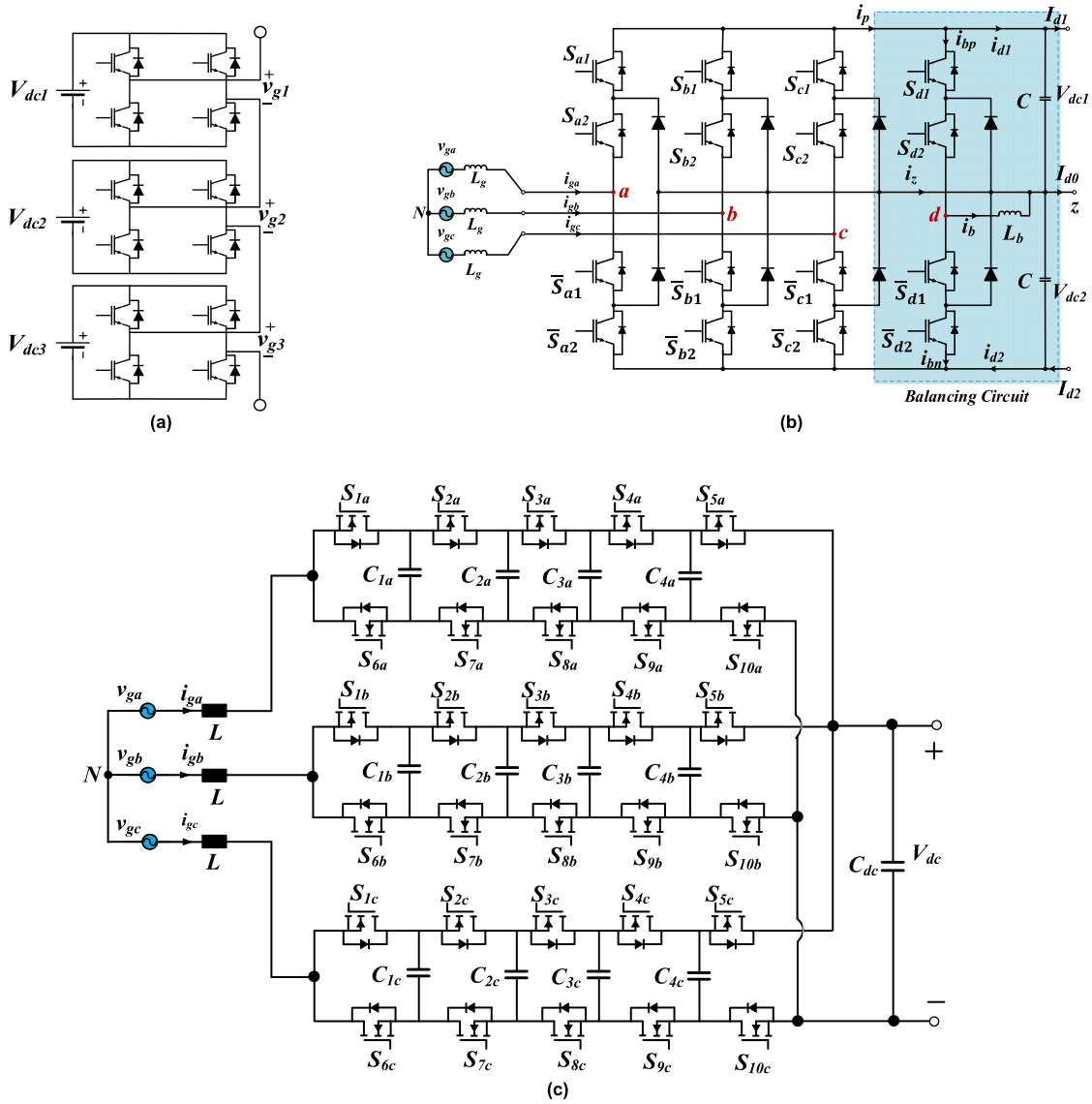

FIGURE 5. Circuit schematics of multilevel converter for AC-DC power stage: (a) Cascaded H-bridge (CHB) rectifier. (b) Three-phase neutral point clamped (NPC) rectifier with voltage balancing circuit in bipolar dc bus structure. (c) Three-phase 6-level flying capacitor multilevel ac-dc converter.

to desirable gate pulses. Despite its simplicity, robustness, and easy implementation, issues such as voltage balancing across the capacitors and inefficiency to deliver maximum modulation index are unavoidable, degrading converter performance [92]. On the other hand, SVPWM technique provides greater flexibility by allowing adjustable duty cycles and optimization of redundant switching sequences. As a consequence, power loss of the ultra-fast charging station can be lowered to a great extent [89]. Further, this method ensures proper utilization of the dc bus voltage, ability to operate at maximum modulation index, and low current ripple. However, if the number of levels of MLC gets high, execution of SVPWM becomes challenging as there are n^3 switching states and $6(n\text{-}1)^2$ triangles in the space vector diagram of a three-phase n-level converter [93]. Therefore, modifications of SVPWM are required so that the benefits of the conventional SVPWM can be retained and dependency on the level of MLC is diminished for a multi-phase system [94].

Since each component of modular MLC may be vulnerable to potential failure, reliability is a major concern here [95]. Though optimization of redundant switching states improves reliability as mentioned earlier, fault detection and bypassing faulty components within a short time are crucial. The most common failure of a power converter originates from power semiconductor devices. The protection system must sense the fault and disable the gate signal before 10 μs [96], as the power device can withstand this event for a very short time. To fulfill this objective, a large number of voltage and current sensors as well as communication channels are required that add to system complexity and cost. Further, pre-charging of floating capacitors without inrush current becomes another problem for MLC [97].

TABLE 5. Design specifications and comparison of various AC-DC rectifiers in EV chargers.

Topology	Ref.	Structure	Power (kW)	Freq. (kHz)	Out. Volt. (V)	No. of Sw./ Diodes	V2G	THD (%)	Peak Efficie–ncy (%)	Merits/Demerits
Three phase buck rectifier (TPBR) and Swiss Rectifier	[53]	Conventional structure +split capacitor and didoes	1.5	200	400	6/8	No	<1.77 %	98.2%	High efficiency, TPBR is bidirectional if output polarity is inverted, low THD. High voltage stress on the switches for conventional TPBR, reduced soft switching capability if working as a single-stage charger, Swiss Rectifier is unidirectional, complex control, cost is higher due to increased number of components.
	[52]	Conventional structure with split free-wheeling diodes	–	60	400	6/8	No	5%	98.1%	
	[55]	Conventional structure with split capacitors	1	200	200	6/7	No	<2%	–	
	[57]	3-phase isolated buck matrix rectifier (single-stage)	5	50	380	12/4	No	1.6%	–	
	[48]	Conventional Swiss	2.5	20	200	8/9	No	–	97.52%	
	[64]	Extended Swiss for bidirectionality	7.5	36	400	16/0	Yes	<1.6	96.8%	
	[62]	Full bridge Swiss (Unfolder + isolated dc-dc)	10	90	400	14/10	No	<3%	95%	
Vienna Rectifier	[196]	Conventional	1.8	50	700	6/6	No	3.5%	98.84%	Less switches, bipolar bus compatible, neutral connection free structure, T-type PFC structure supports V2G operation. Unidirectional power flow (Conventional), suffers from common drawback of three-level converters.
	[63]	Conventional	10	72	700	6/6	No	<5%	97.3%	
	[63]	Conventional	10	250	700	6/6	No	<5%	96.7%	
	[71]	Bidirectional VR (three-level T-type PFC structure)	15	70	800	12/0	Yes	<5%	>98%	
Three-Phase Boost Rectifier	[76]	Three-step and six-step TPSSBR	3	20	400	6/0	Yes	<5%	–	Simple architecture, low THD, continuous input current, bidirectionality, less current stress, low switching count. Switching loss is higher compared to VR, harmonics appear at the dc link under unbalanced ac system.
	[77]	Sensor less TPSSBR	6	100	650	6/0	Yes	4.1%	98.3%	
	[84]	Conventional+ (auxiliary switch, resonant inductor, capacitor)	4	12.8	620	7/0	Yes	3.29%	96.5%	
Multilevel AC-DC Converter	[98]	Cascaded H-bridge (two cell)	2	20	540	8/0	Yes	Low	95.4%	High power capability, high power density, high efficiency, very low THD, less voltage stress on the switches, modular, NPC is compatible with bipolar dc bus structure, FCMLC supports high frequency operation. Voltage balancing is challenging for CHB, inability of CHB to operate at maximum modulation index, reliability is a big concern for MLC due to high number of switches, unbalancing problem is critical for NPC due to uncertainties, high cost in FCMLC.
	[99]	Three-phase Hybrid Cascaded H-bridge	0.55	10		30/0	Yes	<5%	~97%	
	[113]	Four leg three-phase NPC with voltage balance circuit	3.6	1.08/device	~450	16/8	Yes	5.39%	–	
	[111]	Three-level NPC	30	10	858	12/6	Yes	2%	–	
	[111]	Three-level NPC	1.2	1.08/device	~210	12/6	Yes	2.95%	–	
	[117]	Three-phase three-level stacked NPC	2	25	110	18/6	Yes	2.03%	97%	
	[119]	Single-phase seven-level active NPC	50	333	1000	18/0	Yes	–	–	
	[104]	Seven-level FCMLC	1.5	150	400	8/0	Yes	<3.5 %	99.07%	
	[105]	Interleaved 6-level FCMLC	7	720	400	24/0	Yes	<3%	98.9%	

2) FLYING CAPACITOR MULTILEVEL AC–DC CONVERTER

A serious demerit of the modular MLC is that its voltage ripple at the fundamental frequency of the ac side requires larger energy storage for the submodule capacitors [100]. However, Flying Capacitor Multilevel Converter (FCMLC), another variant of MLC, allows for smaller storage requirement for the capacitors when switching frequency is increased. Generally, three-phase MLC is preferred in EV charging

due to its high power delivery capability. But, three-phase rectifiers cannot be designed with very low conduction loss, if they are compared to single-phase rectifiers using the unfolding technique, because current generated in one phase is returned through the other two phases [101], [102]. In a three-phase system, where dc link voltage is near 800V, researchers have shown that three-level MLC cannot provide the same performance compared to single-phase 400V dc link voltage benchmark [102]. In fact, seven-level FCMLC can nearly achieve the same efficiency and performance. FCMLC, along with the unfolder stage, can be used as rectifiers. In [103] and [104], a seven-level FCMLC have been demonstrated. Further, in study [105] and [106], authors have presented an interleaved six-level FCMLC for the purpose of achieving high efficiency and high-power density. In [107], a three-phase FCMLC has been designed in which each input phase is connected to six-level FCMLC as shown in Fig. 5(c). Another advantage of FCMLC lies in the moderate requirement of PWM modulator due to high switching node frequency in FCMLC without using PWM frequency that results in increased PWM resolution [108].

To deal with the issue of double line frequency pulsation, active buffer is adopted as a power decoupling stage [103], [106]. Since FCMLC scales down the filter size significantly with high frequency operation, utilization of smaller inductor causes current phase leading and bring challenges for PFC control. The work presented in [104] describes feedforward control to address this issue. Further, in study [109], authors have proposed a control method to address issues regarding voltage spikes and loss carrier signals operating near zero current ripple. Furthermore, authors have employed a hybrid control that incorporates valley current detection and constant effective duty cycle control to balance the capacitors of 4-level FCMLC for the full range of load [110].

3) NEUTRAL POINT CLAMPED MULTILEVEL AC–DC CONVERTER

Another category of MLC is known as neutral point clamped (NPC) ac-dc converter that allows low distortion in output voltage waveform, medium voltage operation, reduced dv/dt stress across the switch, and input current with low THD. A three-phase three-level NPC ac-dc converter has been illustrated in Fig. 5(b). All the switches need to block half of the dc link voltage and so, switching loss is minimized. Moreover, for example, 500V switches inherit faster technology in comparison with 1000V switches which further cuts down switching loss. In [112], authors have proposed an EV charging station that incorporates a central ac-dc converter with NPC topology connected to medium voltage grid on one side and bipolar dc bus on the other side. Utilization of NPC with bipolar dc bus brings several benefits: 1) reduction of the step-down effort by the dc-dc fast chargers [113], 2) improved reliability as one unit of dc-dc stage can supply power if other unit fails or during maintenance, 3) increases power capacity of the charging station as dc-link capacitance is doubled [114]. However, unbalancing problem is more critical for bipolar dc bus structure which cannot be solved with modulation stage unlike unipolar bus structure [115], [116]. Additionally, uncertainties, e.g., random arrival of vehicles and different battery technologies, worsen the unbalancing problem even more. This issue can be resolved by adding a voltage balance circuit that acts as an additional leg with the three legs of NPC topology as shown in Fig. 5(b) [113], [114]. The work in [117] highlights three-level stacked NPC as an ac-dc power stage, exhibiting superior performance over three-level NPC because of increased switching frequency and better total loss balancing. Asymmetrical distribution of power losses among switches and diodes in NPC poses troubles in the design of the converter and its thermal management system. The losses in the most stressed device may limit converter switching frequency and maximum phase current [118]. This problem gives rise to active NPC (ANPC) topology which is a derivative of NPC topology and uses additional active switches in antiparallel to NPC diodes. With redundancies in zero voltage level switching states and possible commutations that can be chosen through proper modulation methods, ANPC mitigates the uneven distribution of conduction and switching losses among the switches [119], [120]. However, each switch requires a linked gate drive circuit and the control is quite challenging to implement because of high number of switches.

V. TOPOLOGIES FOR DC–DC CONVERSION STAGE

The dc-dc stage is directly connected to EV and so, isolation is essential during high power flow unless isolation is guaranteed in front of ac-dc rectifiers. Here, we analyze the details of both isolated and non-isolated dc-dc converters appropriate for dc fast off-board chargers. The summaries of the experimentally validated isolated and non-isolated dc-dc converters are shown in Table 6 and Table 7 respectively.

A. LLC RESONANT CONVERTER

Owing to various advantages of *LLC* dc-dc converter shown in Fig. 6(a) compared to other resonant topologies, it has been widely used as a dc-dc power stage of the EV charger in recent times. The key advantages are: 1) output voltage regulation capability at light load condition, 2) ZVS over a wide range of output voltage, 3) ZCS switching capability for the rectifier diodes that diminishes diode recovery losses, 4) one capacitor as an output filter [121], [122]. The output voltage is regulated by varying the converter switching frequency. The gain of the converter depends on resonant tank gain, switching bridge gain and transformer turns ratio.

LLC converter has three operational modes depending on the comparative values of switching frequency, f_s and resonant frequency, f_r. At resonant frequency operation ($f_s = f_r$), the resonant tank has unity gain and the converter is in the best-optimized mode of operation. Hence, transformer turns ratio is designed in such a way that the converter operates at the resonant frequency at nominal input and output voltage. When $f_s > f_r$, switching loss is increased, the primary

side switches have higher turn-off losses and secondary rectifier diodes have hard commutation, but conduction losses are lower because of the reduced circulating energy. The converter has a step-down gain in this mode and provides buck operation. On the other hand, if $f_s < f_r$, secondary diodes maintain soft switching, but higher conduction losses occur due to increased circulating energy. The converter has a step-up gain in this mode and provides boost operation.

Despite having high efficiency, high power density, and low EMI due to soft switching capability, *LLC* converter suffers from several critical issues. Design optimization is highly significant when *LLC* output is connected to EV battery rather than some passive loads [123]. Output voltage of the converter depends on the SoC of battery and charging profile, leading to nonlinear load characteristics. Therefore, design procedure of *LLC* turns out to be complicated. In addition, battery voltage, V_{bat} largely varies while charging and discharging. For example, a single Li-ion cell has a voltage range between 2.75V and 4.2V based on the minimum and maximum SoC of the cell. So, for a 400V battery pack, the load voltage variation could be higher than 100V. *LLC* converter needs to regulate wide output voltage range when load current is not constant. Moreover, Li-ion battery is charged through constant current (CC) and constant voltage (CV) charging process including trickle charging state, especially for deeply depleted cells. Light load efficiency becomes a critical issue for *LLC* when battery is in CV mode or trickle stage, since battery current, I_{bat} is low. Also, *LLC* needs to be designed in a specific region of the characteristic curve so that primary side ZVS and secondary side ZCS can be accomplished simultaneously to enhance efficiency.

The authors have adopted a voltage double circuit along with *LLC* converter in [124] for charging the deeply depleted battery cell. To do so, the frequency range of *LLC* should be large enough to generate wide voltage gains. However, f_s of *LLC* cannot be 2-2.5 times of f_r in practical applications owing to the existing parasitic capacitance of the transformer's secondary winding and junction capacitances of output diodes. The voltage double circuit mitigates the negative effect of the parasitic capacitors, shifting the second resonant frequency to a very far away and consequently, the operating range of the converter is extended. The disadvantage of this circuit configuration is having lower efficiency as ZVS is not fully achieved.

The work in [125], highlights *LLC* converter operating in three modes such as full-bridge converter with frequency modulation, dual-phase half-bridge *LLC* converter, and single-phase half-bridge *LLC* converter to improve efficiency at low voltage and light load condition. Integration of the resonant inductor to the transformer provides higher power density. The dual-phase structure allows the converter to turn off one phase when the output power is below half of the rated value to improve light load efficiency. Moreover, ZVS is achieved in the active switches in all three modes for the entire operational range.

Bidirectional power flow is an essential functionality of an EV charger for vehicle-to-grid (V2G) applications in which excess energy from the EV battery can be injected to the grid. Asymmetrical resonant tank in *LLC* converter causes a difference between reverse and forward operation, making the design quite challenging for the converter to be operated in bidirectional mode. In [126] and [127], authors have designed *CLLC* dc-dc converter by adding another capacitor on the secondary side. This extra capacitor creates symmetry in the resonant tank during forward and reverse operation and hence, similar characteristics are attainable in both modes. To keep the converter near resonant frequency and maximize efficiency as V_{bat} varies, adjustable dc link voltage, V_{dc} is adopted that corresponds to load voltage variation in *CLLC* converters. Similarly, adding extra L and C on the secondary side to design *CLLLC* converter ensures bidirectional operation [128]. Also, soft switching is maintained here for a wide voltage range. As an extra inductor adds bulkiness to the circuit, a *CLLC* network has been derived from the *CLLLC* design, improving its power density. The article in [129], discusses *LLC* converter including interleaved bridgeless totem-pole PFC stage. Here, bidirectionality becomes feasible with a voltage gain compensation control. Although reverse voltage gain of the *LLC* converter is generally lower than unity, it is compensated by increasing the bus voltage at the front-end side of the *LLC* converter, utilizing V_{dc} as extra control freedom. This control shifts the voltage regulation burden from the *LLC* to the PFC stage and thus, confirms bidirectional power flow for V2G applications. Voltage regulation range of the dc link voltage, V_{dc} is reported to be between 400V and 700V for forward and reverse operation.

B. DUAL ACTIVE BRIDGE CONVERTER

Dual active bridge (DAB) topology consists of a full-bridge structure with active switches on the primary and secondary sides, connected by a high-frequency transformer as shown in Fig. 6(b). DAB is a suitable candidate for the dc-dc power stage due to its high efficiency, high power density, bidirectional power flow, inherent soft switching, galvanic isolation, and wide range of voltage transfer ratio [130]. DAB's modularity allows it to be scaled to the higher power level. Bidirectional power flow is achieved by controlling the phase shift angle between the voltage waveforms of the two bridges. When the phase shift angle is positive between the input and output bridge voltage, power flows from left to right. Changing the polarity of the phase shift angle enables reverse power flow and hence, bidirectionality can easily be achieved with simpler control for the DAB topology compared to the resonant converters.

Different types of switching modulation techniques such as single-phase shift (SPS) with variable of phase shift angle, dual-phase shift (DPS) with variables of phase shift angle and duty ratio of one bridge, and triple-phase shift (TPS) with variables of phase shift angle and duty ratios of two bridges are utilized for DAB [131]. Although DAB uses

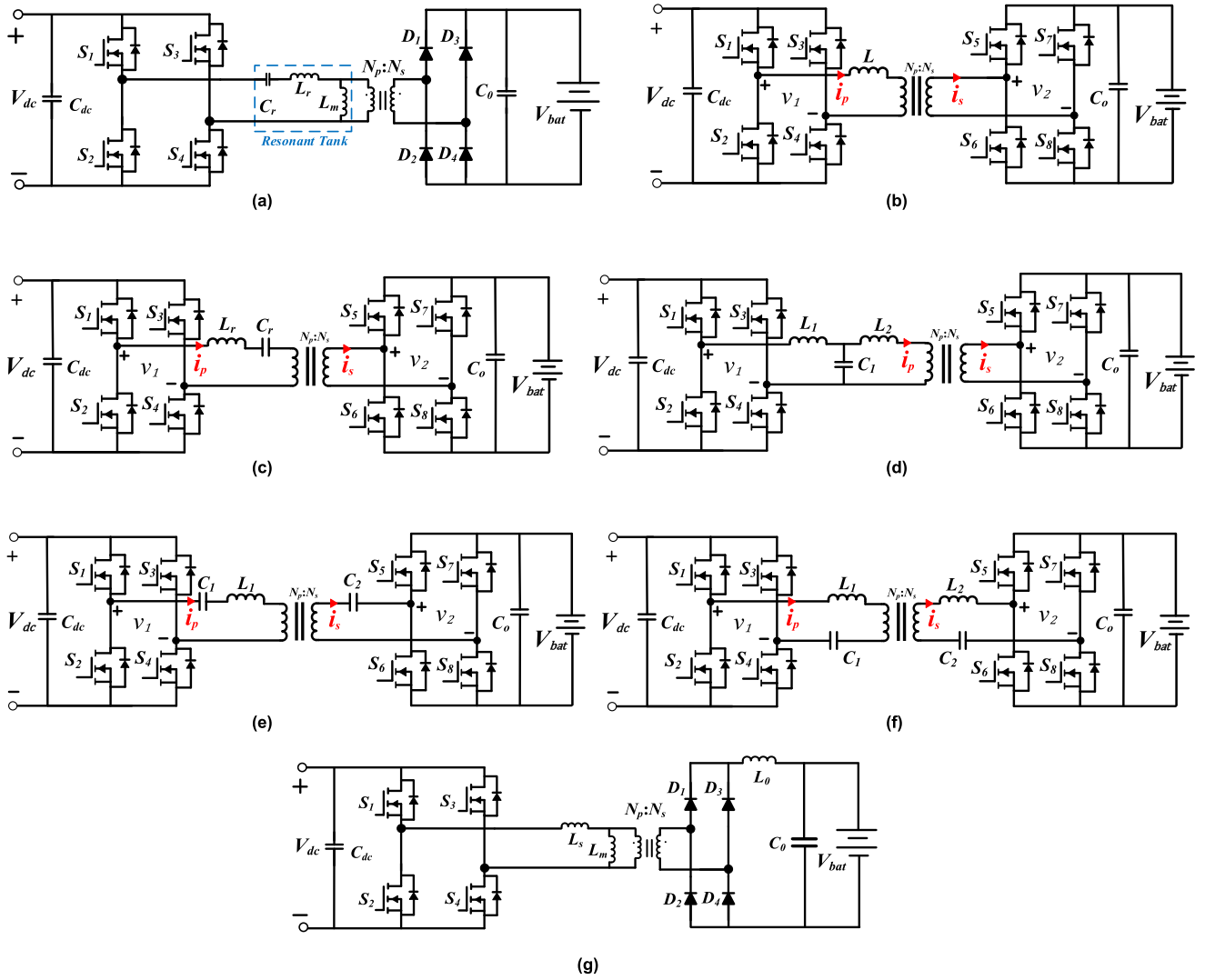

FIGURE 6. Topologies for isolated DC-DC power stage: (a) LLC resonant converter. (b) Dual active bridge converter. (c) Dual active bridge series resonant (LC) converter. (d) Dual active bridge converter with LCL resonant tank. (e) Dual active bridge converter with CLC resonant tank. (f) Dual active bridge converter with CLLC resonant tank. (g) Phase-shifted full-bridge converter.

fewer passive components compared to resonant converters, securing ZVS switching for a wide range of EV battery voltage especially at light to medium load is quite challenging with SPS modulation. DPS can extend the ZVS range but during light load condition, ZVS cannot be fully secured for all eight switches. TPS confirms ZVS for all switches even at no load condition; however, it increases the turn-off current. Therefore, in study [132], SPS, DPS, and TPS are incorporated in order to guarantee ZVS of all switches for the entire operating range of load.

The reactive current causes additional conduction losses for DAB converter with SPS modulation. This problem can be well addressed by utilizing TPS modulation with the optimization of reactive current. In addition, transformer peak current contributes to losses which decrease the efficiency of the converter more. In [133], authors have demonstrated a control method based on DPS modulation, minimizing the transformer peak current to reduce its hysteresis loss. The optimal duty ratios that lead to the lowest peak current are obtained using the Lagrange multiplier method. Another critical issue for DAB originates from the transformer's operation in saturation region [134]. A large magnetic flux density offset can drive the transformer to its saturation point of B-H curve that results in current spikes, increased losses, and damages to the converter. High switching frequency can reduce the magnetic flux swing and transformer core volume while increasing the safety margin to avoid saturation. A saturation prevention algorithm presented in [135], provides a safety margin of the magnetic flux near saturation. The algorithm detects the current slope of the converter instantaneously and so, the onset of saturation is identified and taken care of.

Wide voltage gain is an important factor of DAB converter in EV charging applications. For the voltage-fed DAB

converter, when the input voltage, V_{dc} is equal to nV_{bat}, ZVS can be achieved for all switches, while in other cases, ZVS range is limited. The work in [136], introduces a three-level DAB converter that generates square wave of four different amplitudes and thus, allows adaptation to a wide voltage range. In a similar study presented in [137], a five-level DAB converter is employed to achieve wide voltage gain. Both [136] and [138] optimize transformer RMS current to enhance efficiency. Moreover, wide voltage gain can be achieved with a novel circuit architecture based on dual transformer in DAB [139]. Dual outputs are adjusted successively due to dual-mode (primary side and secondary side phase shift) control, securing a very wide output range with the sacrifice of bidirectionality. Current-fed DAB can also be employed as a dc-dc power stage of the EV charger owing to its wide voltage gain and clamping voltage capability that matches primary and secondary side voltages. However, efficiency of the converter drops as the extra inductor suffers from losses [140].

Another key issue regarding DAB converter is the high frequency current ripple which is generated because of the conventional circuit design, causing negative impacts on battery lifetime. To reduce the current ripple, three-phase DAB structure can be utilized as a straightforward solution. Unlike single-phase DAB, three-phase architecture can triple the effective efficiency and reduces the amplitude of the ripple. Consequently, input and output filter requirements become less. Moreover, a three-phase DAB converter provides lower transformer RMS current and higher power density [138]. Alternatively, current-fed DAB with hybrid phase shift control is a viable solution for achieving low current ripple and increasing battery lifetime [141], [142].

C. DUAL ACTIVE BRIDGE RESONANT CONVERTER

In conjunction with the advanced modulation scheme, using a resonant tank between the two bridges of the DAB converter extends the ZVS range of battery charging [144]–[154]. A variety of resonant tanks such as *CLC* [144], *LLL* [145], *CLLC* [146]–[148], *LC* [149]–[152], *LCL* [153] are found in the existing literature. DAB converter with series *LC* network shown in Fig. 6(c) is preferred due to its low resonant component count [150], [151]. The leakage inductance of the transformer can be used as a series inductor and the additional capacitor has dc blocking capability. However, this topology suffers from hard switching in certain operating regions under wide variations of battery voltage. In study [149], authors have added a switch-controlled inductor network in DAB series resonant converter (*LC*-type) to confirm ZVS at the primary side and ZCS at the secondary side for a wide range of battery voltage. Authors in [152] have adopted four degrees of freedom modulation strategy with optimization for DAB series resonant converter to achieve soft switching, minimum resonant tank current, and complete elimination of reactive power under wide variations in battery voltage. The circuit schematics of DAB resonant converter with *LCL* and *CLC* resonant tank have been exhibited in Fig. 6(d) and Fig. 6(e) respectively. The bridge currents are almost sinusoidal and in phase (or anti-phase for reverse operation) with their respective voltages for both *LCL* and *CLC* type DAB resonant converter [144], [153]. Therefore, reactive power is significantly reduced and thus, efficiency is increased. *CLC* structure has a higher power density as magnetizing inductance can be used for the resonant component. In addition, the series capacitor in *CLC* structure prevents transformer core saturation during abnormal operating conditions. Although both structures extend soft switching range and reduce conduction loss compared to DAB converter, soft switching cannot be secured for a wide range of battery voltage. The authors in [154], have introduced a reconfigurable resonant DAB converter that operates in full-bridge mode for 50%-100% load and reconfigured to half-bridge mode of operation in case load falls below 50%. Desirable soft switching characteristics are achieved in full-bridge mode, while half-bridge mode operation aims at reducing the circulating current with improved light load efficiency. However, additional active devices and passive components increment volume and cost. In article [145], a TPS controlled DAB with *LLL* tank is demonstrated that features ZVS for the entire operating range of the converter, enabling high frequency operation. A schematic of DAB converter with *CLLC* resonant tank is exhibited in Fig 6(f). A complete soft switching can be achieved for the entire load range with appropriate design of DAB *CLLC* converter [147]. In [148], a three-level *CLLC* DAB resonant converter has been introduced which provides the inherited features of DAB resonant converter and reduces voltage stress on the switches due to multilevel configuration. The major drawback of DAB-based resonant converter is synchronization and paralleling which demands exhaustive effort in control, attributable to asymmetrical tank and complex mathematical model.

D. PHASE-SHIFTED FULL-BRIDGE CONVERTER

Phase-shifted full-bridge (PSFB) converter shown in Fig. 6(g) is related to the family of DAB converters where the major difference lies on the secondary side. Active switches on the secondary side are replaced by diodes that allow power flow in one direction. PSFB has proved its potential for EV chargers owing to its attractive features such as soft switching capability of the primary active switches, simple PWM control with a fixed frequency, modularity, reduced current stress on the devices, and low EMI. The power flow occurs due to the variation of the phase between the switches on the primary side. For this topology, ZVS turn-on of one leg and low voltage turn-on of the other leg in the primary side are achievable while the secondary side diodes suffer from hard switching. In fact, in EV charging applications, this converter experiences non ZVS turn-on when the battery current is low. The circulating current in the primary side during the freewheeling period causes additional losses. A large output inductor on the secondary side increases the cost and reduces power density. Additionally, voltage overshoot across the

TABLE 6. Technical specifications and comparison of isolated DC-DC converters in EV chargers.

Topology	Ref.	Structure	Power (kW)	Freq. (kHz)	Output voltage (V)	No. of S/D	V2G	Effic–iency (%)	Modulation method	Major Advantages/Disadvantages
Resonant Converter	[129]	*LLC*	6.6	300	240~420	8/0	Yes	96%	Pulse Frequency	Wide range of ZVS, output voltage regulation capability at light load condition, high-efficiency, compact size, low EMI. Bidirectionality is not normally obtained [117], [124], switching frequency is close to resonant frequency, design procedure is complex to achieve wider output voltage range.
	[124]	Interleaved *LLC* + cascaded voltage doubler rectifiers	1.5	70.96-472	50~420	4/4	No	95.65 %	Pulse Frequency	
	[123]	*LLC* Full bridge	3.3	83.33-220	250-450	4/4	No	98.2%	Pulse Frequency	
	[125]	Hybrid *LLC*	3.2	75-300	250-400	4/4	No	98.5%	Pulse Frequency	
	[122]	Full bridge 3-level *LLC*	6.6	90	225-378	6/6	No	98.14 %	Pulse width+ Phase shift	
	[128]	*CLLLC*	3.5	40-200	250-450	8/0	Yes	~98.1 %	Pulse Frequency	
	[126]	*CLLC*	6.6	325-700	250-450	8/0	Yes	96%	Pulse Frequency	
Dual Active Bridge (DAB) Converter	[135]	DAB+ Saturation Mitigation	6.6	125	320-450	8/0	Yes	96.8%	Single Phase Shift	High efficiency and power density, bidirectionality, inherent soft switching, wide voltage transfer ratio, flexibility in modulation, modularity. Securing ZVS at light load condition is challenging for SPS, high frequency current ripple, transformer saturation.
	[132]	Conventional DAB	20	100	200-450	8/0	Yes	~96%	Single + Dual +Triple Phase shift	
	[143]	Medium voltage DAB	12	50/10	520-820	8/0	Yes	–	Single Phase Shift	
	[136]	Three-level DAB + Blocking Capacitor	3.5	50	200-700	16/8	Yes	~97.5 %	Single Phase Shift	
DAB Resonant Converter	[144]	DAB+ *CLC*	4	50	~400	8/0	Yes	95%	Phase shift PWM	Extended ZVS range, high efficiency, transformer core saturation is avoidable. Power density is decreased, and cost is increased due to added components, control and synchronization becomes complex.
	[145]	DAB+*LLL*	1	100	~270	8/0	Yes	~96%	Triple phase shift	
	[147]	DAB+*CLLC*	1	170	200-420	8/0	Yes	96%	Pulse Frequency	
	[148]	Three level DAB+*CLLC*	3.5	31-70	200-700	16/8	Yes	~96.8 %	Pulse Frequency	
	[150]	DAB with series resonant tank	4.5	109.6	~200	8/0	Yes	–	Phase shift	
	[152]	DAB with series resonant tank	1	100	~250	8/0	Yes	97.7%	Triple Phase Shift	
	[153]	DAB+*LCL*	2.5	50	~380	8/0	Yes	96%	Triple Phase Shift	
Phase-Shifted Full-Bridge (PSFB) Converter	[157]	Full-bridge + passive auxiliary circuit	1.2	100	209-350	4/6	No	95%	Asymmetrical PWM/Phase shift PWM	Modularity, simple PWM modulation, reduces current stresses on devices, no circulating current on both primary and secondary side [146], and low EMI. Bidirectionality is compromised due to diodes, efficiency decreases as diodes incur higher losses, non ZVS turn-off for the diodes.
	[155]	Secondary side phase-shifted full-bridge	1	50	200-330	6/4	No	~94%	Phase shift PWM	
	[158]	PSFB with center tapped clamp circuit	3.3	50	270-420	4/6	No	98.3%	Phase shift PWM	
	[159]	Half-bridge integrated PSFB with center tapped clamp circuit	3.3	50	270-420	4/6	No	98.5%	Phase shift PWM	

full-bridge rectifier is severe as the output voltage is typically high in EV charging. Moreover, reverse recovery losses of the diodes are the obvious disadvantages of this topology for high power flow. In [155] and [156], authors bring some modifications in the circuit structure such as utilizing the leakage inductance of the transformer and using turn-off

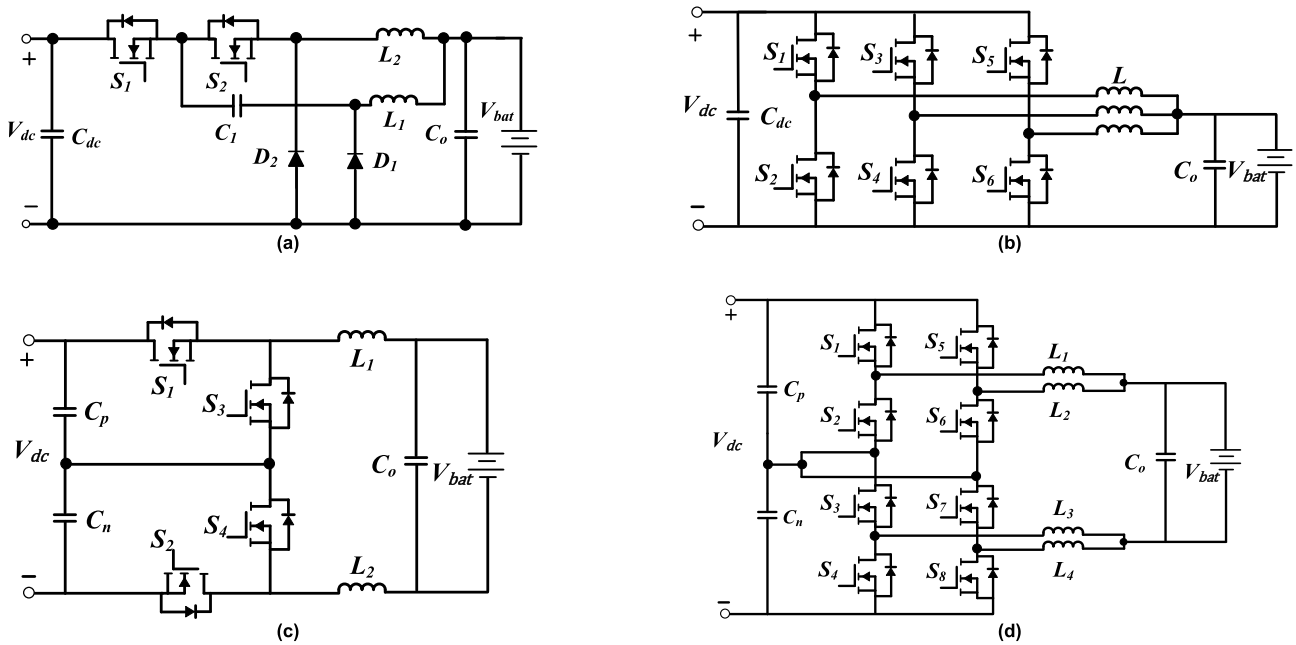

FIGURE 7. Topologies for non-isolated dc-dc power stage: (a) Interleaved two-phase buck converter. (b) Interleaved three-phase buck converter used in ABB terra HP150 ultra-fast charger. (c) Three-level buck converter. (d) Parallel three-level buck converter.

snubber in combination with controlled output rectifier to eliminate circulating current and improve soft switching for full load range. In study [157], a passive auxiliary circuit is included on the primary side so that ZVS turn-on for the entire battery range is ensured and the voltage spikes on the secondary diodes are significantly minimized. However, they contribute to the losses because of the additional components. The authors in [158] and [159], utilize a center tap clamp circuit on the secondary to achieve high efficiency and high-power density. All the aforementioned major drawbacks of the PSFB converter including the size of the output inductor can be mitigated with this modified architecture while charging the EV battery. Moreover, a hybrid converter comprising of PSFB converter and *LLC* series resonant converter is presented in [160] to improve the limitations of conventional PSFB converter and increase power density and efficiency.

E. NON-ISOLATED DC–DC CONVERTER

A non-isolated dc-dc converter is well-suited for a charging station where the line-frequency transformer exists before the ac-dc power stage. The voltage in the input side of the dc-dc converter in dc fast charging is typically higher than the EV battery voltage. Therefore, a single-phase buck converter can theoretically be used for charging the EV. However, there are two major issues associated with the conventional buck converter. First, it is necessary to keep the current ripple of the dc-dc power stage low which will reduce charging/discharging losses as well as aging of the battery [162], [163]. To achieve this, inductor of the conventional buck converter must be sufficiently large and so, power density is reduced. Second, the power rating of this converter is limited as only one switch carries the total current.

Unlike single-phase buck converter with one inductor, interleaved buck converter (IBC) with multiple inductors has many benefits such as smaller current ripple and inductor volume, modularity, better power, and thermal management [164]. However, the voltage stress on all the switches of conventional IBC is equal to the input voltage that incurs high switching loss and diode recovery loss in high voltage applications like EV fast charging. A non-isolated interleaved 2-phase buck converter is demonstrated in Fig. 7(a). In [165]–[167], modified IBCs with distinct architectures have been proposed to achieve low switching loss, reduced voltage stress on the switches, minimized current ripple, and improved step-down conversion ratio. The study in [165] shows that voltage stress across all the active switches is half of the input voltage before turn-on or after turn-off and extra circuitry is not required to balance the current. Owing to inherent charge balance of the blocking capacitors, the converters in [166] and [167], provide current sharing between the interleaved phases without any additional circuit and control module. Moreover, a 3× three-phase interleaved dc-dc buck converter has been presented in which each module contains six identical switches and three inductors [168], [169]. This modular architecture has been used in ABB Terra HP150 ultra-fast charger [170]. The circuit schematic of one module is exhibited in Fig. 7(b). This configuration provides several merits such as modularity, high power (150 kW), low-cost design, and balanced power sharing among the phases. Further, extremely low output current ripple has been reported compared to other IBCs. However, if the number of the interleaved phases gets higher,

TABLE 7. Technical specifications and comparison of non-isolated DC-DC converters in EV chargers.

Topology	References	Structure	Power (kW)	Freq. (kHz)	Output voltage (V)	No. of S/D	V2G	Effic–iency	Modulation	Major Advantages/Disadvantages
Non – Isolated DC-DC Converter	[161]	2-phase IBC	1	16-32	~350	4/0	No	98.5 %	PWM	Avoid losses caused by transformer, interleaving reduces current ripple and inductor volume, high power operation is feasible, modularity. Voltage stresses across switches of conventional buck converter are high, absence of isolation, current sharing becomes issue for high number of phases.
	[168]	3-phase interleaved chopper (6 cells)	150	16	200-800	6/0 (each)	No	–	PWM	
	[173]	3-phase interleaved	100	25	~450	6/0	Yes	98%	PWM (DCM)	
	[180]	Parallel 3-level with separate inductors	1.2	4.32	–	8/0	No	–	PWM	
	[177]	3-level asymmetrical voltage source converter	40	20	200-500	4/0	Yes	–	PWM	

obtaining similar phase characteristics becomes burdensome due to variation in the component tolerances. Different phases can suffer from different losses and thus, average current among the interleaved phases will be different. Additionally, current sharing among the phases is sensitive to duty cycle fluctuation [171]. Therefore, current equalization is important for an interleaved converter where the phase number is comparatively high. Authors have introduced an eight-phase synchronous interleaved buck converter and developed sliding mode control including current equalization algorithm in [172] to accomplish robust voltage regulation, frequency regulation, and phase current equalization.

To increase the power density, the buck converter can be designed to operate in discontinuous conduction mode (DCM), since a smaller inductor size is selected. Large ripple in DCM can be alleviated by increasing the number of interleaved phases. However, high turn-off losses and ringing effects among the switches are the major disadvantages in DCM. To overcome these challenges, authors in [173], have proposed gate complementary control including snubber so that currents in the nonactive switches are diverted to the anti-parallel diodes, and hence, ZVS turn on is achieved. Moreover, splitting the input voltage is a solution to the increased stress on the switches [174]. The only concern with this method is that V_{bat} must be in the range between the split voltage and the input voltage which limits the charger operation.

Another way of decreasing the voltage stress on the switches is to use a non-isolated three-level dc-dc converter which allows to choose lower rated switches as well as high frequency operation [175]–[180]. In this way, smaller inductor can be chosen that reduces extra cost and volume. Output and inductor current ripples are cut down significantly for this topology compared to IBC and conventional buck/boost converter [176]. A bidirectional three-level asymmetrical voltage converter shown in Fig. 7(c) has a similar working principle as IBC by adopting an advanced control method [177], [178]. The converter is controlled with a single controller operating at one frequency and the resulting frequency in the coupling filter is double the switching frequency. Current ripple here is significantly lower compared to the half-bridge structure of non-isolated dc-dc converters. A new circuit structure consisting of two parallel three-level converters shown in Fig. 7(d) is proposed to achieve high power operation [179]. This topology is compatible with bipolar dc bus structure and eliminates the balancing circuit for NPC ac-dc converter due to the proposed active dc power management algorithm. However, with this configuration, high dc link voltage ripple and circulating current exist if multiple fast chargers operate simultaneously. To address this issue, authors in [180] have modified a parallel three-level dc-dc converter with an integrated inductor structure. The inductor contains integrated magnetic core with output and circulating windings that filter output currents and thus, circulating current produced by the ac-dc power stage is reduced.

VI. MULTIPORT CONVERTER BASED EV CHARGING SYSTEM

In the last few years, there has been a growing interest in the advancement of multiport converters for EV charging that can integrate various dc sources (PV, Energy Storage), grid, and multiple loads (EV Battery) with only one single-stage power conversion system [181], [182]. In a smart microgrid, combining EVs and renewable energy sources including energy storage units provides electricity to the loads during peak hours resulting in minimization of load shedding and additionally, improving power quality. Utilization of multiport converters as an EV charger guarantees higher efficiency due to reduced number of power stages and dc power flow between PV and EV battery directly, high-power density, small scale communication infrastructure requirement, and cost reduction. An EV charging station based on solar panels, energy storage devices, and multiport inverters in ac connected system is shown in Fig. 8. In [183], authors have designed a 10 kW EV charger that receives

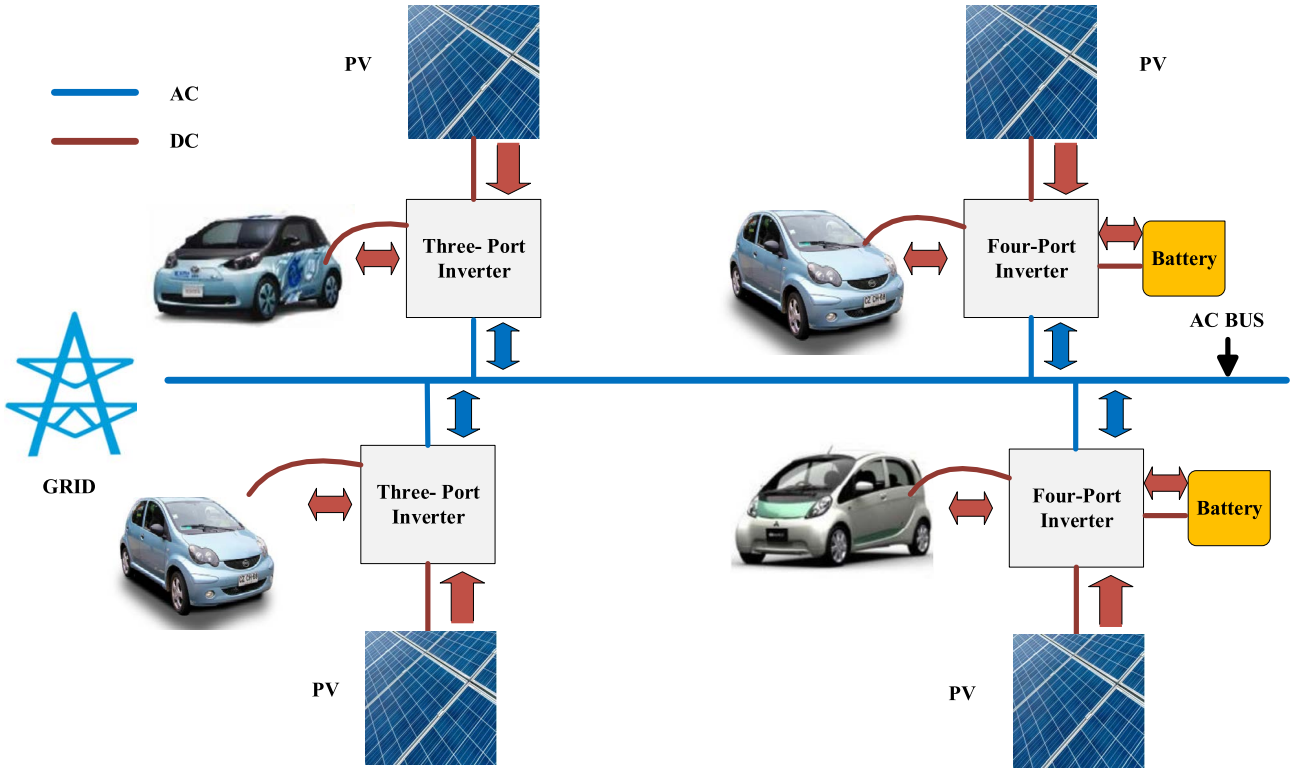

FIGURE 8. Block diagram of an EV off-board charging station including energy storage (ES) and PV panels based on the multiport inverter.

power from PV arrays and three-phase ac grid. The three-port EV charger consists of a unidirectional dc-dc power stage based on interleaved boost topology for the PV, a bidirectional dc-ac inverter (three-phase voltage source inverter) for the grid, and a bidirectional isolated dc-dc converter based on interleaved flyback topology for the EV side. An internal dc link is used to exchange power due to the dc nature of EV and PV and hence, overall system efficiency is increased. Further, bidirectionality of the power converter for the grid and EV side facilitates V2G operation. The interleaved flyback converter operates in quasi-resonant soft switching while interleaved boost and three-phase voltage source inverter maintain hard switching. The developed closed-loop control allows four different power flow modes, i.e., PV to EV, grid to EV, PV to grid, EV to grid. The research work presented in [184], introduces an isolated multiport converter to integrate PV, grid, energy storage, and EV. The main converter is basically designed by incorporating triple active bridge (TAB) converter, bidirectional dc-dc converter for EV interface, dc-dc unidirectional converter for PV port, and ac-dc bidirectional converter in the grid side. One major benefit of this configuration is that it can be extended to N different dc buses through a multi-winding transformer and thereby, integration of various dc sources is done reliably. Despite the inherent soft switching offered by the TAB converter, other power stages suffer from hard switching significantly while delivering high power. In [185], a four-port converter has been proposed that integrates PV, EV, energy storage, and ac grid aiming at achieving high-power density and compact design with the sacrifice of galvanic isolation. Three sub-converters within the main four-port converter are connected via a dc bus. The dc-dc power stage for EV port is unidirectional and so, V2G operation is not feasible here. In study [186], authors have proposed a three-port converter for dc/dc/dc system considering both single-phase and three-phase ac ports. The total number of switches for single and three-phase three-port converter are four and six respectively. In both configurations, i.e., two legs like an H bridge or three legs like the conventional three-phase inverter, each leg can be used as an inverter and as a buck-boost converter simultaneously. The power flow between the ac port and dc port-1 is based on conventional full-bridge topology, whereas, the converter acts as a buck-boost converter between dc port-1 and dc port-2. Simplicity in design, higher power density, bidirectionality in all ports, and modularity make it an appropriate multiport converter for EV charging applications. The power flow modes among the three ports are managed by developing multivariable control method such as finite control set model predictive control. However, hard switching and non-isolation among ports are the major disadvantages. Further, in article [187], an EV station has been proposed based on 100kW three-phase four-port converter integrating PV, energy storage, EV, and ac grid. Unlike several power converters connecting to a common dc bus, this architecture offers lower power conversion stages and so, the number of electrical components is highly reduced. Power converter

TABLE 8. Summary of existing multiport EV chargers.

Ref.	No. of Ports and Interface	Topology	Power (kW)	Power Flow Modes/ Peak efficiency	Advantages	Disadvantages
[183]	3 Ports: PV, 3-phase AC grid, EV	Interleaved Boost (PV), 3-phase VSC (grid), Interleaved Flyback (EV)	10	PV→EV(95.2%), PV→grid(96.4%), grid→EV(95.4%), EV→grid(95.4%)	Electrical isolation, V2G operation, higher partial and peak load efficiency, high power density, quasi resonant soft switching (Flyback), modular (Scaling up to 100kW).	Hard switching (Interleaved Boost, 3-phase VSC), no SoC Control, sophisticated control for sub converters, reliability issues due to series connection between EV and PV, No usage of energy storage.
[184]	4 Ports: PV, AC grid, EV, Energy Storage	Triple Active Bridge, Boost (PV), Bidirectional DC-DC (Energy Storage, EV)	–	PV→EV, PV→grid, grid→EV, EV→grid, PV→ES, ES→grid, ES→EV, grid→ES	Electrical isolation, V2G operation, soft switching (TAB), modular, supports wide variety of dc sources through multi-winding transformer.	Hard switching (Boost), absence of detailed analysis on control, transformer design is challenging for high power flow.
[185]	4 Ports: PV, AC grid, EV, Energy Storage	Full-Bridge, Boost	16	PV→EV, ES→EV, PV→ES, grid→EV, PV→grid	Compact and simple design, high power density, simple control.	No electrical isolation, hard switching for all modes of power flow, V2G is not possible, no state of charge (SoC) control.
[186]	3 Ports: PV, AC grid, EV	Conventional Full-Bridge (AC port and DC port), Buck-Boost (among DC ports)	3	PV→EV, PV→grid, grid→EV, EV→grid (95.94%)	Low cost, simple design and control, high power density, only 4 & 6 switches in single-phase and three-phase configuration respectively, modular, scaled up to high power, V2G operation.	No electrical isolation, hard switching for all power flow modes, no usage of energy storage
[187]	4 Ports: PV, AC grid, EV, Energy Storage	Similar to Full-Bridge (AC grid), External Buck (EV side)	100	PV→EV, PV→grid, grid→EV, PV→ES, ES→grid, ES→EV, grid→ES	Suitable for high power and fast charging, usage of energy storage, simple and effective control, low THD, high power factor.	No electrical isolation, hard switching, No V2G operation, reliability issues due to series connection between EV and energy storage.
[188]	3 Ports: AC grid, Energy Storage, EV	Cascaded H-bridge, Dual half-bridge	–	grid→EV, grid→ES, ES→grid, Static Synchronous Compensator Mode	Modular, ultra-fast charging, Low THD, isolation, soft switching over wide range, very low charging current ripple, SoC self -balancing.	No V2G operation, renewable energy sources are not considered.
[189]	3 Ports: DC source, (after AC-DC rectifier), EV, EV/Energy Storage	Triple Active Bridge, Dual Active Bridge, Series Resonant	5	grid→EV-1, grid→EV-2/ES, ES→grid, grid→EV-1 & EV-2/ES (Simultaneously) 98.2%	Low cost, electrical isolation, modular, soft switching over wide range, multiple EV charging, high power density, high efficiency.	No V2G operation for fast charging, renewable energy source is not considered, transformer design is challenging for high power flow.
[190]	3 Ports: DC source, (after AC-DC rectifier), EV-1, EV-2	Triple Active Bridge	50	grid→EV-1, grid→EV-2, EV-1→grid, EV-2→grid	Low cost, modular, inherent soft switching, electrical isolation, high power density.	No usage of energy storage, renewable energy sources are not considered, V2G is not possible.
[191]	3 Ports: AC grid, PV, EV	Dual Active Bridge, Interleaved Boost	0.2	grid→EV, (96%) EV→grid, (96%) PV→EV, (96.5%) PV→grid, (95.5%)	High power density, electrical isolation, soft switching, modular, simple control, scaled up to high power.	No usage of external ES, boost inductors suffer from significant losses, large output filter is needed to keep THD low.
[192]	3 Ports: AC grid, PV, EV	Full-Bridge (AC), Half Bridge (PV, EV)	3.5	grid→EV, PV→grid, EV→grid, PV→EV	Simplicity in design, bidirectionality, high power density, low THD, unitary power factor, low cost.	No electrical isolation, no usage of energy storage, hard switching.

connected in ac port exchanges power with utility grid while maintaining low THD and high-power factor. EV port is connected through an external buck converter that supports unidirectional power flow and therefore, V2G is not possible here. In addition, the architecture employs a series power conversion structure from EV port to energy storage,

contributing to single point of failure and thereupon, the reliable operation becomes an issue. Furthermore, an EV ultra-fast charging station based on CHB converter for medium voltage grid is proposed [188]. The cost and weight of the low frequency transformer for medium voltage grid can be saved by using CHB converter, as THD becomes low. The charging station is constituted by CHB converter, split energy storage, and medium frequency transformer-based dual half-bridge dc-dc converter. Dual half-bridge converter offers isolation, better control capabilities, bidirectionality, and soft switching over a wide operating range. This modular architecture is capable of handling high power and charging multiple EVs at the same time. The key demerit lies in the absence of renewable energy port. The work in [189], illustrates a three-port converter that performs the task of dc-dc power stage in EV charger. The three-port converter comprises DAB converter and series resonant converter for slow and fast charging respectively. On the port-2 side, the series resonant tank is followed by full-bridge rectifier, whereas, on the port-3, there is only an active bridge rectifier for slow charging. EV battery or energy storage can be connected in port-3, while only EVs are connected on port-2. The three ports are coupled by a three-winding transformer that offers isolation and turns ratios for different voltage levels. This architecture improves power density and lowers component cost. Also, high power can be delivered due to modularity while charging multiple EVs simultaneously. To reduce switching loss in the input active bridge and transformer RMS current, a control method using phase shift and frequency modulation has been developed. One disadvantage of the converter is that port-2 is unidirectional which disables V2G operation during fast charging. In [190], a similar converter structure is proposed as a dc-dc power stage except for the port-2 side. The converter looks like a TAB converter where the secondary side is connected to the primary side through a multi- winding transformer. Isolation, bidirectionality in all ports, high efficiency, and better control capabilities are the main advantages. However, these three-port converters in [188]–[190] neglect the inclusion of PV as a power source. An interleaved boost and DAB-based novel single-stage three-port converter has been proposed in [191] for the dc-dc-ac system. Between the dc and ac port, the converter works based on DAB topology, while between the dc ports, the main topology is interleaved boost. SPWM modulation along with DPS modulation is used here which requires neither optimization nor complex control. The total number of switches is eight and ac output is achievable through modulation without any additional stage on the secondary side. Although soft switching is preserved inherently in DAB, hard switching is common for interleaved boost converter. In [192], a 3.5 kW three-port converter consisting of full-bridge rectifier in ac grid and two half-bridge dc-dc converters in EV and PV side is demonstrated. Simple design and control, bidirectionality in ac port, low THD, and unitary power factor are the advantages, whereas, absence of electrical isolation and hard switching are the impediments for utilizing it as an EV charger practically. A summary of the reviewed multiport EV chargers has been presented in Table 8.

VII. CONTROL METHODS FOR AC–DC RECTIFIERS

The main control goals for the ac-dc power stage include power factor correction, drawing sinusoidal input current, and regulation of dc link voltage. In this section, control methods of the previously mentioned topologies in ac-dc rectification are studied extensively. Our review here is mainly focused on fulfilling control objectives for EV charging. Also, a comparison of the various control methods used for different ac-dc rectifiers is provided in Table 9 and Table 10.

A. CONTROL OF THREE-PHASE BUCK AND SWISS RECTIFIER

The present Swiss Rectifier (SR) utilizes a double loop PWM control scheme that includes dc link voltage and current control loop. In addition, a feed-forward control loop is incorporated to directly generate input current forming voltage [48], [58]. The switching signals of SR are generated based on the modulation ratio and phase information. Analogously, in [61], a feedback PWM control is described for five-level three-phase buck rectifiers to regulate dc link voltage and ac currents. The overall control architecture consists of three control loops, i.e., a slow outer control loop for regulating dc link voltage and two fast inner current control loops for generating dc link voltage references which are eventually used to determine the relative on-time of the active switches. This control method is capable of achieving uniform distribution of current in the dc link inductors. The abovementioned PWM control strategies lead to duty cycle loss and hence, modulation ratio is automatically increased. As a consequence, input current distortion is not minimized. The control method introduced in [62], not only employs dual-loop control as discussed earlier but also mitigates the detrimental impacts of duty cycle loss by incorporating phase shift angle compensation into the closed-loop control according to adaptive algorithm as shown in Fig. 9.

B. CONTROL OF VIENNA RECTIFIER

Several control methods of VR have been employed in the literature for EV charging applications such as hybrid linear-nonlinear control [193], mixed-signal based control [194], model predictive control [195], synergetic vector control [67], and voltage oriented control [196] in order to fulfill certain objectives; for instance, PFC control, neutral point voltage balancing, current tracking under disturbances, reduction of dc link voltage ripple, mitigation of THD in the input current, attaining unity power factor, and reducing the losses. The comprehensive control structure of VR as an EV charger contains three necessary functional blocks such as output current control, grid current control, and dc link voltage control as depicted in Fig. 10 [67]. The output current control block having the lowest bandwidth sets output current

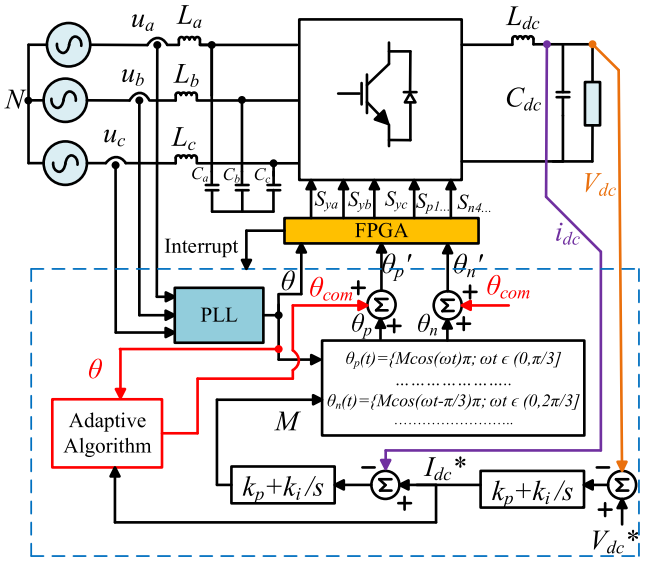

FIGURE 9. Control scheme of a three-phase Swiss rectifier.

reference and determines input conductance of the rectifier by measuring the output voltage. Reference phase currents are compared with the measured phase current in grid current control block, resulting in generating the references of ac input voltage. Finally, dc link voltage control is utilized to regulate dc link voltage and load current. Interaction of these three functional blocks leads to the generation of three-level duty cycle that fulfills the overall control objectives.

C. CONTROL OF THREE-PHASE BOOST RECTIFIER

Several current control strategies can be applied on TPSSBR to attain high quality input currents [197]. Direct current control methods provide better performance in comparison with direct power control methods due to disturbances and voltage spikes from the grid [198]. Average current control scheme is one kind of direct current control method for digital implementation [199]. TPSSBR can also be controlled using simple hysteresis control [200]. However, this method yields variable switching frequency and hence, EMI filter design becomes difficult. In study [77], a control strategy has been developed that minimizes the input current harmonics by adding a common mode duty ratio term to the feedback controller's output. In addition, the method does not require ac voltage sensors and hence, cost is reduced. Input voltages are estimated through mathematical modeling of dc-link voltage ripple, PWM states, and phase currents. As mentioned before, under unbalanced operating conditions, harmonics appear at the dc-link voltage. An analytical expression of instantaneous power at the dc link side has been derived in [79] that suggests a link between second-order harmonic term and dc-link voltage ripple under unbalanced voltage supply. A PI cascaded control strategy has been implemented to remove the harmonic component and maintain constant dc-link voltage. Besides, the developed control keeps the power factor close to unity under unbalanced voltage supply conditions. In [78], a control scheme of two parallel TPSSBRs for high power operation is discussed. Average model of the parallel converters has been developed and then, zero-sequence dynamics have been predicted. A zero-sequence current control loop is designed to reduce the circulating current generated by the parallel operation. The average current control can be implemented on TPSSBR based on six-step PWM and three-step PWM methods. In six-step PWM method, line cycle of input phase voltages is split into six 60° segments in such a way that none of the three phase voltages alter their signs on that segment. In contrast, for three-step PWM method, line cycle of input voltages is divided into three 120° segments and one phase voltage must be greater or smaller than the other two phase voltage on that segment. The authors in [76] have provided a comparison between these two PWM methods for TPSSBR and it has been found that three-step PWM displays lower THD and higher power factor compared to six-step PWM method. A space vector control architecture based on d-q transformation for TPSSBR is exhibited in Fig. 11. Implementation of this control method ensures power factor correction, drawing sinusoidal input current, and regulating dc-link voltage. AC quantities are transformed into d-q domain which leads to negligible tracking error while using the PI controllers. Three PI controllers are utilized to control current components (i_d, i_q) and dc-link voltage. Current control is achieved using inner current control loop and dc link voltage is regulated by outer voltage control loop. To achieve the unit power factor, reference q axis current, i_q^* is set to zero. In [201], a start-up process for TPSSBR is discussed in detail which guarantees that inrush currents do not go beyond the specified limit. In addition, dc-link voltage increases gradually to its reference value and does not show any overshoot. Initially, all the switches are off and at this moment, bulk capacitor is pre-charged through antiparallel diodes and inrush limiting resistors. When the boost operation of the switches is enabled, a duty cycle soft start control is implemented to restrict the inrush current with overcurrent protection level.

D. CONTROL OF MULTILEVEL AC–DC CONVERTER

1) CONTROL OF FLYING CAPACITOR MULTILEVEL AC–DC CONVERTER

For FCMLC, capacitor voltage balancing is a prime control task to perform; otherwise, voltage stress across the switches will be increased, requiring high-rated switches. Valley current mode control- a sort of current limit control, is used to balance the capacitor voltage [203]. Based on capacitor voltage states, a set of essential conditions is developed to ensure the balance of median capacitor voltage levels. Undamped dynamics of FCMLC capacitor voltage states are considered, as they represent the worst-case scenario of voltage balancing. However, this method doesn't work well at light load condition. To cover both heavy and light load condition, constant effective duty cycle compensation

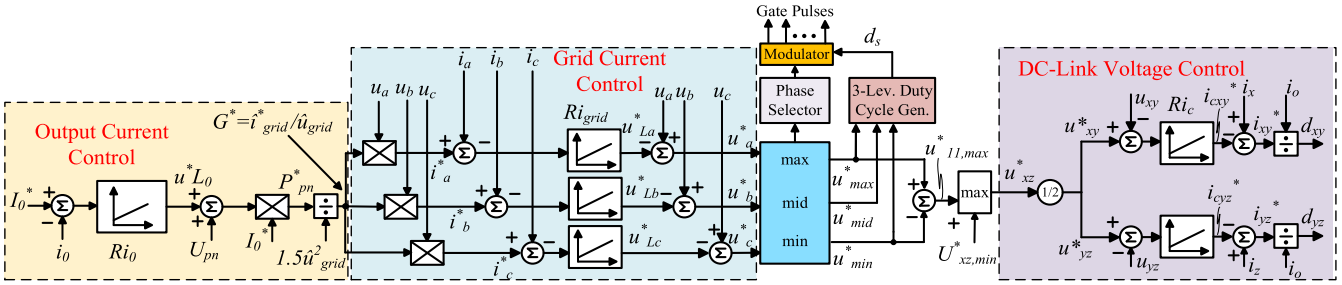

FIGURE 10. Control structure of a three-phase vienna rectifier including output current control, grid current control, and dc link voltage control blocks.

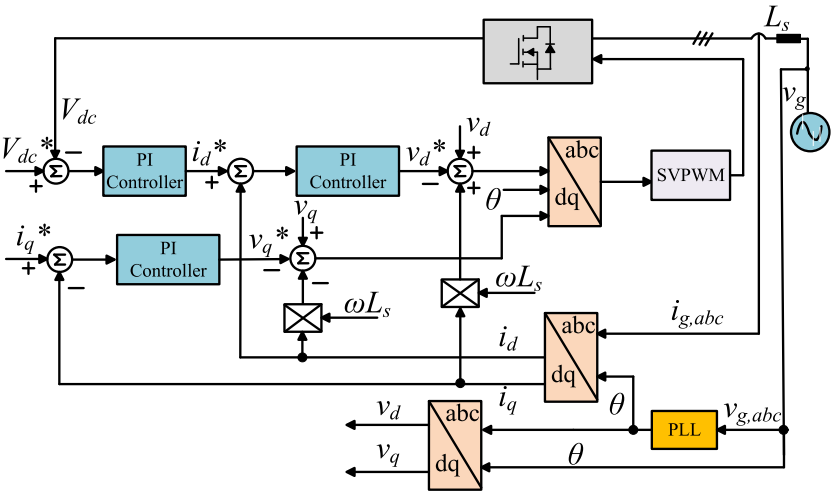

FIGURE 11. Control method of a three-phase boost rectifier based on d-q axis transformation.

is implemented [110]. The main control principle is about adjusting the duty cycles and the phase shifts of switching signals so that capacitor charging and discharging become independent of load. After sampling and averaging the valley current, the farthest current value from the average value is determined. Difference from the average current is considered as an error and later used to adjust the duty cycle and the phase shift. In [97], a start-up controller is developed for the modular FCMLC converter to avoid inrush current during pre-charging of floating capacitors. Further, inner current loop controls the charging current, whereas, outer voltage loop regulates the average dc voltage. Furthermore, the feedforward loop, the reference voltages, and currents are generated by the PI controller and so, equal charging of the submodule's outer capacitors is ensured. FCMLC necessitates smaller filter inductors due to its high operating frequency. This poses challenges in PFC control, as current phase leading is larger. To overcome this issue, a PFC control method similar to conventional multiloop control is developed as shown in Fig. 12 [104]. Achieving unit power factor and low THD in input current depends on producing in-phase current reference, $i*$ for the inner control loop. A PLL based on adaptive notch filter is developed to confirm that input current and voltage phase match very well. The inner current loop generates duty ratio which in turn guarantees that the average inductor current tracks $i*$ properly. By scaling the magnitude of the input current, the outer voltage loop regulates the dc-link voltage. PI controller is used as a compensator for the voltage loop gain. The crossover frequency should be selected in a way such that dc-link voltage ripple at twice line frequency is attenuated. Finally, the feedforward control term is added to the duty ratio to predict the disturbance from the rectified sine wave and thus, its impact is neutralized. Moreover, in [106], similar PFC control is adopted for the interleaved FCMLC converter that performs additional control tasks considering equal current sharing between the interleaved stages.

2) CONTROL OF CASCADED H-BRIDGE MULTILEVEL AC–DC CONVERTER

The control objectives of the CHB multilevel converter mainly consist of active and reactive power control on the grid side, minimization of grid impact caused by unbalanced load condition, balancing of capacitor voltages in CHB submodules, and facilitating charging and discharging for the dc-dc stage. The work reported in [89], presents a control technique with SVPWM regarding voltage control on the grid side. Capacitor voltage balancing is also accomplished

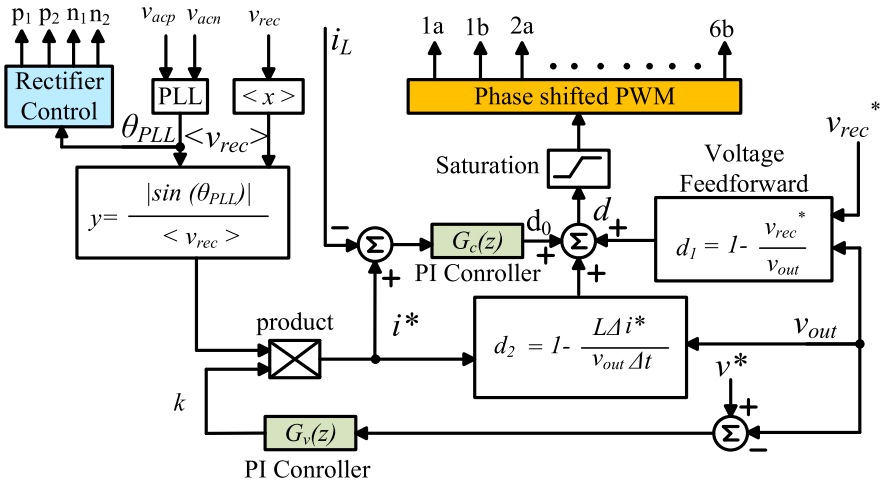

FIGURE 12. Control scheme of a 7-level flying capacitor multilevel converter.

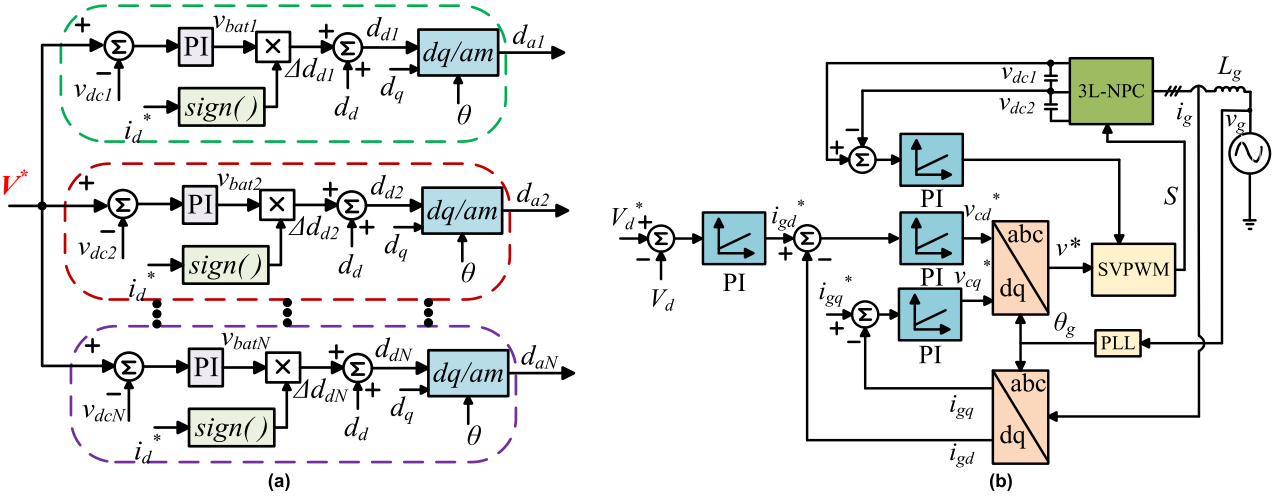

FIGURE 13. (a) Control method of a modular multilevel converter based on cascaded H-bridge structure. (b) Voltage-oriented control of a 3-level neutral point clamped multilevel converter.

with the implementation of this method. In [204], authors have adopted a voltage-oriented control as a conventional grid connection solution to balance the dc link capacitors. The control structure is formed by the combination of cascaded control loop, synchronous frame transformation, and PLL. The outer control loop regulates the dc-link voltage which is adjusted by the requirement of active power of the system. Additionally, inner loop controls d-q axis current components and then, reference voltages are modulated with phase-shifted PWM. Likewise, a d-q control is designed in [86], which sets active current reference and reactive current reference for dc-link voltage regulation and unity power factor. SPWM is used here for switching pulse generation. Similar active and reactive power control has been developed that features independent control of i_d and i_q [87]. In [98], a single-phase d-q decoupled controller is used to control the power factor and regulate individual dc voltages of the CHB converter. By applying grid voltage-oriented method, active and reactive power can be decoupled. Active and reactive power references are set and thereby, reactive power is compensated at the grid side. Also, a unified control method to balance the CHB dc voltages is shown in Fig. 13(a). which works in both charging and discharging modes of the EV battery. If reference current, i_d^* is negative, the power flow occurs from EV to grid while positive i_d^* specifies power direction from grid to EV. During charging, Δd_{d1} will decrease to make modulation index, M_1 smaller and thus, the disturbance will be rejected. Conversely, while battery is being discharged, with this control method, Δd_{d1} will increase to make M_1 larger and so, the disturbance is suppressed, as dc bus voltage is also increased.

3) CONTROL OF NEUTRAL POINT CLAMPED MULTILEVEL AC–DC CONVERTER

For controlling the NPC multilevel converter, similar approaches as CHB dc link voltage control can be employed.

TABLE 9. Summary of existing control methods for AC-DC rectifiers in EV chargers.

Topology	Ref.	Controller type	Objectives	Sensor Signal	Control Variable	Features
Swiss Rectifier	[48], [58]	Feedback PWM control based on output voltage controller and output current controller	To perform EV battery charging	u_{pn}, I_{dc}, $u_{D\bar{a}x,p}$, $u_{Dz\bar{a},n}$	Duty cycle	Performs single-stage EV charging with high power factor and low THD, simple control, dual loop control: voltage and current control loop regulate battery voltage and current respectively, feedforward loop facilitates generating input current forming voltage.
	[62]	Dual control loop: output direct voltage and current control including phase shift angle compensation	To minimize low order harmonics caused by duty cycle loss	u_{dc}, I_{dc}, u_a, u_b, u_c	Duty cycle	Output voltage and current control loop can regulate battery voltage and current respectively, utilizes PLL block to generate synchronized phase angle, utilization of FPGA and DSP board makes it expensive.
Vienna Rectifier	[67]	Synergetic control utilizing both power stages: output current control, grid current control and dc link voltage control	To regulate dc link voltage and reduce input current harmonics	u_a, u_b, u_c, i_a, i_b, i_c, V_{dc}, I_{bat}, V_{bat},	Duty cycle	Cascaded method consisting of three essential functional blocks controls battery current, grid current, and dc-link voltage, utilizes phase selector block to generate duty cycle, three control loops can interact with each other, capable of varying the dc link voltage with six times the mains frequency.
	[196]	Voltage-oriented control including current control (2-PI controller) and voltage control (1-PI controller)	To reduce THD in input current, maintain unitary power factor and reduce output voltage ripple	u_a, u_b, u_c, V_{dc}, i_a, i_b, i_c	Duty cycle	Provides good steady state performance and fast dynamic response, reduces output voltage ripple, control structure is simple, performs CC-CV charging, utilizes positive and negative synchronous reference frames, minimizes input disturbance.
	[195]	Moving average based finite set model predictive control	To track input current according to reference current so that THD can be reduced	u_a, u_b, u_c, V_{dc}, i_a, i_b, i_c	Duty cycle	Does not require the values of converter nonidealities, free of control loop or sensor circuit, handles constraints very well, minimizes tracking error, improves current quality.
Three Phase Six Switch Boost Rectifier	[79]	Cascaded PI control	To remove harmonics from dc link voltage & keep high power factor under unbalanced ac system	u_a, u_b, V_{dc}, i_a, i_b	Duty cycle	Less sensors are required, power factor is close to unity under unbalanced ac condition, utilizes *d-q* synchronous frame current regulator.
	[77]	Outer voltage control loop and inner current control loop with common mode duty ratio injection	To reduce THD in input current, maintain unitary power factor, track dc link voltage	V_{dc}, i_a, i_b	Duty cycle	Eliminates two input voltage sensors, estimates input voltages, addresses the existence of floating potential between source neutral and dc-link negative terminal, control is not affected by source disturbance.
	[78]	Zero sequence current control for parallel TPSSBR	To eliminate the circulating current from parallel TPSSBR	u_{a1}, u_{b1}, i_{a1}, i_{b1}	Duty cycle	Develops average models of the parallel converters, zero sequence current control strategy is built for individual converter to facilitate modular design.
	[202]	Outer voltage control loop, voltage feedforward, inner current control loop	To improve THD of input current, regulate dc link voltage	u_a, u_b, u_c, V_{dc}, i_a, i_b, i_c	Duty cycle	Utilizes duty cycle feedforward and zero sequence signal injection, capable of regulating dc-link voltage for wider input range, current controller is built with both PI and P compensation, P compensation is better in improving output voltage transient.

In study [205], the output control loop regulates dc-link voltage and the inner current loop addresses the dc side voltage imbalance. On top of this, feedforward compensation is adopted to minimize dynamic coupling between the grid and NPC ac-dc converter. In bipolar dc bus architecture, voltage-oriented control has three main blocks, namely, *dq* to *abc* transformation block, PLL and PI controller blocks for the regulation of NPC as shown in Fig. 13(b). Besides, a voltage balance circuit controller is required to extend the bipolar NPC operation for the entire load range. The fundamental idea of this control is to generate reference balancing current which is minimal to keep the system balanced [113]. Further, in [116], another voltage balance control with an extended controllable region has been proposed that eliminates the requirement of voltage balance circuit in bipolar bus NPC structure. To implement the control, three different coordination rules are followed: 1) if the fast charger (dc-dc) is not working, NPC multilevel converter is responsible for voltage balance control; 2) when the fast chargers are operating and unbalanced power ratio

TABLE 10. Summary of control methods for AC-DC multilevel converters in EV chargers.

Topology	Ref.	Controller type	Objectives	Sensor Signal	Control Variable	Features
Cascaded H-Bridge (CHB) Multilevel AC-DC Converter	[98]	Single-phase *d-q* coupled control based on PI controller including voltage balancing scheme	To maintain high power factor, regulate individual dc voltages, balance capacitor voltages	v_g, i_g	Duty cycle, phase shift	Active and reactive power control is decoupled, PI controller tracks the reference accurately, supports active/reactive power in V2G mode, voltage balancing control works in both charging and discharging of the EV battery.
	[86]	*d-q* control including PI controller and PLL	To control power factor and regulate dc link voltage	v_g, i_g, V_{dc}	Duty cycle, phase shift	Simple control implementation, low cost, PLL is used to achieve the phase angle of grid voltage, voltage balancing is accomplished, power factor is high.
Neutral Point Clamped (NPC) Multilevel AC-DC Converter	[113]	Voltage-oriented control based on PI controller and PLL.	To maintain high power factor, regulate input current and balance the voltage	v_g, i_g, V_{d1}, V_{d2}	Duty cycle (SVPWM)	Supports bipolar dc bus structure, space vector pulse width modulation (SVPWM) is utilized, PI controller adjusts the dc link voltage, voltage balancing is achieved, PI controller regulates the input current of voltage balancing circuit.
	[206]	Average current mode control comprising differential voltage loop, current loop, and dc link voltage loop	To keep high power factor, reduce THD, regulate dc link voltage, and balance capacitor voltages	v_g, i_g, V_{dc}	Duty Cycle	Current loop makes input current to become sinusoidal, external dc-link voltage loop regulates V_{dc}, differential voltage loop balances capacitor voltages, unsophisticated control, requires transfer function development.
Flying Capacitor Multilevel AC-DC Converter (FCMLC)	[106], [104]	Interleaved [102] PFC control based on voltage, current compensator, and partial feedforward term	To keep high power factor, reduce THD, regulate dc link voltage	V_g, V_{dc}, i_{L1}, i_{L2}, V_{rec}	Duty cycle, phase shift	Feedforward term solves the problem of input current phase leading caused by small inductor, equal current sharing in each leg of the inductor is accomplished [106], dc link voltage is adjusted according to EV battery, enables bidirectional power flow modes.

falls into the controllable region, dc-dc power stage controls voltage balancing; 3) if the fast chargers are working and unbalanced power ratio is not limited to controllable region, both dc-dc converter and NPC multilevel ac-dc converter perform voltage balancing task. This control strategy is built on three separate sections, i.e., constant current and constant voltage charging method, voltage balance control of dc-dc stage and NPC, and voltage-oriented control. Reference current and voltage for charging process are set according to EV battery charging profile and converter output current is regulated by PI controller. Voltage-oriented control is conventional and at the end, it generates modulation vector and angle for SVPWM. Further, in [206], an average current mode control is presented for three-level stacked NPC converter to achieve high power factor and bidirectional power flow. The objectives of the three control loops are summarized: maintaining high power factor, minimization of THD, regulating dc-link voltage, and the output filter capacitor voltage balancing. Internal current loop takes care of the power factor issue, external voltage loop is responsible for dc-link voltage regulation and finally, differential voltage loop keeps the voltages of the output capacitors balanced.

VIII. CONTROL METHODS FOR DC–DC CONVERTERS

In this section, control strategies of the aforementioned topologies for the dc-dc power stages are discussed. Although the converters have a wide range of available control methods for several applications, we will limit our review here to the control techniques of EV chargers only. The key control tasks include regulating the battery voltage and supervising battery charging and discharging. Summaries of the control methods for different isolated and non-isolated dc-dc converters in terms of controller type, sensor signal, control input, and features are presented in Table 11 and Table 12 respectively.

A. CONTROL OF LLC RESONANT CONVERTER

There are a few control objectives that need to be fulfilled while implementing an *LLC* converter with superior performance. Light load efficiency improvement is one of the pivotal control targets to accomplish for EV charging. From the characteristic curve of the *LLC* converter, it is noticeable that, while delivering power to light load, converter switching frequency requires to be increased, resulting in poor efficiency [123]. Burst mode control with constant burst-on time and optimal switching pattern based on optimal trajectory control can be employed to improve light load efficiency [207]. When the load changes, burst-off time is modulated, but the burst-on time remains the same to keep the battery voltage ripple very low. PWM and pulse frequency modulation (PFM) based hybrid modulation is also used to deal with this issue. PFM is activated for heavy load, and then, it is switched to PWM during light load condition. With the

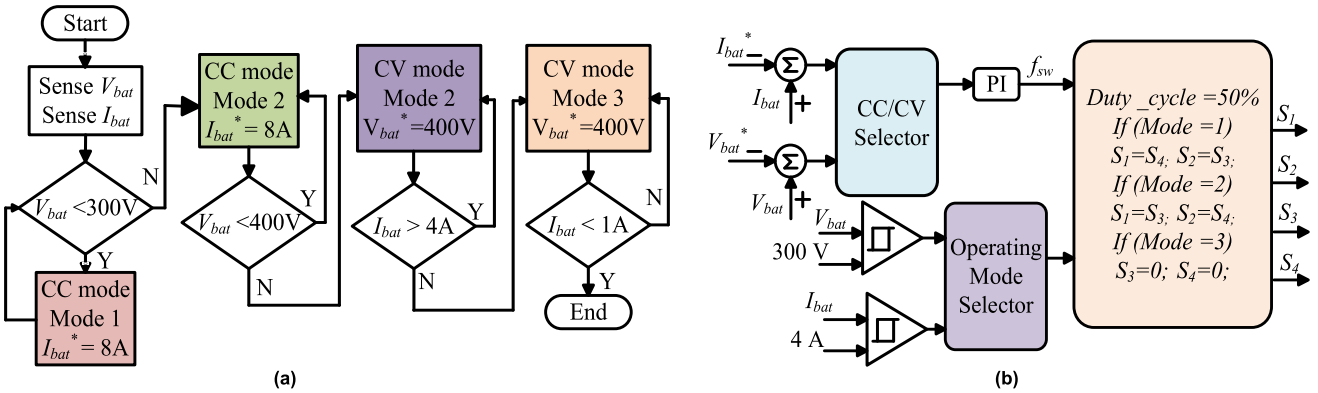

FIGURE 14. (a) Control strategy of EV battery charging with LLC converter. (a) Algorithm for charging mode selection. (b) Implementation of CC/CV charging.

variation of the duty cycle of PWM, the voltage gain of the *LLC* converter can be regulated and hence, ZCS is achieved for the rectifier diodes, improving the efficiency [208]. Moreover, PWM plus PFM hybrid modulation can overcome the PFM resolution limitation issue stemming from high frequency operation while regulating the output voltage.

Operation near resonant frequency, *fr* leads to minimum circulating current as well as ensuring ZVS and ZCS on the primary and secondary switches respectively. Synchronous rectification control method can track *fr* very well [209]. The secondary side current is in phase with the gate driving signal at $fs = fr$, and synchronous rectifier should be turned off as the secondary side current goes to zero for tracking *fr*. Variable dc-link voltage control is another method used in EV charging for the *CLLC* resonant converter to operate near *fr* [126]. The overall control structure is divided into current and voltage control loop which regulates the battery voltage and adjusts dc link voltage respectively [127]. DC link voltage is increased with the battery voltage during charging, whereas, the voltage drops at the time of discharging. The maximum limit of dc link voltage is determined by the power rating of the switching devices and capacitors. On the contrary, minimum dc link voltage limitation is caused by ac-dc front-end rectifier power requirement.

In general, frequency control method can be applied for the *LLC* converter to charge the EV battery. The study in [124], describes a control strategy based on frequency variation for the interleaved *LLC* converter that allows independent mode (converter-1) and simultaneous mode (converter-1 & converter-2) of operation to cover a wide range of voltage (i.e. 50V-420V). The switching frequency is controlled by compensating the error between reference charging current and output current in CC charging mode. Once the battery voltage increases up to its certain set value (i.e. 100V), the converter switches into simultaneous mode from independent mode while being charged by constant current. Later, when the voltage reaches a higher level (i.e. 250V), charging mode switches to CV charging in which the frequency is controlled by compensating error between the reference voltage and battery voltage. Similarly, the converter designed in [125], goes into transition among three modes such as full-bridge converter with frequency modulation, dual-phase half-bridge *LLC*, single-phase half-bridge *LLC* to facilitate CC charging and CV charging. Initially, when the voltage is low, the frequency is higher so that small current can be generated. In that case, the converter may operate in burst mode control if the switching frequency exceeds the limitation. Finally, as the reverse maximum voltage gain of *LLC* converter is unity, a voltage compensation control method is used where dc link voltage is increased so that dc-ac inverter can be grid-tied and hence, V2G operation becomes feasible with *LLC* [129]. A control algorithm to select and implement proper battery charging mode with *LLC* dc-dc converter is demonstrated in Fig. 14.

B. CONTROL OF DUAL ACTIVE BRIDGE CONVERTER

For the implementation of dynamic control of DAB converter, common practices among researchers include small signal modeling and discrete-time average method for multi-phase shift modulation that can capture the dynamics of the system [131], [210]. The dynamic control mechanisms are usually categorized mostly into three types such as power computation-based control, direct inductance current control, and load current feedforward technique [211]. The active power flow between the two bridges for SPS modulation can be written as below,

$$P_o = \frac{V_{in} V_o D(1-D) T_S}{2nL} \tag{1}$$

where, D is the phase shift ratio for SPS modulation, L is the equivalent inductance, n is transformer ratio, and V_{in}, V_o are the input and output voltages respectively. Direct power control strategy can be applied with PI controller of control input D based on mathematical power model, regulating the output voltage well [212]. This method brings significant advantages in a control system where input and output voltage fluctuations are high. Unlike the conventional current mode controller, load current feedforward method improves output transient response of DAB converter under load disturbance without the inclusion of any inner current modulator. For

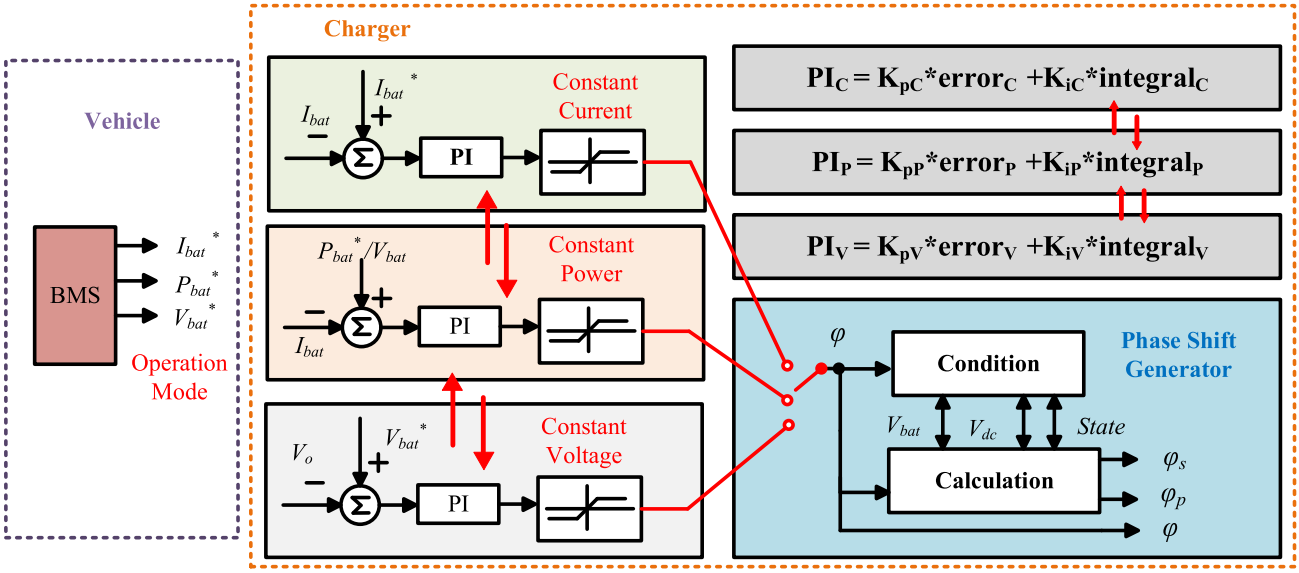

FIGURE 15. Control method of EV battery charging with dual active bridge topology.

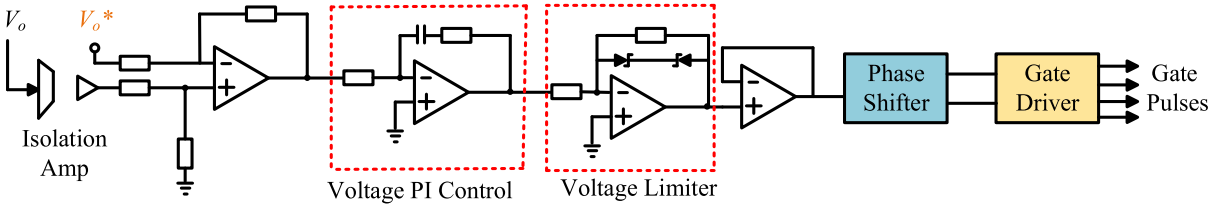

FIGURE 16. Control method for battery voltage regulation with phase-shifted full-bridge converter.

direct inductance current control, inductor current is sensed and with a novel modulation method like asymmetric double side modulation in which D has varying nature, fast transient response is achieved [213].

Although DPS and TPS modulation can extend the ZVS range of DAB, they both incur large turn-off current. Therefore, authors in [132], have utilized a combination of SPS, DPS, and TPS based on optimized operational states to secure ZVS for a wide output voltage and power range with reduced turn-off current. In addition, dead band impact is embedded into ZVS boundary for further extension ranging from 200V to 450V. Prior to connecting to the EV battery, output capacitor of the DAB should be pre-charged at no load condition. The reference voltage of the closed-loop control for charging should be increased slowly until it matches the EV battery voltage. It is worth mentioning that due to the higher dc link voltage (e.g. 800V) compared to the initial output capacitor voltage (e.g. 0V), primary side voltage waveform is a sort of narrow pulse while the secondary side voltage is like a square waveform. This impedes switches from damaging by large leakage inductor current. After the pre-charging process, constant current (CC), constant power (CP), and constant voltage (CV) charging take place sequentially. Each charging mode corresponds to separate operational modes of DAB converter on the basis of switching modulation. As shown in Fig. 15, three PI controllers are used for three charging modes and communications within the controller allow smooth transitions from one operational mode to another [132]. Besides, V2G and G2V transitions are very easy and simple to execute attributable to the symmetrical nature of the structure and waveform of the DAB primary and secondary bridge.

In study [136], operation modes based on minimum transformer RMS current are selected for the three-level DAB converter with blocking capacitors. Generally, DAB converter suffers from conduction and copper losses due to high transformer RMS current. An algorithm is developed considering the mathematical model of normalized active power, phase shift ratio, and normalized transformer current to eliminate five operating modes out of sixteen modes that generate high transformer RMS current.

DC link capacitor between the ac-dc and dc-dc power stage is a key obstacle to achieve high-power density for the EV charger because of the fact that its volume is dependent on the ripple power at the double line frequency while charging the dc current. To address this issue, the concept of sinusoidal charging which allows power ripple at two times the line frequency to the EV battery is utilized so that ripple power

stored in the dc link capacitor can be reduced [214]. The charging current of the battery will be as follows,

$$i_{bat} = \sqrt{2}\, V_{ac} \sin(\omega t) \frac{\sqrt{2} I_{ac} \sin(\omega t)}{V_{bat}} = I_{bat}\,(1 - cos2\omega t) \quad (2)$$

where, I_{bat} is the average charging current and V_{bat} is the EV battery voltage. DAB converter is responsible for the sinusoidal charging while ac-dc stage performs PFC and dc link voltage regulation. Unlike a low bandwidth PI controller, achieving sinusoidal charging requires a high bandwidth control method so that power between the ac grid and the EV battery is balanced. Control input (phase shift ration, D) to output (battery current, i_{bat}) transfer function is obtained after developing the small signal modeling of DAB converter. Low pass filter is used here to attenuate the switching noise. The reference value of i_{bat} is taken from the EV charging profile and phase details are extracted from the PLL.

C. CONTROL OF PHASE-SHIFTED FULL-BRIDGE CONVERTER

Control objectives of a phase-shifted full-bridge (PSFB) converter can be accomplished in a similar manner to DAB converter control. SPS modulation is a very common switching technique when it comes to control the PSFB converter. The output power and voltage can be controlled with the slight change of a phase shift angle. When the charging continues in CC mode, V_{bat} increases linearly with the decrease of the phase shift angle. After reaching up to a certain rated value, CV charging mode is initiated. In CV mode, the output voltage is regulated with the gradual increase of phase shift angle as shown in Fig. 16. Soft switching is achieved with SPS-PWM technique for the entire CC and CV region [155]. However, at light load condition, soft switching is difficult to achieve and the duty cycle is small. As a consequence, circulating loss and switching loss turn out to be significant. The unified control method presented in [215], can be divided into three parts: phase shift control under heavy load, PWM switching control under light load, and PWM switching control with burst mode under no load condition. PWM switching control results in lower circulating loss compared to phase shift control and hence, transition to PWM during light load condition increases efficiency. Switching loss is also reduced by PWM switching control under light load condition but full ZVS range cannot be secured without increasing the resonant inductor value. Further, burst mode at no load condition improves efficiency too. Employing this control under light load condition, efficiency is reported to be increased by 26%. In work [216], another hybrid mode control is adopted to improve efficiency in both heavy load and light load condition. The main idea is to decrease the turns ratio of the transformer and thereby, the circulating current is reduced using only phase shift control. Additionally, applying asymmetrical PWM can provide stability including higher battery voltage if the turns ratio is smaller. Finally, adaptive dead time control

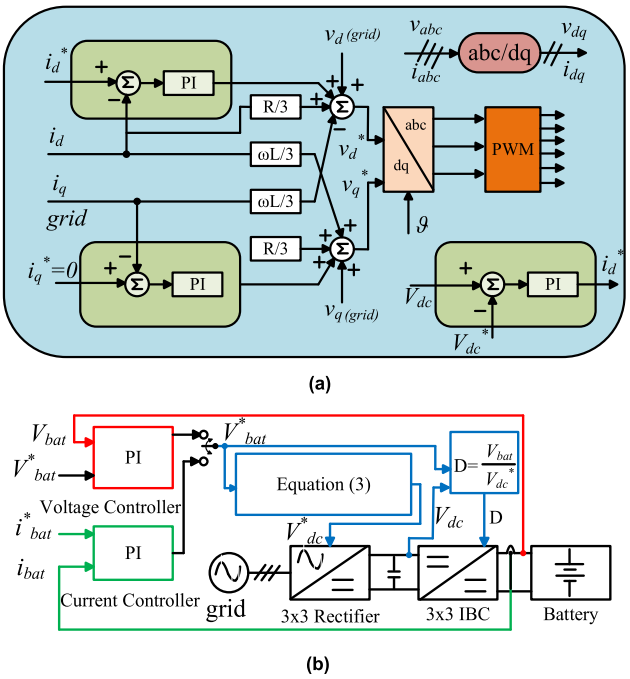

FIGURE 17. Control of EV battery charging with three-phase interleaved charger (a) dc link voltage and grid current control (b) EV battery current and voltage regulation.

is combined with the previously mentioned techniques, developing hybrid control for PSFB to reduce the loss further. Despite the simplicity and popularity of PI controller for PSFB converter, model predictive control (MPC) is highly effective nowadays to deal with multiple physical constraints of the system while optimizing the cost function considering multiple objectives. The study presented in [217], discusses the MPC strategy that uses the system dynamics to transform nonlinear peak inductor current constraint into a dynamic linear constraint. The control objective of this method is to track the battery voltage according to the set values while satisfying several constraints in the system. Authors have also reported better performance by MPC technique compared to PI controller in terms of mean square error while rejecting disturbance. Moreover, common duty ratio control has been designed in [218] for multiple connected PSFB converters to deliver high power. The primary purpose of this control is to ensure equal sharing of the dc link voltage and load current among the connected converters so that circulating losses are minimized and power imbalance does not occur. Small signal average model, as well as steady state dc model have been developed, and Type II compensator is considered as a voltage and current controller.

D. CONTROL OF NON-ISOLATED CONVERTER

Interleaving technique offers many benefits such as high-power flow capability, lower stress on power devices, reduction of current ripple, and possibility of increased switching frequency in EV charger applications. The very common control target of an interleaved converter is to ensure

TABLE 11. Summary of control methods for isolated DC-DC converters in EV chargers.

Topology	Ref.	Controller type	Objectives	Sensor Signal	Control Param.	Features
Resonant Converter: *LLC*	[129]	Voltage gain compensation: dual control loop	Reverse *LLC* operation, voltage gain regulation	V_{bat}, I_{bat}	f_s	Enables V2G for *LLC*, performs pre-charging, CV-CC charging, integrated with adaptive synchronous rectifier driving scheme.
	[125]	PI control with operating mode selection algorithm based on EV charging profile	Operation mode selection and execution based on V_{bat}, I_{bat}	V_{bat}, I_{bat}	f_s	Simple control implementation, performs CV-CC charging by the selection of proper operating mode, enhances efficiency at light load condition.
	[124]	Two PI controllers with operating mode selection algorithm based on EV charging profile	To maintain power flow for CC-CV charging	V_{bat}, I_{bat}	f_s	Simple control, allows interleaving operation, enables extended voltage range for deeply depleted battery, performs CV-CC charging.
Resonant Converter: *CLLC*	[127]	Dual control loop: inner current control and outer voltage control	Regulating I_{bat}, keeping f_s close to f_r, adjusting V_{dc}	V_{bat}, I_{bat}	f_s	Implementation is simple, can be combined with PFC control, allows reverse mode of operation, switching frequency, f_s tracks resonant frequency, f_r despite wide range of EV battery voltage.
	[126]	Dual control loop structure	Eliminating second order harmonic ripple in I_{bat}, following EV charging profile	V_{bat}, I_{bat}	f_s	Performs CV-CC charging, can be combined with PFC control, output current ripple is reduced to increase battery lifetime.
Dual Active Bridge (DAB) Converter	[132]	Three PI controllers for constant current (CC), constant power (CP), and constant voltage (CV) charging mode	To pre-charge and charge battery in G2V mode, control power flow in V2G mode	V_{bat}, I_{bat}	Phase shift angle	Comprises individual PI controller for each mode, e.g., CC, CP, and CV; allows V2G operation, provides pre-charging at no-load condition, integrates SPS, DPS and TPS modulation to extend ZVS range.
	[214]	Closed-loop feedback control to track reference battery current and dc link voltage ripple	To achieve sinusoidal charging, regulate battery current, reduce dc link voltage ripple	V_{bat}, i_{bat}, V_{dc}	Phase shift angle	Dual control loop that achieves sinusoidal charging and reduces dc link voltage ripple respectively, integrated with PFC control, implementation is easy and requires small signal model and transfer function formulation.
	[212]	Virtual direct power control based on PI controller and phase shift ratio estimation	To regulate battery voltage accurately under all working conditions.	V_{bat}, I_{bat}, V_{dc}	Phase shift angle	Unsophisticated feedback control loop, achieves very fast dynamic response, fulfil objectives under all working conditions, i.e., start up, sudden load change, no-load, input voltage fluctuation; no overshoot, not sensitive to parameter variation.
Phase-Shifted Full-Bridge (PSFB) Converter	[155]	Closed loop feedback control based on voltage PI controller	To achieve soft switching for whole range of CC-CV charging process; voltage and power regulation	V_{bat}	Phase shift angle	Low cost implementation, utilizes voltage PI controller, achieves wide range of output power and voltage regulations, adopts SPS PWM modulation, output power can be controlled from full load to no load.
	[215]	Closed loop feedback control incorporating PWM switching and phase shift switching	To increase efficiency in light load condition	V_{bat}, I_{bat}	Phase shift angle, duty cycle	Employs PWM and phase shift switching control, PWM switching control is activated under light load condition to remove circulating loss, phase shift control is activated under heavier load condition to achieve ZVS.
	[217]	Model predictive control using Laguerre Functions	To regulate battery voltage while maintaining non-linear peak input current constraint	V_{bat}, i_L	Duty cycle	Tracks the reference signal efficiently, transforms the nonlinear peak inductor current into the dynamic linear constraints, generates predicted samples based on plant model, computationally efficient, improves switching frequency.

equal current sharing among the phases, avoiding power imbalance and overall efficiency reduction. The control method introduced in [168], provides a wide battery voltage range with ripple-free battery current as shown in Fig. 17. The general equation to determine the dc link reference voltage, V_{dc}^* can be written as follows,

$$V_{dc}^* = \begin{cases} \dfrac{N}{floor(\frac{NV_{bat}^*}{V_{dc,min}})} & V_{bat}^* V_{bat}^* \leq V_{dc,min} \\ V_{bat}^* & V_{bat}^* \geq V_{dc,min} \end{cases} \quad (3)$$

Although there is no contemporary unanimity on the allowable battery current ripple for fast chargers, the best practice is to keep it as minimum as possible for the longevity of the battery life. Two separate PI controllers for voltage and current control purposes have been designed during CV and CC charging. In case of both modes, the controller adapts reference battery voltage, V^*_{bat} which in turn changes duty ratio to track reference battery current and voltage. Battery current is free of ripple for both modes of operation and EV battery voltage range between 200V and 800V can be achieved with the adoption of this method. In study [167], a novel interleaved buck converter is proposed where C_{in1} and C_{in2} are used to equalize the current between the two phases if there exists any duty cycle mismatch. In addition, a simple PI controller has been designed to regulate the battery voltage. The work in [219], presents a decoupling control method including PI controller, where three independent control loops are formulated to track reference battery current and make the circulating current zero. The reference battery current varies according to the oncoming vehicles in the charging station. This control scheme has been developed digitally and experimentally validated in a hardware in loop (HIL) testbed. The study in [220], describes a discrete-time model of the converter followed by the introduction of one primary PID controller and multiple secondary PI controllers which regulate current for each leg of the converter and maintain robustness under load variations. During pre-charging, the current controller guarantees a gradual ramp up of battery current and later, constant current flow increases the battery voltage until the constant voltage mode is initiated. The output battery current control and inductor current sharing problem are addressed separately by average duty cycle control and circulating current control. Moreover, sliding mode control which is very popular in power electronics owing to its robustness with respect to variations in parameters and disturbances is adopted for the eight-phase synchronous buck converter to fulfill goals such as robust output voltage regulation, phase current equalization, and switching frequency regulation [171]. The control scheme is set up as a master and slave configuration where each phase is triggered as the master one. The overall control structure comprises three tasks- a power management algorithm that decides whether the phases should be connected or not based on the power delivery to the load, a rotatory master technique that balances the working of the phases, and a frequency controller that regulates the switching frequency.

IX. GRID IMPACTS

Unplanned installation of fast charging stations and uncontrolled fast charging may pose several critical issues such as peak loading, power quality degradation, reduce reserve margins, grid stability degradation, voltage deviations, economic loss, grid asset loss, overloading, and reliability problems [221]–[239]. A fast charger requires significant amount of power within a short period of time which reshapes the load curve and the situation gets worse if multiple EVs are being charged simultaneously [221]. Therefore, integration of renewable energy sources, smart charging techniques, location planning, and EV scheduling are indeed necessary to supervise the peak demand efficiently [222]–[226]. Various power quality issues such as harmonic distortion, voltage fluctuations, and supra-harmonics appear due to the integration of fast charging stations [227]–[231]. The power electronics system of EV charger is responsible for the harmonic injection to the grid. For ABB Terra 53J charging station, it has been found that the average current THD is around 11% in CC charging mode, whereas, the current THD range lies between 9.3% and 30.7% in CV charging mode [228]. The harmonic analysis is typically done in the frequency range below 2kHz. In case of the fast charging station, as the trend is to increase the frequency to reduce the size of passive components, it may lead to supra-harmonics (2kHz -150kHz) distortions [229]. Supra-harmonics can cause excessive heating, lifetime shortening, malfunctioning of the grid equipment including tripping of residual current devices. Impacts may become more severe for the weak grid which is characterized by low short circuit ratio, low X/R ratio of distribution line, and high impedance [230]. Harmonic distortion and supra-harmonics can be alleviated by the selection and proper design of ac-dc front end rectifier and input filter. Another power quality issue, namely, voltage fluctuations arise due to fast charging of EVs. In study [231], authors have demonstrated that voltage fluctuation increases on the bus increases if the charging power goes up. Voltage deviations beyond specified limit lead to economic penalty. In [232], authors have proposed a charging control method to mitigate voltage fluctuation and light flicker. In article [233], authors have described that distribution network suffers from voltage instability, reliability issues, power losses, and economic losses if EV charging station is placed on weak buses. Grid stability is a major concern if fast charging is not controlled properly. In [234], authors have performed a stability test on IEEE 3-bus system which demonstrates that fast charging station reduces the grid stability. Also, it takes a higher time to settle back into pre-disturbance conditions once the disturbance is removed from the system. Authors in [235], have modeled the fast-charging station in d-q frame and from the analysis, it is apparent that source side and load side parameters of the charging station influence the stability. Additionally, it has been shown in [236] that CC charging pushes the grid closer to the unstable region more in comparison with CV charging. Integration of renewable energy sources and energy storage to the charging station can improve the stability. Grid assets such as transformers and line cables are affected by the integration of fast charging stations [237]–[239]. Fast charging can overload the distribution transformers which may lead to insulation failure [237]. Further, the necessity for installing underground cable, overhead line, and transformer with higher capacity is increased. Furthermore, transformer lifetime is reduced with the increased penetration of the

TABLE 12. Summary of control methods for NON-ISOLATED interleaved DC-DC converters in EV chargers.

Topology	Ref.	Controller type	Objectives	Sensor Signal	Control Variable	Features
Non-isolated Interleaved DC-DC Converter	[219]	Feedback control based on Hardware-in-Loop (HIL) testbed	To control battery current and circulating current	I_{bat}, i_{L1}, i_{L2}, i_{L3}	Duty cycle	Output current control is decoupled from the circulating current control, HIL implementation, includes inductor current sharing control, confirms zero circulating current if inductor parameter changes, computationally efficient.
	[220]	Feedback control based on PI and PID controller	To regulate current flow in each leg of the converter	I_{bat}, i_{L1}, i_{L2}, i_{L3}	Duty Cycle	Maintains CC-CV charging, small signal model development is required, digital controller implementation, mitigates the drawbacks of average duty cycle control and circulating current control, simple and precise, addresses total output control and inductor current sharing control.
	[172]	Sliding Mode Control including power management algorithm	To ensure equal current among phases	I_{bat}, V_{bat}, i_{L1}, x_1, ... i_{L8}, x_8,	Duty cycle	Robust output voltage regulation, equalization of the phase current, frequency regulation, utilizes two current sensors in each leg, power management algorithm increases the efficiency, adopts master-slave control architecture.
	[168]	Feedback control based on voltage and current PI controller	To performs CC-CV charging with ripple free current	I_{bat}, V_{bat}, V_{dc}	Duty cycle	Simple and low-cost implementation, can be combined with PFC control stage, adjusts V_{dc} according to V_{bat}, zero output ripple current for entire output voltage range.

EVs [238]. Several smart charging strategies have been proposed to mitigate the impact of the EV fast charging on the transformer aging, loss, and overloading [240]–[242]. V2G is an emerging technology that can lessen the negative influences of fast charging and provides various merits such as active power regulation, reactive power support, grid stability improvement, current harmonics minimization, peak load shaving, reliability improvement, frequency and voltage regulation, and support to renewable energy sources [243].

X. SUMMARY

In this section, the overall synthesis of the fast charging station architecture and the power converter topologies for the ac-dc and dc-dc power stage is presented. The two common architectures of the EV off-board charging station based on ac and dc connected system have been discussed in this paper. DC connected off-board chargers provide various benefits such as flexible integration of renewable energy sources, reduced number of power conversion stages, higher efficiency, and simple control for the transition between islanding and grid-connected mode. However, power rating of the central ac-dc rectifier is very high. In addition, overall system reliability depends immensely on the central ac-dc rectifier. Complex protection devices are required, and the protection guidelines are not well established for this architecture. In case of V2G operation, the situation becomes worse. On the other hand, although ac connected system has a higher number of power stages and low efficiency, the overall system reliability is improved. Additionally, the power rating of the ac-dc rectifier is comparatively lower. The protection devices are not sophisticated and there are matured protection guidelines and standards available for the ac connected system. Therefore, EV charging station based on ac connected system is preferable. Until now, most of the renowned EV charging facilities such as ABB, Tesla, Porsche adopts ac connected system for their off-board chargers.

For the ac-dc power stage of an EV off-board charger, seven topologies have been discussed exhaustively in the previous sections. Boost-type rectifiers are more suitable for high power applications as the current is lower. In contrast, buck-type rectifiers such as TPBR and SR increase the current which leads to additional challenges and higher cost in the design of the off-board charger. Both TPSSBR and VR step up the voltage at the dc-link and hence, current is decreased. Although TPSSBR provides simplicity, VR has higher power density and lower switching loss. In addition, VR being a three-level topology has lower input current ripple and less voltage stress on the devices compared to the two-level topology of TPSSBR. Multilevel ac-dc converter topologies such as CHB, NPC, and FCMLC feature improved power quality, modularity, and reduced stress on the switches. However, in general, reliability and cost are the major concerns due to the high number of switches and associated driving circuitry. In case of NPC, additional balancing circuit is required, and thermal management is difficult due to unsymmetrical loss distribution. Control of FCMLC is challenging and to be more specific, the situation gets worse in the three-phase configuration of FCMLC with increased levels due to the high number of voltage vectors and computational burden. There are two configurations of VRs (unidirectional and bidirectional) presented in this paper. The bidirectional VR (also known as three-phase three-level T-type rectifier) which utilizes bidirectional switches instead of diodes in the bridge supports V2G operation and provides higher efficiency as well. Therefore, taking several criteria such as efficiency, power density, reliability, bidirectionality, cost, power quality, modularity, and control into consideration, it can be deduced that bidirectional VR is

the most suitable topology for the ac-dc power stage of EV off-board charger.

For the dc-dc power stage, both isolated and non-isolated converters have been reviewed comprehensively that provide modularity, high power operation, high efficiency, high power density, and high reliability. Along with these advantages, *LLC* resonant converter also features soft switching capabilities which facilitate high frequency operation. However, the voltage gain is less than unity in reverse operation which causes difficulties in V2G mode especially when the battery voltage is lower. In addition, as the battery voltage is regulated by frequency, it is very challenging to operate near resonant frequency given that EVs have a very wide range of battery voltage. DAB is another isolated dc-dc topology in which bidirectional operation can be achieved very easily by changing the polarity of the phase shift between input and output bridge switching waveforms. Also, battery voltage is regulated by phase shift rather than frequency. With TPS modulation, DAB converter can achieve soft switching for a very wide range of battery voltage. However, the circulating current generated by the DAB converter operation increases the conduction loss. PSFB converter brings simplicity in control compared to DAB and *LLC* converter. But the efficiency is reduced due to the diodes in the output bridge and the absence of soft switching for a wide range of battery voltage if it is compared with the DAB converter. Further, bidirectional power flow cannot be achieved which is a major drawback. Soft switching range of the DAB converter can be extended by adding a resonant tank in the conventional DAB architecture. This configuration is known as DAB resonant converter which reduces the circulating current and with proper optimization, reactive power can be fully eliminated. Additionally, sinusoidal current flows through the transformer and thereby, conduction loss is less compared to DAB converter where inductor current contains higher-order harmonics leading to high RMS current. Magnetic and leakage inductance of the transformer can be used as a resonant component and hence, the power density is not reduced that much compared to DAB. DAB *CLLC* converter has a symmetrical resonant tank and so, bidirectional operation is accomplished easily. With proper design and modulation strategy, DAB *CLLC* provides better performance compared to other DAB resonant converters and can achieve soft switching for the complete range of EV battery voltage. Based on the comparative discussion regarding isolated dc-dc converter, it can be inferred that DAB *CLLC* is the most attractive choice for the dc-dc power stage of an EV off-board charger. In case of non-isolated dc-dc converter, as the galvanic isolation is performed by low frequency transformer, cost and size of the system are enhanced. The benefit lies in the simple design and control of a non-isolated converter. To exploit the benefit of easy design and hardware implementation including bidirectional power flow control, a three-phase interleaved buck converter is an appropriate choice that provides modularity, high power operation, high efficiency, extremely low output ripple, and low cost.

XI. FUTURE RESEARCH TRENDS

The future research prospects should be directed in such a way so that several barriers to the successful growth and maturity of the EV industry can be dealt with systematically and efficiently. Ultra-fast charging station development can provide the EV users a fueling experience by charging the EV battery within 10-15 minutes. This necessitates exhaustive research in charging cable, cooling method, protection devices, efficient power converter design with wide band-gap semiconductor devices to handle high power, solid-state transformers, integration of PV, and energy storage. The partial power converters are gaining interest for EV fast charging that process only a fraction of the full power available [244]–[246]. This design reduces size and cost while increasing the efficiency of the system. Utilization of well-suited topologies for EV fast charging in partial power processing framework can be investigated in the upcoming days. Besides, the research trend is heading towards wireless charging which can be categorized as inductive power transfer, magnetic power transfer, and capacitive power transfer [247], [248]. Vehicle to grid (V2G) and vehicle to home (V2H) technology are not still matured yet. Further, research and development in wireless V2G operation are essential. Although grid following control methods such as droop control, real and reactive control are well established in the literature, grid forming control for the charging station equipped with renewable energy sources or for V2H operation, is an emerging topic [249]–[255]. Rapid discharging during V2G operation causes negative impacts on the battery health. Attention should be given to the development of solid-state battery, cell and pack design, battery management system, and electrolyte/electrode stability [256]. With the exponential expansion of EV charging stations, environment compatibility is a big concern which creates research needs in heat dissipation, noise mitigation, and shielding against EMI of the charging station. Also, the grid must be capable of delivering a huge amount of power to the increased EVs on the road without causing negative impacts. Smart charging should be implemented in which charging behavior is shaped based on peak demand, renewable source generation, dynamic price, and need of EV owners [257]–[259]. Artificial intelligence-based control algorithms can provide a superior performance when it comes to take a smart decision regarding EV charging load prediction, driving range estimation, and dynamic pricing [260]–[262]. Moreover, cyber security assessment of the charging infrastructure as well as the vehicle is an important factor to consider. Critical data related to the charging system, location, vehicle owner, payment info can be stolen [263]. In addition, accessibility in the remote control of the EV is possible through malicious cyber-attacks. Therefore, research efforts must be made on cyber security, resiliency, reliability, protection of user and grid data against malicious attacks. Although ac charging is available in residential areas at present times, low power dc charging stations will be established at home and workplace in the future. Moreover, charging infrastructure should be

intelligent, digitalized, smart grid compatible, and embedded with the advanced communication system.

XII. CONCLUSION

This paper comprehensively discusses the present status, technical details, and challenges of the power converter topologies and their control methods for the EV off-board chargers. To reduce the charging time significantly, high-power dc fast and ultra-fast off-board chargers are being developed which are located outside the vehicle, unlike on-board chargers. Extensive analysis of ac-dc rectifier and dc-dc converter topologies suitable for fast charging is provided here. Additionally, a comparative investigation of the power converter topologies in terms of various parameters such as power, frequency, voltage range, THD, peak efficiency, switching modulation including merits and demerits has been carried out. Since EVs extract a high amount of power from the grid, a multiport EV charger integrating PV, energy storage, EV, and grid is an attractive solution to reduce the high demand charges during peak hours. A review of the existing three-port and four-port converters used in EV charging is presented in this article. Moreover, control methods of the ac-dc rectifiers and dc-dc converters are thoroughly studied for EV fast charging applications. The common control objectives of the ac-dc rectifiers include reduction of THD, maintaining high power factor, and regulating dc link voltage. The dc-dc converters control techniques mainly aim at facilitating CC-CV charging, regulating battery voltage, enabling V2G operation, and reducing current ripple. Control schemes of multiport EV chargers are at an early stage and require exhaustive research efforts in the future. An overall summary focusing on preferable architecture and power converter topology of the EV fast charging station is provided. Installation of the fast charging station has several impacts on the grid and thus, proper planning, coordination, and control are required. The widespread deployment of EV relies immensely on the efficiency, cost, size, reliability, advanced control algorithm, and functionalities of the converter topologies. Therefore, this paper is a valuable source of information for researchers and engineers intending to design and develop EV off-board dc fast chargers.

REFERENCES

[1] B. Maclnnis and J. A. Krosnick. (Oct. 2020). Climate insights 2020: Electric vehicles. Resources for the Future (RFF). [Online]. Available: https://www.rff.org/publications/reports/climateinsights2020-electric-vehicles

[2] United States Environmental Protection Agency. (Apr. 2021). *Inventory of U.S. Greenhouse Gas Emissions and Sinks*. [Online]. Available: https://www.epa.gov/ghgemissions/inventory-us-greenhouse-gas-emissions-and-sinks

[3] International Energy Agency. (Apr. 2021). *Global EV Outlook*. [Online]. Available: https://iea.blob.core.windows.net/assets/ed5f4484-f556-4110-8c5c-4ede8bcba637/GlobalEVOutlook2021.pdf

[4] C. McKerracher *et al.*, "Electric vehicle outlook 2021," BloombergNEF, London, U.K., Tech. Rep., Aug. 2021. [Online]. Available: https://about.bnef.com/electric-vehicle-outlook/

[5] M. Yilmaz and P. T. Krein, "Review of battery charger topologies, charging power levels, and infrastructure for plug-in electric and hybrid vehicles," *IEEE Trans. Power Electron.*, vol. 28, no. 5, pp. 2151–2169, May 2013.

[6] A. Konig, L. Nicoletti, D. Schroder, S. Wolff, A. Waclaw, and M. Lienkamp, "An overview of parameter and cost for battery electric vehicles," *World Electr. Vehicle J.*, vol. 12, no. 21, pp. 1–29, Feb. 2021.

[7] (Dec. 2020). *Battery Pack Prices Cited Below $100/kWh for the First Time in 2020, While Market Average Sits at $137/kWh*. [Online]. Available: https://about.bnef.com/blog/battery-pack-prices-cited-below-100-kwh-for-the-first-time-in-2020-while-market-average-sits-at-137-kwh/

[8] (Aug. 2020). *Electric Car Costs to Remain Higher Than Traditional Engines*. [Online]. Available: https://www.ft.com/content/a7e58ce7-4fab-424a-b1fa-f833ce948cb7

[9] (Sep. 2020). *EVs Are Still 45% More Expensive to Make Than Combustion-Engined Cars*. [Online]. Available: https://insideevs.com/news/444542/evs-45-percent-more-expensive-make-ice/

[10] M. Adhikari, L. P. Ghimire, Y. Kim, P. Aryal, and S. B. Khadka, "Identification and analysis of barriers against electric vehicle use," *Sustainability*, vol. 12, pp. 1–20, Jun. 2020.

[11] G. Krishna, "Understanding and identifying barriers to electric vehicle adoption through thematic analysis," *Transp. Res. Interdiscipl. Perspect.*, vol. 10, pp. 1–9, Apr. 2021.

[12] T. R. Board and N. R. Council, *Overcoming Barriers to Deployment of Plug-in Electric Vehicles*. Washington, DC, USA: Nat. Acad. Press, 2015.

[13] C. C. Chan and K. T. Chau, "An overview of power electronics in electric vehicles," *IEEE Trans. Ind. Electron.*, vol. 44, no. 1, pp. 3–13, Feb. 1997.

[14] B. Singh, B. N. Singh, A. Chandra, K. Al-Haddad, A. Pandey, and D. P. Kothari, "A review of three-phase improved power quality AC-DC converters," *IEEE Trans. Ind. Electron.*, vol. 51, no. 3, pp. 641–660, Jun. 2004.

[15] H. F. Farahani, A. Rabiee, and M. Khalili, "Plug-in electric vehicles as a harmonic compensator into microgrids," *J. Cleaner Prod.*, vol. 159, pp. 388–396, Aug. 2017.

[16] S. Srdic and S. Lukic, "Toward extreme fast charging: Challenges and opportunities in directly connecting to medium-voltage line," *IEEE Electrific. Mag.*, vol. 7, no. 1, pp. 22–31, Mar. 2019.

[17] J. Y. Yong, V. K. Ramachandaramurthy, K. M. Tan, and N. Mithulananthan, "A review on the state-of-the-art technologies of electric vehicle, its impacts and prospects," *Renew. Sustain. Energy Rev.*, vol. 49, pp. 365–385, Sep. 2015.

[18] M. Ashfaq, O. Butt, J. Selvaraj, and N. Rahim, "Assessment of electric vehicle charging infrastructure and its impact on the electric grid: A review," *Int. J. Green Energy*, vol. 18, no. 7, pp. 657–686, Mar. 2021.

[19] I. Rahman, P. M. Vasant, M. Singh, M. Abdullah-Al-Wadud, and N. Adnan, "Review of recent trends in optimization techniques for plug-in hybrid, and electric vehicle charging infrastructures," *Renew. Sustain. Energy Rev.*, vol. 58, pp. 1039–1047, May 2016.

[20] T. Chen, X. Zhang, J. Wang, J. Li, C. Wu, M. Hu, and H. Bian, "A review on electric vehicle charging infrastructure development in the U.K.," *J. Mod. Power Syst. Clean Energy*, vol. 8, no. 2, pp. 193–205, Mar. 2020.

[21] A. Ahmad, Z. A. Khan, M. S. Alam, and S. Khateeb, "A review of the electric vehicle charging techniques, standards, progression and evolution of EV technologies in Germany," *Smart Sci.*, vol. 6, no. 1, pp. 36–53, Dec. 2017.

[22] V. Krithika and C. Subramani, "A comprehensive review on choice of hybrid vehicles and power converters, control strategies for hybrid electric vehicles," *Int. J. Energy Res.*, vol. 42, no. 5, pp. 1–24, Dec. 2017.

[23] A. Khaligh and M. D'Antonio, "Global trends in high-power on-board chargers for electric vehicles," *IEEE Trans. Veh. Technol.*, vol. 68, no. 4, pp. 3306–3324, Apr. 2019.

[24] I. Subotic, N. Bodo, E. Levi, B. Dumnic, D. Milicevic, and V. Katic, "Overview of fast on-board integrated battery chargers for electric vehicles based on multiphase machines and power electronics," *IET Electr. Power Appl.*, vol. 10, no. 3, pp. 217–229, Mar. 2016.

[25] S. F. Tie and C. W. Tan, "A review of energy sources and energy management system in electric vehicles," *Renew. Sustain. Energy Rev.*, vol. 20, pp. 82–102, Apr. 2013.

[26] H. Ramakrishnan and J. Rangaraju, "Power topology considerations for electric vehicle stations," Texas Instrum. Appl. Rep., Texas Instrum., Dallas, TX, USA, Tech. Rep. SLLA497, Sep. 2020. [Online]. Available: https://www.ti.com/lit/an/slla497/slla497.pdf?ts=1633058316605

[27] S. Chakraborty, H. N. Vu, M. M. Hasan, D. D. Tran, M. E. Baghdadi, and O. Hegazy, "DC–DC converter topologies for electric vehicles, plug-in hybrid electric vehicles and fast charging stations: State of the art and future trends," *Energies*, vol. 12, no. 8, pp. 1–43, Apr. 2019.

[28] H. Tu, H. Feng, S. Srdic, and S. Lukic, "Extreme fast charging of electric vehicles: A technology overview," *IEEE Trans. Transport. Electrific.*, vol. 5, no. 4, pp. 861–878, Dec. 2019.

[29] *SAE Electric Vehicle and Plug-In Hybrid Electric Vehicle Conductive Charge Coupler*, SAE Standard J1772, 2010.

[30] *Plugs, Socket-Outlets, Vehicle Connectors and Vehicle Inlets-Conductive Charging of Electric Vehicles-Part 1, 2, 3*, Standard IEC 62196, 2014.

[31] (2017). *Plug-in Around the EV World*. [Online]. Available: http://www.ev-institute.com/images/media/Plug_World_map_v4.pdf

[32] U.S. Department of Energy. (Oct. 2017). *Enabling Extreme Fast Charging: A Technology Gap Assessment*. [Online]. Available: https://www.energy.gov/eere/vehicles/downloads/enabling-extreme-fast-charging-technology-gap-assessment

[33] D. Aggeler, F. Canales, H. Z.-D. La Parra, A. Coccia, N. Butcher, and O. Apeldoorn, "Ultra-fast DC-charge infrastructures for EV-mobility and future smart grids," in *Proc. IEEE PES Innov. Smart Grid Technol. Conf. Eur. (ISGT Europe)*, Oct. 2010, pp. 1–8.

[34] G. Rajendran, C. A. Vaithilingam, N. Misron, K. Naidu, and M. R. Ahmed, "A comprehensive review on system architecture and international standards for electric vehicle charging stations," *J. Energy Storage*, vol. 42, pp. 1–31, Aug. 2021.

[35] M. Adil, J. Ali, Q. T. H. Ta, M. Attique, and T.-S. Chung, "A reliable sensor network infrastructure for electric vehicles to enable dynamic wireless charging based on machine learning technique," *IEEE Access*, vol. 8, pp. 187933–187947, 2020.

[36] D. Wang, X. Qu, Y. Yao, and P. Yang, "Hybrid inductive-power-transfer battery chargers for electric vehicle onboard charging with configurable charging profile," *IEEE Trans. Intell. Transp. Syst.*, vol. 22, no. 1, pp. 592–599, Jan. 2021.

[37] S. Augustine, J. E. Quiroz, M. J. Reno, and S. Brahma, "DC microgrid protection: Review and challenges," Sandia Nat. Lab., Albuquerque, NM, USA, Tech. Rep. SAND2018-8853, 2018.

[38] M. Eull, W. Wang, L. Zhou, and M. Preindl, "Zero sequence voltage control enabling transformerless electric vehicle chargers," in *Proc. IEEE Transp. Electrific. Conf. Expo (ITEC)*, Jun. 2021, pp. 861–868.

[39] *Residual Direct Current Detecting Device (RDC-DD) to be Used for Mode 3 Charging of Electric Vehicles*, Standard IEC 62955:2018, 2018.

[40] *Electric Vehicle Conductive Charging System—Part 1: General Requirements*, Standard IEC 61851-1:2017, 2017.

[41] J. Wang, Y. Zhang, M. Elshaer, W. Perdikakis, C. Yao, K. Zou, Z. Xu, and C. Chen, "Nonisolated electric vehicle chargers: Their current status and future challenges," *IEEE Electrific. Mag.*, vol. 9, no. 2, pp. 23–33, Jun. 2021.

[42] Y. Tahir, I. Khan, S. Rahman, M. F. Nadeem, A. Iqbal, Y. Xu, and M. Rafi, "A state-of-the-art review on topologies and control techniques of solid-state transformers for electric vehicle extreme fast charging," *IET Power Electron.*, pp. 1560–1576, May 2021.

[43] R. Greul, S. D. Round, and J. W. Kolar, "Analysis and control of a three-phase, unity power factor Y-rectifier," *IEEE Trans. Power Electron.*, vol. 22, no. 5, pp. 1900–1911, Sep. 2007.

[44] T. B. Soeiro and J. W. Kolar, "Analysis of high-efficiency three-phase two- and three-level unidirectional hybrid rectifiers," *IEEE Trans. Ind. Electron.*, vol. 60, no. 9, pp. 3589–3601, Sep. 2013.

[45] L. Huber, M. Kumar, and M. M. Jovanovic, "Analysis, design, and evaluation of three-phase three-wire isolated AC-DC converter implemented with three single-phase converter modules," in *Proc. IEEE Appl. Power Electron. Conf. Expo. (APEC)*, Mar. 2016, pp. 38–45.

[46] J. W. Kolar and T. Friedli, "The essence of three-phase PFC rectifier systems—Part I," *IEEE Trans. Power Electron.*, vol. 28, no. 1, pp. 176–198, Jan. 2013.

[47] Y. Jang, M. M. Jovanovic, and J. M. Ruiz, "A new three-phase two-switch ZVS PFC DCM boost rectifier," in *Proc. 27th Annu. IEEE Appl. Power Electron. Conf. Expo. (APEC)*, Feb. 2012, pp. 807–814.

[48] M.-C. Ancuti, C. Sorandaru, S. Musuroi, and V.-N. Olarescu, "High efficiency three-phase interleaved buck-type PFC rectifier concepts," in *Proc. 41st Annu. Conf. IEEE Ind. Electron. Soc. (IECON)*, Nov. 2015, pp. 7763–7768.

[49] B. Chae, T. Kang, T. Kang, and Y. Suh, "Carrier based PWM for three-phase three-switch buck-type rectifier in EV rapid charging system," in *Proc. 9th Int. Conf. Power Electron. ECCE Asia (ICPE-ECCE Asia)*, Jun. 2015, pp. 881–889.

[50] M. Baumann and J. W. Kolar, "Parallel connection of two three-phase three-switch buck-type unity-power-factor rectifier systems with DC-link current balancing," *IEEE Trans. Ind. Electron.*, vol. 54, no. 6, pp. 3042–3053, Dec. 2007.

[51] T. Nussbaumer and J. W. Kolar, "Improving mains current quality for three-phase three-switch buck-type PWM rectifiers," *IEEE Trans. Power Electron.*, vol. 21, no. 4, pp. 967–973, Jul. 2006.

[52] J. Lei, S. Feng, J. Zhao, W. Chen, P. Wheeler, and M. Shi, "An improved three-phase buck rectifier topology with reduced voltage stress on transistors," *IEEE Trans. Power Electron.*, vol. 35, no. 3, pp. 2458–2466, Mar. 2020.

[53] Q. Chen, J. Xu, F. Zeng, R. Huang, and L. Wang, "An improved three-phase buck rectifier with low voltage stress on switching devices," *IEEE Trans. Power Electron.*, vol. 36, no. 6, pp. 6168–6174, Jun. 2021.

[54] Q. Chen, J. Xu, R. Huang, W. Wang, and L. Wang, "A digital control strategy with simple transfer matrix for three-phase buck rectifier under unbalanced AC input conditions," *IEEE Trans. Power Electron.*, vol. 36, no. 4, pp. 3661–3666, Apr. 2021.

[55] Q. Chen, J. Xu, L. Wang, R. Huang, and H. Ma, "Analysis and improvement of the effect of distributed parasitic capacitance on high-frequency high-density three-phase buck rectifier," *IEEE Trans. Power Electron.*, vol. 36, no. 6, pp. 6415–6428, Jun. 2021.

[56] A. K. Singh, E. Jeyasankar, P. Das, and S. K. Panda, "A matrix-based nonisolated three-phase AC–DC rectifier with large step-down voltage gain," *IEEE Trans. Power Electron.*, vol. 32, no. 6, pp. 4796–4811, Jun. 2017.

[57] J. Afsharian, D. Xu, B. Wu, B. Gong, and Z. Yang, "A new PWM and commutation scheme for one phase loss operation of three-phase isolated buck matrix-type rectifier," *IEEE Trans. Power Electron.*, vol. 33, no. 11, pp. 9854–9865, Nov. 2018.

[58] T. B. Soeiro, T. Friedli, and J. W. Kolar, "Swiss rectifier—A novel three-phase buck-type PFC topology for electric vehicle battery charging," in *Proc. 27th Annu. IEEE Appl. Power Electron. Conf. Expo. (APEC)*, Feb. 2012, pp. 2617–2624.

[59] M. A. Ahmed, J. D. Dasika, M. Saeedifard, and O. Wasynczuk, "Interleaved Swiss rectifiers for fast EV/PHEV battery chargers," in *Proc. IEEE Appl. Power Electron. Conf. Expo. (APEC)*, Mar. 2014, pp. 3260–3265.

[60] L. Schrittwieser, M. Leibl, M. Haider, F. Thony, J. W. Kolar, and T. B. Soeiro, "99.3% efficient three-phase buck-type all-SiC Swiss rectifier for DC distribution systems," *IEEE Trans. Power Electron.*, vol. 34, no. 1, pp. 126–140, Jan. 2019.

[61] T. B. Soeiro, M. L. Heldwein, and J. W. Kolar, "Three-phase modular multilevel current source rectifiers for electric vehicle battery charging systems," in *Proc. Brazilian Power Electron. Conf.*, Oct. 2013, pp. 623–629.

[62] B. Zhang, S. Xie, X. Wang, and J. Xu, "Modulation method and control strategy for full-bridge-based Swiss rectifier to achieve ZVS operation and suppress low-order harmonics of injected current," *IEEE Trans. Power Electron.*, vol. 35, no. 6, pp. 6512–6522, Jun. 2020.

[63] T. Friedli, M. Hartmann, and J. W. Kolar, "The essence of three-phase PFC rectifier systems—Part II," *IEEE Trans. Power Electron.*, vol. 29, no. 2, pp. 543–560, Feb. 2014.

[64] L. Schrittwieser, J. W. Kolar, and T. B. Soeiro, "Novel Swiss rectifier modulation scheme preventing input current distortions at sector boundaries," *IEEE Trans. Power Electron.*, vol. 32, no. 7, pp. 5771–5785, Jul. 2017.

[65] R. Gowthamraj, C. V. Aravind, and O. K. S. Prakash, "Modeling of VIENNA rectifier with PFC controller for electric vehicle charging stations," in *Proc. 12th Int. Eng. Res. Conf. (EURECA)*, 2019, p. 2137.

[66] S. Liu, J. Jiang, and G. Cheng, "Research on vector control strategy of three phase VIENNA rectifier employed in EV charger," in *Proc. Chin. Control Decis. Conf. (CCDC)*, Jun. 2019, pp. 4914–4917.

[67] J. A. Anderson, M. Haider, D. Bortis, J. W. Kolar, M. Kasper, and G. Deboy, "New synergetic control of a 20 kW isolated VIENNA rectifier front-end EV battery charger," in *Proc. 20th Workshop Control Modeling Power Electron. (COMPEL)*, Jun. 2019, pp. 1–8.

[68] L. Zhang, R. Zhao, P. Ju, C. Ji, Y. Zou, Y. Ming, and Y. Xing, "A modified DPWM with neutral point voltage balance capability for three-phase VIENNA rectifiers," *IEEE Trans. Power Electron.*, vol. 36, no. 1, pp. 263–273, Jan. 2021.

[69] S. M. H. Khorasgani, A. Izadinia, and H. R. Karshenas, "Finite control set model predictive control for DC voltage balancing in VIENNA rectifier," in *Proc. 24th Iranian Conf. Electr. Eng. (ICEE)*, May 2016, pp. 687–692.

[70] Q. Wang, X. Zhang, R. Burgos, D. Boroyevich, A. M. White, and M. Kheraluwala, "Design and implementation of a two-channel interleaved VIENNA-type rectifier with >99% efficiency," *IEEE Trans. Power Electron.*, vol. 33, no. 1, pp. 226–239, Jan. 2018.
[71] J. Halbig, "15 kW bidirectional VIENNA PFC," presented at the STMicroelectronics APEC, Aug. 2020. [Online]. Available: https://www.st.com/content/dam/AME/2020/apec-2020/presentations/APEC2020_Vienna_Rectifier-virtual-FINAL.pdf
[72] R. Lai, F. Wang, R. Burgos, D. Boroyevich, D. Jiang, and D. Zhang, "Average modeling and control design for VIENNA-type rectifiers considering the DC-link voltage balance," *IEEE Trans. Power Electron.*, vol. 24, no. 11, pp. 2509–2522, Nov. 2009.
[73] L. Hang, B. Li, M. Zhang, Y. Wang, and L. M. Tolbert, "Equivalence of SVM and carrier-based PWM in three-phase/wire/level VIENNA rectifier and capability of unbalanced-load control," *IEEE Trans. Ind. Electron.*, vol. 61, no. 1, pp. 20–28, Jan. 2014.
[74] X. Zhang, Q. Wang, R. Burgos, and D. Boroyevich, "Discontinuous pulse width modulation methods with neutral point voltage balancing for three phase VIENNA rectifiers," in *Proc. IEEE Energy Convers. Congr. Expo. (ECCE)*, Sep. 2015, pp. 225–232.
[75] T. Wang, C. Chen, P. Liu, T. Liu, Z. Chao, and S. Duan, "A hybrid space-vector modulation method for harmonics and current ripple reduction of interleaved VIENNA rectifier," *IEEE Trans. Ind. Electron.*, vol. 67, no. 10, pp. 8088–8099, Oct. 2020.
[76] L. Huber, M. Kumar, and M. M. Jovanović, "Performance comparison of three-step and six-step PWM in average-current-controlled three-phase six-switch boost PFC rectifier," *IEEE Trans. Power Electron.*, vol. 31, no. 10, pp. 7264–7272, Oct. 2016.
[77] A. Mallik, W. Ding, C. Shi, and A. Khaligh, "Input voltage sensorless duty compensation control for a three-phase boost PFC converter," *IEEE Trans. Ind. Appl.*, vol. 53, no. 2, pp. 1527–1537, Mar./Apr. 2017.
[78] Z. Ye, D. Boroyevich, J.-Y. Choi, and F. C. Lee, "Control of circulating current in two parallel three-phase boost rectifiers," *IEEE Trans. Power Electron.*, vol. 17, no. 5, pp. 609–615, Sep. 2002.
[79] X. H. Wu, S. K. Panda, and J. X. Xu, "Analysis of the instantaneous power flow for three-phase PWM boost rectifier under unbalanced supply voltage conditions," *IEEE Trans. Power Electron.*, vol. 23, no. 4, pp. 1679–1691, Jul. 2008.
[80] P. N. Enjeti and S. A. Choudhury, "A new control strategy to improve the performance of a PWM AC to DC converter under unbalanced operating conditions," *IEEE Trans. Power Electron.*, vol. 8, no. 4, pp. 493–500, Oct. 1993.
[81] M. Malinowski, M. Jasinski, and M. P. Kazmierkowski, "Simple direct power control of three-phase PWM rectifier using space-vector modulation (DPC-SVM)," *IEEE Trans. Ind. Electron.*, vol. 51, no. 2, pp. 447–454, Apr. 2004.
[82] H.-S. Song and K. Nam, "Dual current control scheme for PWM converter under unbalanced input voltage conditions," *IEEE Trans. Ind. Electron.*, vol. 46, no. 5, pp. 953–959, Oct. 1999.
[83] Y. Jiang, H. Mao, F. C. Lee, and D. Borojevic, "Simple high performance three-phase boost rectifiers," in *Proc. Power Electron. Spec. Conf. (PESC)*, 1994, pp. 1158–1163.
[84] D. Xu, B. Feng, R. Li, K. Mino, and H. Umida, "A zero voltage switching SVM (ZVS–SVM) controlled three-phase boost rectifier," *IEEE Trans. Power Electron.*, vol. 22, no. 3, pp. 978–986, May 2007.
[85] R. Hariri, F. Sebaaly, and H. Y. Kanaan, "A review on modular multilevel converters in electric vehicles," in *Proc. 46th Annu. Conf. IEEE Ind. Electron. Soc. (IECON)*, Oct. 2020, pp. 1993–4987.
[86] J. Maneiro and F. Hassan, "A flexible modular multi-level converter for DC microgrids with EV charging stations," in *Proc. 28th Annu. IEEE Appl. Power Electron. Conf. Expo. (APEC)*, Mar. 2013, pp. 1316–1320.
[87] F. Ciccarelli, A. Del Pizzo, and D. Iannuzzi, "An ultra-fast charging architecture based on modular multilevel converters integrated with energy storage buffers," in *Proc. 8th Int. Conf. Exhib. Ecol. Vehicles Renew. Energies (EVER)*, Mar. 2013, pp. 1–6.
[88] U. Abronzini, C. Attaianese, M. D'Arpino, M. Di Monaco, A. Rufer, and G. Tomasso, "Dead time and non-linearities compensation for CHB multi-level converters with integrated ESS feeding EV's ultra-fast charging stations," in *Proc. Int. Conf. Electr. Syst. Aircr., Railway, Ship Propuls. Road Vehicles, Int. Transp. Electrific. Conf. (ESARS-ITEC)*, Nov. 2016, pp. 1–5.
[89] U. Abronzini, C. Attaianese, M. D. Monaco, G. Tomasso, and M. DrArpino, "Optimal control for CHB multi-level converter with integrated ESS for EV ultra-fast charging station," in *Proc. IEEE Int. Conf. Electr. Syst. Aircr., Railway, Ship Propuls. Road Vehicles, Int. Transp. Electrific. Conf. (ESARS-ITEC)*, Nov. 2018, pp. 1–6.
[90] Z. Yan, Z. Yin, X. Yang, K. Zhang, J. Shi, and L. Wang, "Research and simulation of centralized charge and discharge technology of EVs based on MMC," in *Proc. 2nd Int. Conf. Power Renew. Energy (ICPRE)*, Sep. 2017, pp. 800–804.
[91] P. Qashqai, A. Sheikholeslami, H. Vahedi, and K. Al-Haddad, "A review on multilevel converter topologies for electric transportation applications," in *Proc. IEEE Vehicle Power Propuls. Conf. (VPPC)*, Oct. 2015, pp. 1–6.
[92] S. Vadhiraj, K. N. Swamy, and B. P. Divakar, "Generic SPWM technique for multilevel inverter," in *Proc. IEEE PES Asia–Pacific Power Energy Eng. Conf. (APPEEC)*, Dec. 2013, pp. 1–5.
[93] B. P. McGrath, D. G. Holmes, and T. Lipo, "Optimized space vector switching sequences for multilevel inverters," *IEEE Trans. Power Electron.*, vol. 18, no. 6, pp. 1293–1301, Nov. 2003.
[94] Y. Deng, Y. Wang, K. H. Teo, and R. G. Harley, "A simplified space vector modulation scheme for multilevel converters," *IEEE Trans. Power Electron.*, vol. 31, no. 3, pp. 1873–1886, Mar. 2016.
[95] D. Ronanki and S. S. Williamson, "Modular multilevel converters for transportation electrification: Challenges and opportunities," *IEEE Trans. Transport. Electrific.*, vol. 4, no. 2, pp. 399–407, Jun. 2018.
[96] N. Badawi, A. E. Awwad, and S. Dieckerhoff, "Robustness in short-circuit mode: Benchmarking of 600 V GaN HEMTs with power Si and SiC MOSFETs," in *Proc. IEEE Energy Convers. Congr. Expo. (ECCE)*, Sep. 2016, pp. 1–7.
[97] A. Dekka, B. Wu, and N. R. Zargari, "Start-up operation of a modular multilevel converter with flying capacitor submodules," *IEEE Trans. Power Electron.*, vol. 32, no. 8, pp. 5873–5877, Aug. 2017.
[98] D. Sha, G. Xu, and Y. Xu, "Utility direct interfaced charger/discharger employing unified voltage balance control for cascaded H-bridge units and decentralized control for CF-DAB modules," *IEEE Trans. Ind. Electron.*, vol. 64, no. 10, pp. 7831–7841, Oct. 2017.
[99] Z. Zheng, K. Wang, L. Xu, and Y. Li, "A hybrid cascaded multilevel converter for battery energy management applied in electric vehicles," *IEEE Trans. Power Electron.*, vol. 29, no. 7, pp. 3537–3546, Jul. 2014.
[100] T. Modeer, C. Barth, Y. Lei, and R. Pilawa-Podgurski, "An analytical method for evaluating the power density of multilevel converters," in *Proc. IEEE 17th Workshop Control Modeling Power Electron. (COMPEL)*, Jun. 2016, pp. 1–5.
[101] Q. Huang and A. Q. Huang, "Review of GaN totem-pole bridgeless PFC," *CPSS Trans. Power Electron. Appl.*, vol. 2, no. 3, pp. 187–196, Sep. 2017.
[102] J. Azurza Anderson, G. Zulauf, P. Papamanolis, S. Hobi, S. Miric, and J. W. Kolar, "Three levels are not enough: Scaling laws for multilevel converters in AC/DC applications," *IEEE Trans. Power Electron.*, vol. 36, no. 4, pp. 3967–3986, Apr. 2021.
[103] Y. Lei *et al.*, "A 2-kW single-phase seven-level flying capacitor multilevel inverter with an active energy buffer," *IEEE Trans. Power Electron.*, vol. 32, no. 11, pp. 8570–8581, Nov. 2017.
[104] S. Qin, Y. Lei, Z. Ye, D. Chou, and R. C. N. Pilawa-Podgurski, "A high-power-density power factor correction front end based on seven-level flying capacitor multilevel converter," *IEEE Trans. Emerg. Sel. Topics Power Electron.*, vol. 7, no. 3, pp. 1883–1898, Sep. 2019.
[105] D. Chou, K. Fernandez, and R. C. N. Pilawa-Podgurski, "An interleaved 6-level GaN bidirectional converter for level II electric vehicle charging," in *Proc. IEEE Appl. Power Electron. Conf. Expo. (APEC)*, Mar. 2019, pp. 594–600.
[106] Z. Liao, D. Chou, K. Fernandez, Y. L. Syu, and R. C. N. Pilawa-Podgurski, "Architecture and control of an interleaved 6-level bidirectional converter with an active energy buffer for level-II electric vehicle charging," in *Proc. IEEE Energy Convers. Congr. Expo. (ECCE)*, Oct. 2020, pp. 4137–4142.
[107] Y.-L. Syu, Z. Liao, N.-T. Fu, Y.-C. Liu, H.-J. Chiu, and R. C. N. Pilawa-Podgurski, "Design and control of a high power density three-phase flying capacitor multilevel power factor correction rectifier," in *Proc. IEEE Appl. Power Electron. Conf. Expo. (APEC)*, Jun. 2021, pp. 613–618.
[108] A. Syed, E. Ahmed, D. Maksimovic, and E. Alarcon, "Digital pulse width modulator architectures," in *Proc. IEEE 35th Annu. Power Electron. Spec. Conf.*, Jun. 2004, pp. 4689–4695.

[109] L. Lu, A. Prodic, G. Calabrese, G. Frattini, and M. Granato, "Current programmed mode control of multi-level flying capacitor converter near zero-ripple current region," in *Proc. IEEE Appl. Power Electron. Conf. Expo. (APEC)*, Mar. 2019, pp. 3064–3070.

[110] A. Stillwell, E. Candan, and R. C. N. Pilawa-Podgurski, "Active voltage balancing in flying capacitor multi-level converters with valley current detection and constant effective duty cycle control," *IEEE Trans. Power Electron.*, vol. 34, no. 11, pp. 11429–11441, Nov. 2019.

[111] T. Kang, C. Kim, Y. Suh, H. Park, B. Kang, and D. Kim, "A design and control of bi-directional non-isolated DC–DC converter for rapid electric vehicle charging system," in *Proc. 27th Annu. IEEE Appl. Power Electron. Conf. Expo. (APEC)*, Feb. 2012, pp. 14–21.

[112] L. Tan, B. Wu, and S. Rivera, "A bipolar-DC-bus EV fast charging station with intrinsic DC-bus voltages equalization and minimized voltage ripples," in *Proc. 41st Annu. Conf. IEEE Ind. Electron. Soc. (IECON)*, Nov. 2015, pp. 2190–2195.

[113] S. Rivera, B. Wu, S. Kouro, V. Yaramasu, and J. Wang, "Electric vehicle charging station using a neutral point clamped converter with bipolar DC bus," *IEEE Trans. Ind. Electron.*, vol. 62, no. 4, pp. 1999–2009, Apr. 2015.

[114] S. Rivera, B. Wu, J. Wang, H. Athab, and S. Kouro, "Electric vehicle charging station using a neutral point clamped converter with bipolar DC bus and voltage balancing circuit," in *Proc. 39th Annu. Conf. IEEE Ind. Electron. Soc. (IECON)*, Nov. 2013, pp. 6219–6226.

[115] N. Celanovic and D. Boroyevich, "A comprehensive study of neutral-point voltage balancing problem in three-level neutral-point-clamped voltage source PWM inverters," *IEEE Trans. Power Electron.*, vol. 15, no. 2, pp. 242–249, Mar. 2000.

[116] L. Tan, B. Wu, V. Yaramasu, S. Rivera, and X. Guo, "Effective voltage balance control for bipolar-DC-bus-fed EV charging station with three-level DC–DC fast charger," *IEEE Trans. Ind. Electron.*, vol. 63, no. 7, pp. 4031–4041, Jul. 2016.

[117] F. E. U. Reis, R. P. Torrico-Bascopé, F. L. Tofoli, and L. D. S. Bezerra, "Bidirectional three-level stacked neutral-point-clamped converter for electric vehicle charging stations," *IEEE Access*, vol. 8, pp. 37565–37577, 2020.

[118] T. Bruckner, S. Bernet, and H. Guldner, "The active NPC converter and its loss-balancing control," *IEEE Trans. Ind. Electron.*, vol. 52, no. 3, pp. 855–868, Jun. 2005.

[119] M. Abarzadeh, W. A. Khan, N. Weise, K. Al-Haddad, and A. M. El-Refaie, "A new iguration of paralleled modular ANPC multilevel converter controlled by an improved modulation method for 1 MHz, 1 MW EV charger," *IEEE Trans. Ind. Appl.*, vol. 57, no. 3, pp. 3164–3178, Jun. 2021.

[120] S. R. Pulikanti, G. Konstantinou, and V. G. Agelidis, "Hybrid seven-level cascaded active neutral-point-clamped-based multilevel converter under SHE-PWM," *IEEE Trans. Ind. Electron.*, vol. 60, no. 11, pp. 4794–4804, Nov. 2013.

[121] H. Wang, S. Dusmez, and A. Khaligh, "Design and analysis of a full-bridge LLC-based PEV charger optimized for wide battery voltage range," *IEEE Trans. Veh. Technol.*, vol. 63, no. 4, pp. 1603–1613, Apr. 2014.

[122] H. Haga and F. Kurokawa, "Modulation method of a full-bridge three-level LLC resonant converter for battery charger of electrical vehicles," *IEEE Trans. Power Electron.*, vol. 32, no. 4, pp. 2498–2507, Apr. 2017.

[123] J. Deng, S. Li, S. Hu, C. C. Mi, and R. Ma, "Design methodology of LLC resonant converters for electric vehicle battery chargers," *IEEE Trans. Veh. Technol.*, vol. 63, no. 4, pp. 1581–1592, May 2014.

[124] M. I. Shahzad, S. Iqbal, and S. Taib, "Interleaved LLC converter with cascaded voltage-doubler rectifiers for deeply depleted PEV battery charging," *IEEE Trans. Transport. Electrific.*, vol. 4, no. 1, pp. 89–98, Mar. 2018.

[125] L. A. D. Ta, N. D. Dao, and D.-C. Lee, "High-efficiency hybrid LLC resonant converter for on-board chargers of plug-in electric vehicles," *IEEE Trans. Power Electron.*, vol. 35, no. 8, pp. 8324–8334, Aug. 2020.

[126] B. Li, F. C. Lee, Q. Li, and Z. Liu, "Bi-directional on-board charger architecture and control for achieving ultra-high efficiency with wide battery voltage range," in *Proc. IEEE Appl. Power Electron. Conf. Expo. (APEC)*, Mar. 2017, pp. 3688–3694.

[127] C. Liu, B. Sen, J. Wang, C. Gould, and K. Colombage, "A CLLC resonant converter based bidirectional EV charger with maximum efficiency tracking," in *Proc. 8th IET Int. Conf. Power Electron., Mach. Drives (PEMD)*, 2016, pp. 1–6.

[128] Z. U. Zahid, Z. M. Dalala, R. Chen, B. Chen, and J.-S. Lai, "Design of bidirectional DC–DC resonant converter for vehicle-to-grid (V2G) applications," *IEEE Trans. Transport. Electrific.*, vol. 1, no. 3, pp. 232–244, Oct. 2015.

[129] H. Li, Z. Zhang, S. Wang, J. Tang, X. Ren, and Q. Chen, "A 300-kHz 6.6-kW SiC bidirectional LLC onboard charger," *IEEE Trans. Ind. Electron.*, vol. 67, no. 2, pp. 1435–1445, Feb. 2020.

[130] R. W. De Donker, D. M. Divan, and M. H. Kheraluwala, "A three-phase soft-switched high-power-density DC/DC converter for high-power applications," *IEEE Trans. Ind. Appl.*, vol. 27, no. 1, pp. 63–73, Jan./Feb. 1991.

[131] M. Safayatullah and I. Batarseh, "Small signal model of dual active bridge converter for multi-phase shift modulation," in *Proc. IEEE Energy Convers. Congr. Expo. (ECCE)*, Oct. 2020, pp. 5960–5965.

[132] Y. Yan, H. Bai, A. Foote, and W. Wang, "Securing full-power-range zero-voltage switching in both steady-state and transient operations for a dual-active-bridge-based bidirectional electric vehicle charger," *IEEE Trans. Power Electron.*, vol. 35, no. 7, pp. 7506–7519, Jul. 2020.

[133] Y.-C. Wang, Y.-C. Wu, and T.-L. Lee, "Design and implementation of a bidirectional isolated dual-active-bridge-based DC/DC converter with dual-phase-shift control for electric vehicle battery," in *Proc. IEEE Energy Convers. Congr. Expo.*, Sep. 2013, pp. 5468–5475.

[134] G. Ortiz, J. Mühlethaler, and J. W. Kolar, "'Magnetic ear'-based balancing of magnetic flux in high power medium frequency dual active bridge converter transformer cores," in *Proc. 8th Int. Conf. Power Electron. (ECCE Asia)*, 2011, pp. 1307–1314.

[135] S. A. Assadi, H. Matsumoto, M. Moshirvaziri, M. Nasr, M. S. Zaman, and O. Trescases, "Active saturation mitigation in high-density dual-active-bridge DC–DC converter for on-board EV charger applications," *IEEE Trans. Power Electron.*, vol. 35, no. 4, pp. 4376–4387, Apr. 2020.

[136] Y. Xuan, X. Yang, W. Chen, T. Liu, and X. Hao, "A three-level dual-active-bridge converter with blocking capacitors for bidirectional electric vehicle charger," *IEEE Access*, vol. 7, pp. 173838–173847, 2019.

[137] P. A. M. Bezerra, F. Krismer, R. M. Burkart, and J. W. Kolar, "Bidirectional isolated non-resonant DAB DC–DC converter for ultra-wide input voltage range applications," in *Proc. Int. Power Electron. Appl. Conf. Expo.*, Nov. 2014, pp. 1038–1044.

[138] D. D. Nguyen, N. T. Bui, and K. Yukita, "Design and optimization of three-phase dual-active-bridge converters for electric vehicle charging stations," *Energies*, vol. 13, no. 1, p. 150, Dec. 2019.

[139] K. Shi, D. Zhang, Z. Zhou, M. Zhang, and Y. Gu, "A novel phase-shift dual full-bridge converter with full soft-switching range and wide conversion range," *IEEE Trans. Power Electron.*, vol. 31, no. 11, pp. 7747–7760, Nov. 2016.

[140] H. Xiao and S. Xie, "A ZVS bidirectional DC–DC converter with phase-shift plus PWM control scheme," *IEEE Trans. Power Electron.*, vol. 23, no. 2, pp. 813–823, Jun. 2008.

[141] Y. Shi, R. Li, Y. Xue, and H. Li, "Optimized operation of current-fed dual active bridge DC–DC converter for PV applications," *IEEE Trans. Ind. Electron.*, vol. 62, no. 11, pp. 6986–6995, Nov. 2015.

[142] D. Sha, F. You, and X. Wang, "A high-efficiency current-fed semi-dual-active bridge DC–DC converter for low input voltage applications," *IEEE Trans. Ind. Electron.*, vol. 63, no. 4, pp. 2155–2164, Apr. 2016.

[143] L. Gill, T. Ikari, T. Kai, B. Li, K. Ngo, and D. Dong, "Medium voltage dual active bridge using 3.3 kV SiC MOSFETs for EV charging application," in *Proc. IEEE Energy Convers. Congr. Expo. (ECCE)*, Sep. 2019, pp. 1237–1244.

[144] R. P. Twiname, D. J. Thrimawithana, U. K. Madawala, and C. A. Baguley, "A dual-active bridge topology with a tuned CLC network," *IEEE Trans. Power Electron.*, vol. 30, no. 12, pp. 6543–6550, Dec. 2015.

[145] S. S. Muthuraj, V. K. Kanakesh, P. Das, and S. K. Panda, "Triple phase shift control of an LLL tank based bidirectional dual active bridge converter," *IEEE Trans. Power Electron.*, vol. 32, no. 10, pp. 8035–8053, Oct. 2017.

[146] W. L. Malan, D. M. Vilathgamuwa, and G. R. Walker, "Modeling and control of a resonant dual active bridge with a tuned CLLC network," *IEEE Trans. Power Electron.*, vol. 31, no. 10, pp. 7297–7310, Oct. 2016.

[147] P. He and A. Khaligh, "Comprehensive analyses and comparison of 1 kW isolated DC–DC converters for bidirectional EV charging systems," *IEEE Trans. Transport. Electrific.*, vol. 3, no. 1, pp. 147–156, Mar. 2017.

[148] Y. Xuan, X. Yang, W. Chen, T. Liu, and X. Hao, "A novel three-level CLLC resonant DC–DC converter for bidirectional EV charger in DC microgrids," *IEEE Trans. Ind. Electron.*, vol. 68, no. 3, pp. 2334–2344, Mar. 2021.

[149] M. Yaqoob, K. H. Loo, and Y. M. Lai, "Extension of soft-switching region of dual-active-bridge converter by a tunable resonant tank," *IEEE Trans. Power Electron.*, vol. 32, no. 12, pp. 9093–9104, Dec. 2017.
[150] L. Corradini, D. Selzer, D. Bloomquist, R. Zane, D. Maksimović, and B. Jacobson, "Minimum current operation of bidirectional dual-bridge series resonant DC/DC converters," *IEEE Trans. Power Electron.*, vol. 27, no. 7, pp. 3266–3276, Jul. 2012.
[151] X. Li and A. K. S. Bhat, "Analysis and design of high-frequency isolated dual-bridge series resonant DC/DC converter," *IEEE Trans. Power Electron.*, vol. 25, no. 4, pp. 850–862, Apr. 2010.
[152] M. Yaqoob, K. H. Loo, and Y. M. Lai, "A four-degrees-of-freedom modulation strategy for dual-active-bridge series-resonant converter designed for total loss minimization," *IEEE Trans. Power Electron.*, vol. 34, no. 2, pp. 1065–1081, Feb. 2019.
[153] R. P. Twiname, D. J. Thrimawithana, U. K. Madawala, and C. A. Baguley, "A new resonant bidirectional DC–DC converter topology," *IEEE Trans. Power Electron.*, vol. 29, no. 9, pp. 4733–4740, Sep. 2014.
[154] Y. P. Chan, K. H. Loo, M. Yaqoob, and Y. M. Lai, "A structurally reconfigurable resonant dual-active-bridge converter and modulation method to achieve full-range soft-switching and enhanced light-load efficiency," *IEEE Trans. Power Electron.*, vol. 34, no. 5, pp. 4195–4207, May 2019.
[155] T. Mishima, K. Akamatsu, and M. Nakaoka, "A high frequency-link secondary-side phase-shifted full-range soft-switching PWM DC–DC converter with ZCS active rectifier for EV battery chargers," *IEEE Trans. Power Electron.*, vol. 28, no. 12, pp. 5758–5773, Dec. 2013.
[156] J. Dudrik, M. Bodor, and M. Pástor, "Soft-switching full-bridge PWM DC–DC converter with controlled output rectifier and secondary energy recovery turn-off snubber," *IEEE Trans. Power Electron.*, vol. 29, no. 8, pp. 4116–4125, Aug. 2014.
[157] V. R. K. Kanamarlapudi, B. Wang, N. K. Kandasamy, and P. L. So, "A new ZVS full-bridge DC–DC converter for battery charging with reduced losses over full-load range," *IEEE Trans. Ind. Appl.*, vol. 54, no. 1, pp. 571–579, Jan./Feb. 2018.
[158] C.-Y. Lim, Y. Jeong, and G.-W. Moon, "Phase-shifted full-bridge DC–DC converter with high efficiency and high power density using center-tapped clamp circuit for battery charging in electric vehicles," *IEEE Trans. Power Electron.*, vol. 34, no. 11, pp. 10945–10959, Nov. 2019.
[159] C.-Y. Lim, Y. Jeong, M.-S. Lee, K.-H. Yi, and G.-W. Moon, "Half-bridge integrated phase-shifted full-bridge converter with high efficiency using center-tapped clamp circuit for battery charging systems in electric vehicles," *IEEE Trans. Power Electron.*, vol. 35, no. 5, pp. 4934–4945, May 2020.
[160] J.-H. Kim, I.-O. Lee, and G.-W. Moon, "Analysis and design of a hybrid-type converter for optimal conversion efficiency in electric vehicle chargers," *IEEE Trans. Ind. Electron.*, vol. 64, no. 4, pp. 2789–2800, Apr. 2017.
[161] M. Jung, G. Lempidis, D. Hölsch, and J. Steffen, "Control and optimization strategies for interleaved DC–DC converters for EV battery charging applications," in *Proc. IEEE Energy Convers. Congr. Expo. (ECCE)*, Sep. 2015, pp. 6022–6028.
[162] K. Uddin, A. D. Moore, A. Barai, and J. Marco, "The effects of high frequency current ripple on electric vehicle battery performance," *Appl. Energy*, vol. 178, pp. 142–154, Sep. 2016.
[163] M. J. Brand, M. H. Hofmann, S. F. Schuster, P. Keil, and A. Jossen, "The influence of current ripples on the lifetime of lithium-ion batteries," *IEEE Trans. Veh. Technol.*, vol. 67, no. 11, pp. 10438–10445, Nov. 2018.
[164] O. Garcia, P. Zumel, A. de Castro, and J. A. Cobos, "Automotive DC–DC bidirectional converter made with many interleaved buck stages," *IEEE Trans. Power Electron.*, vol. 21, no. 3, pp. 578–586, May 2006.
[165] I.-O. Lee, S.-Y. Cho, and G.-W. Moon, "Interleaved buck converter having low switching losses and improved step-down conversion ratio," *IEEE Trans. Power Electron.*, vol. 27, no. 8, pp. 3664–3675, Aug. 2012.
[166] C.-T. Pan, C.-F. Chuang, and C.-C. Chu, "A novel transformerless interleaved high step-down conversion ratio DC–DC converter with low switch voltage stress," *IEEE Trans. Ind. Electron.*, vol. 61, no. 10, pp. 5290–5299, Oct. 2014.
[167] M. Esteki, B. Poorali, E. Adib, and H. Farzanehfard, "Interleaved buck converter with continuous input current, extremely low output current ripple, low switching losses, and improved step-down conversion ratio," *IEEE Trans. Ind. Electron.*, vol. 62, no. 8, pp. 4769–4776, Aug. 2015.
[168] K. Drobnic, G. Grandi, M. Hammami, R. Mandrioli, M. Ricco, A. Viatkin, and M. Vujacic, "An output ripple-free fast charger for electric vehicles based on grid-tied modular three-phase interleaved converters," *IEEE Trans. Ind. Appl.*, vol. 55, no. 6, pp. 6102–6114, Nov. 2019.
[169] M. Hammami, A. Viatkin, M. Ricco, and G. Grandi, "A DC/DC fast charger for electric vehicles with minimum input/output ripple based on multiphase interleaved converters," in *Proc. Int. Conf. Clean Electr. Power (ICCEP)*, Jul. 2019, pp. 187–192.
[170] S. Rivera, S. Kouro, S. Vazquez, S. M. Goetz, R. Lizana, and E. Romero-Cadaval, "Electric vehicle charging infrastructure: From grid to battery," *IEEE Ind. Electron. Mag.*, vol. 15, no. 2, pp. 37–51, Jun. 2021.
[171] P.-W. Lee, Y.-S. Lee, D. K. W. Cheng, and X.-C. Liu, "Steady-state analysis of an interleaved boost converter with coupled inductors," *IEEE Trans. Ind. Electron.*, vol. 47, no. 4, pp. 787–795, Aug. 2000.
[172] V. Repecho, D. Biel, R. Ramos-Lara, and P. G. Vega, "Fixed-switching frequency interleaved sliding mode eight-phase synchronous buck converter," *IEEE Trans. Power Electron.*, vol. 33, no. 1, pp. 676–688, Jan. 2018.
[173] J. Zhang, J.-S. Lai, R.-Y. Kim, and W. Yu, "High-power density design of a soft-switching High-power bidirectional DC–DC converter," *IEEE Trans. Power Electron.*, vol. 22, no. 4, pp. 1145–1153, Jul. 2007.
[174] D. Christen, F. Jauch, and J. Biela, "Ultra-fast charging station for electric vehicles with integrated split grid storage," in *Proc. 17th Eur. Conf. Power Electron. Appl. (EPE ECCE-Europe)*, Sep. 2015, pp. 1–11.
[175] P. J. Grbović, P. Delarue, P. Le Moigne, and P. Bartholomeus, "A bidirectional three-level DC–DC converter for the ultracapacitor applications," *IEEE Trans. Ind. Electron.*, vol. 57, no. 10, pp. 3415–3430, Oct. 2010.
[176] S. Dusmez, A. Hasanzadeh, and A. Khaligh, "Comparative analysis of bidirectional three-level DC–DC converter for automotive applications," *IEEE Trans. Ind. Electron.*, vol. 62, no. 5, pp. 3305–3315, May 2015.
[177] V. Monteiro, J. C. Ferreira, A. A. N. Meléndez, C. Couto, and J. L. Afonso, "Experimental validation of a novel architecture based on a dual-stage converter for off-board fast battery chargers of electric vehicles," *IEEE Trans. Veh. Technol.*, vol. 67, no. 2, pp. 1000–1011, Feb. 2018.
[178] V. Monteiro, J. C. Ferreira, A. A. N. Melendez, J. A. Afonso, C. Couto, and J. L. Afonso, "Experimental validation of a bidirectional three-level DC–DC converter for on-board or off-board EV battery chargers," in *Proc. 45th Annu. Conf. IEEE Ind. Electron. Soc. (IECON)*, Oct. 2019, pp. 3468–3473.
[179] L. Tan, B. Wu, S. Rivera, and V. Yaramasu, "Comprehensive DC power balance management in high-power three-level DC–DC converter for electric vehicle fast charging," *IEEE Trans. Power Electron.*, vol. 31, no. 1, pp. 89–100, Jan. 2016.
[180] L. Tan, N. Zhu, and B. Wu, "An integrated inductor for eliminating circulating current of parallel three-level DC–DC converter-based EV fast charger," *IEEE Trans. Ind. Electron.*, vol. 63, no. 3, pp. 1362–1371, Mar. 2016.
[181] C.-M. Lai and M.-J. Yang, "A high-gain three-port power converter with fuel cell, battery sources and stacked output for hybrid electric vehicles and DC-microgrids," *Energies*, vol. 9, no. 3, p. 180, Mar. 2016.
[182] G. R. C. Mouli, P. Bauer, and M. Zeman, "Comparison of system architecture and converter topology for a solar powered electric vehicle charging station," in *Proc. 9th Int. Conf. Power Electron. ECCE Asia (ICPE-ECCE Asia)*, Jun. 2015, pp. 1908–1915.
[183] G. R. C. Mouli, J. Schijffelen, M. van den Heuvel, M. Kardolus, and P. Bauer, "A 10 kW solar-powered bidirectional EV charger compatible with Chademo and COMBO," *IEEE Trans. Power Electron.*, vol. 34, no. 2, pp. 1082–1098, Feb. 2019.
[184] S. A. Khan, M. R. Islam, Y. Guo, and J. Zhu, "A new isolated multi-port converter with multi-directional power flow capabilities for smart electric vehicle charging stations," *IEEE Trans. Appl. Supercond.*, vol. 29, no. 2, pp. 1–4, Mar. 2019.
[185] Y. Zhang, J. He, and D. M. Ionel, "Modeling and control of a multiport converter based EV charging station with PV and battery," in *Proc. IEEE Transp. Electrific. Conf. Expo (ITEC)*, Jun. 2019, pp. 1–5.
[186] B. Singh, A. Verma, A. Chandra, and K. Al-Haddad, "Implementation of solar PV-battery and diesel generator based electric vehicle charging station," *IEEE Trans. Ind. Appl.*, vol. 56, no. 4, pp. 4007–4016, Aug. 2020.

[187] R. A. da Câmara, L. M. Fernández-Ramírez, P. P. Praça, D. S. de Oliveira, P. García-Triviño, and R. Sarrias-Mena, "An application of the multi-port bidirectional three-phase AC-DC converter in electric vehicle charging station microgrid," in *Proc. IEEE 15th Brazilian Power Electron. Conf., 5th IEEE Southern Power Electron. Conf. (COBEP/SPEC)*, Dec. 2019, pp. 1–6.

[188] M. Vasiladiotis and A. Rufer, "A modular multiport power electronic transformer with integrated split battery energy storage for versatile ultrafast EV charging stations," *IEEE Trans. Ind. Electron.*, vol. 62, no. 5, pp. 3213–3222, May 2015.

[189] N. D. Dao, D.-C. Lee, and Q. D. Phan, "High-efficiency SiC-based isolated three-port DC/DC converters for hybrid charging stations," *IEEE Trans. Power Electron.*, vol. 35, no. 10, pp. 10455–10465, Oct. 2020.

[190] F. Hoffmann, J.-L. Lafrenz, M. Liserre, and N. Vazquez, "Isolated multiport converter as cost efficient solution for DC-fast charger of electric vehicle," in *Proc. 45th Annu. Conf. IEEE Ind. Electron. Soc. (IECON)*, Oct. 2019, pp. 4905–4910.

[191] A. K. Bhattacharjee and I. Batarseh, "An interleaved boost and dual active bridge-based single-stage three-port DC–DC–AC converter with sine PWM modulation," *IEEE Trans. Ind. Electron.*, vol. 68, no. 6, pp. 4790–4800, Jun. 2021.

[192] V. Monteiro, J. G. Pinto, and J. L. Afonso, "Experimental validation of a three-port integrated topology to interface electric vehicles and renewables with the electrical grid," *IEEE Trans. Ind. Informat.*, vol. 14, no. 6, pp. 2364–2374, Jun. 2018.

[193] E. Barbie, R. Rabinovici, and A. Kuperman, "Modeling and simulation of a novel active three-phase multilevel power factor correction front end—The 'Negev' rectifier," *IEEE Trans. Energy Convers.*, vol. 35, no. 1, pp. 462–473, Mar. 2020.

[194] G. Aiello, M. Cacciato, G. Scarcella, G. Scelba, F. Gennaro, and N. Aiello, "Mixed signals based control of a sic VIENNA rectifier for on-board battery chargers," in *Proc. 21st Eur. Conf. Power Electron. Appl. (EPE ECCE Europe)*, Sep. 2019, pp. 1–9.

[195] H. S. Nair and N. Lakshminarasamma, "An improved FS-MPC algorithm for VIENNA rectifier based EV chargers," in *Proc. IEEE Transp. Electrific. Conf. Expo (ITEC)*, Jun. 2020, pp. 1103–1108.

[196] G. Rajendran, C. A. Vaithilingam, N. Misron, K. Naidu, and M. R. Ahmed, "Voltage oriented controller based VIENNA rectifier for electric vehicle charging stations," *IEEE Access*, vol. 9, pp. 50798–50809, 2021.

[197] M. P. Kazmierkowski and L. Malesani, "Current control techniques for three-phase voltage-source PWM converters: A survey," *IEEE Trans. Ind. Electron.*, vol. 45, no. 5, pp. 691–703, Oct. 1998.

[198] M. Hartmann, H. Ertl, and J. W. Kolar, "Current control of three-phase rectifier systems using three independent current controllers," *IEEE Trans. Power Electron.*, vol. 28, no. 8, pp. 3988–4000, Aug. 2013.

[199] M. Fu and Q. Chen, "A DSP based controller for power factor correction (PFC) in a rectifier circuit," in *Proc. 16th Annu. IEEE Appl. Power Electron. Conf. Exposit. (APEC)*, Mar. 2001, pp. 144–149.

[200] R.-J. Tu and C. Chen, "A new space-vector-modulated control for a unidirectional three-phase switch-mode rectifier," *IEEE Trans. Ind. Electron.*, vol. 45, no. 2, pp. 256–262, Apr. 1998.

[201] M. Kumar, L. Huber, and M. M. Jovanovic, "Start-up procedure for three-phase six-switch boost PFC rectifier," in *Proc. IEEE Appl. Power Electron. Conf. Expo. (APEC)*, Mar. 2014, pp. 1852–1859.

[202] L. Huber, M. Kumar, and M. M. Jovanović, "Performance comparison of PI and P compensation in DSP-based average-current-controlled three-phase six-switch boost PFC rectifier," *IEEE Trans. Power Electron.*, vol. 30, no. 12, pp. 7123–7137, Dec. 2015.

[203] J. S. Rentmeister and J. T. Stauth, "A 48 V:2 V flying capacitor multilevel converter using current-limit control for flying capacitor balance," in *Proc. IEEE Appl. Power Electron. Conf. Expo. (APEC)*, Mar. 2017, pp. 367–372.

[204] S. Rivera, B. Wu, R. Lizana, S. Kouro, M. Perez, and J. Rodriguez, "Modular multilevel converter for large-scale multistring photovoltaic energy conversion system," in *Proc. IEEE Energy Convers. Congr. Expo.*, Sep. 2013, pp. 1941–1946.

[205] A. Mortezaei, M. Abdul-Hak, and M. G. Simoes, "A bidirectional NPC-based level 3 EV charging system with added active filter functionality in smart grid applications," in *Proc. IEEE Transp. Electrific. Conf. Expo (ITEC)*, Jun. 2018, pp. 201–206.

[206] F. E. U. Reis, R. P. T. Bascopé, and F. L. Tofoli, "Bidirectional three-phase 3L-SNPC converter for EV charging stations," in *Proc. 13th IEEE Int. Conf. Ind. Appl. (INDUSCON)*, Nov. 2018, pp. 298–304.

[207] W. Feng, F. C. Lee, and P. Mattavelli, "Optimal trajectory control of burst mode for LLC resonant converter," *IEEE Trans. Power Electron.*, vol. 28, no. 1, pp. 457–466, Jan. 2013.

[208] H. Pan, C. He, F. Ajmal, H. Chen, and G. Chen, "Pulse-width modulation control strategy for high efficiency LLC resonant converter with light load applications," *IET Power Electron.*, vol. 7, no. 11, pp. 2887–2894, Jun. 2014.

[209] W. Feng, P. Mattavelli, and F. C. Lee, "Pulsewidth locked loop (PWLL) for automatic resonant frequency tracking in LLC DC–DC transformer (LLC-DCX)," *IEEE Trans. Power Electron.*, vol. 28, no. 4, pp. 1862–1869, Apr. 2013.

[210] S. S. Shah and S. Bhattacharya, "A simple unified model for generic operation of dual active bridge converter," *IEEE Trans. Ind. Electron.*, vol. 66, no. 5, pp. 3486–3495, May 2019.

[211] N. Hou and Y. W. Li, "Overview and comparison of modulation and control strategies for a nonresonant single-phase dual-active-bridge DC–DC converter," *IEEE Trans. Power Electron.*, vol. 35, no. 3, pp. 3148–3172, Mar. 2020.

[212] W. Song, N. Hou, and M. Wu, "Virtual direct power control scheme of dual active bridge DC–DC converters for fast dynamic response," *IEEE Trans. Power Electron.*, vol. 33, no. 2, pp. 1750–1759, Feb. 2018.

[213] X. Li and Y.-F. Li, "An optimized phase-shift modulation for fast transient response in a dual-active-bridge converter," *IEEE Trans. Power Electron.*, vol. 29, no. 6, pp. 2661–2665, Jun. 2014.

[214] L. Xue, Z. Shen, D. Boroyevich, P. Mattavelli, and D. Diaz, "Dual active bridge-based battery charger for plug-in hybrid electric vehicle with charging current containing low frequency ripple," *IEEE Trans. Power Electron.*, vol. 30, no. 12, pp. 7299–7307, Dec. 2015.

[215] B.-Y. Chen and Y.-S. Lai, "Switching control technique of phase-shift-controlled full-bridge converter to improve efficiency under light-load and standby conditions without additional auxiliary components," *IEEE Trans. Power Electron.*, vol. 25, no. 4, pp. 1001–1012, Apr. 2010.

[216] L.-C. Shih, Y.-H. Liu, and H.-J. Chiu, "A novel hybrid mode control for a phase-shift full-bridge converter featuring high efficiency over a full-load range," *IEEE Trans. Power Electron.*, vol. 34, no. 3, pp. 2794–2804, Mar. 2019.

[217] J. Saeed, L. Wang, and N. Fernando, "Model predictive control of phase shift full-bridge DC–DC converter using Laguerre functions," *IEEE Trans. Control Syst. Technol.*, vol. 30, no. 2, pp. 819–826, Mar. 2022.

[218] J. Shi, J. Luo, and X. He, "Common-duty-ratio control of input-series output-parallel connected phase-shift full-bridge DC–DC converter modules," *IEEE Trans. Power Electron.*, vol. 26, no. 11, pp. 3318–3329, Nov. 2011.

[219] G. Balen, A. R. Reis, H. Pinheiro, and L. Schuch, "Modeling and control of interleaved buck converter for electric vehicle fast chargers," in *Proc. Brazilian Power Electron. Conf. (COBEP)*, Nov. 2017, pp. 1–6.

[220] S. Cuoghi, R. Mandrioli, L. Ntogramatzidis, and G. Gabriele, "Multileg interleaved buck converter for EV charging: Discrete-time model and direct control design," *Energies*, vol. 13, no. 2, p. 466, Jan. 2020.

[221] F. H. Malik and M. Lehtonen, "Analysis of power network loading due to fast charging of electric vehicles on highways," in *Proc. Electr. Power Quality Supply Rel. (PQ)*, Aug. 2016, pp. 101–106.

[222] M. Moradzadeh and M. M. A. Abdelaziz, "A new MILP formulation for renewables and energy storage integration in fast charging stations," *IEEE Trans. Transport. Electrific.*, vol. 6, no. 1, pp. 181–198, Mar. 2020.

[223] D. Mao, J. Wang, J. Tan, G. Liu, Y. Xu, and J. Li, "Location planning of fast charging station considering its impact on the power grid assets," in *Proc. IEEE Transp. Electrific. Conf. Expo (ITEC)*, Jun. 2019, pp. 1–5.

[224] I. S. Bayram, G. Michailidis, and M. Devetsikiotis, "Unsplittable load balancing in a network of charging stations under QoS guarantees," *IEEE Trans. Smart Grid*, vol. 6, no. 3, pp. 1292–1302, May 2015.

[225] E. Ucer, I. Koyuncu, M. C. Kisacikoglu, M. Yavuz, A. Meintz, and C. Rames, "Modeling and analysis of a fast charging station and evaluation of service quality for electric vehicles," *IEEE Trans. Transport. Electrific.*, vol. 5, no. 1, pp. 215–225, Mar. 2019.

[226] Q. Yang, S. Sun, S. Deng, Q. Zhao, and M. Zhou, "Optimal sizing of PEV fast charging stations with Markovian demand characterization," *IEEE Trans. Smart Grid*, vol. 10, no. 4, pp. 4457–4466, Jul. 2019.

[227] S. Rahman, I. A. Khan, A. A. Khan, A. Mallik, and M. F. Nadeem, "Comprehensive review and impact analysis of integrating projected electric vehicle charging load to the existing low voltage distribution system," *Renew. Sustain. Energy Rev.*, vol. 153, pp. 1–18, Jan. 2022.

[228] Idaho National Laboratory. (2016). *ABB Terra 53 CJ Charging a 2015 Nissan Leaf*. [Online]. Available: https://avt.inl.gov/sites/default/files/pdf/evse/ABBDCFCFactSheetJune2016.pdf
[229] T. Slangen, T. van Wijk, V. Ćuk, and S. Cobben, "The propagation and interaction of supraharmonics from electric vehicle chargers in a low-voltage grid," *Energies*, vol. 13, no. 15, p. 3865, Jul. 2020.
[230] M. M. Mahfouz and M. R. Iravani, "Grid-integration of battery-enabled DC fast charging station for electric vehicles," *IEEE Trans. Energy Convers.*, vol. 35, no. 1, pp. 375–385, Mar. 2020.
[231] S. M. Alshareef and W. G. Morsi, "Impact of fast charging stations on the voltage flicker in the electric power distribution systems," in *Proc. IEEE Electr. Power Energy Conf. (EPEC)*, Oct. 2017, pp. 1–6.
[232] S. Alshareef, "A novel smart charging method to mitigate voltage fluctuation at fast charging stations," *Energies*, vol. 15, no. 5, p. 1746, Feb. 2022.
[233] S. Deb, K. Tammi, K. Kalita, and P. Mahanta, "Impact of electric vehicle charging station load on distribution network," *Energies*, vol. 11, no. 1, p. 178, Jan. 2018.
[234] O. C. Onar and A. Khaligh, "Grid interactions and stability analysis of distribution power network with high penetration of plug-in hybrid electric vehicles," in *Proc. 25th Annu. IEEE Appl. Power Electron. Conf. Expo. (APEC)*, Feb. 2010, pp. 1755–1762.
[235] X. Wang, Z. He, and J. Yang, "Electric vehicle fast-charging station unified modeling and stability analysis in the dq frame," *Energies*, vol. 11, no. 5, p. 1195, May 2018.
[236] T. Das and D. C. Aliprantis, "Small-signal stability analysis of power system integrated with PHEVs," in *Proc. IEEE Energy Conf.*, Nov. 2008, pp. 1–4.
[237] C. Farmer, P. Hines, J. Dowds, and S. Blumsack, "Modeling the impact of increasing PHEV loads on the distribution infrastructure," in *Proc. 43rd Hawaii Int. Conf. Syst. Sci.*, 2010, pp. 1–10.
[238] G. Razeghi, L. Zhang, T. Brown, and S. Samuelsen, "Impacts of plug-in hybrid electric vehicles on a residential transformer using stochastic and empirical analysis," *J. Power Sources*, vol. 252, pp. 277–285, Apr. 2014.
[239] C. Farkas, G. Szucs, and L. Prikler, "Grid impacts of twin EV fast charging stations placed alongside a motorway," in *Proc. 4th Int. Youth Conf. Energy (IYCE)*, Jun. 2013, pp. 1–6.
[240] M. H. Mobarak and J. Bauman, "Vehicle-directed smart charging strategies to mitigate the effect of long-range EV charging on distribution transformer aging," *IEEE Trans. Transport. Electrific.*, vol. 5, no. 4, pp. 1097–1111, Dec. 2019.
[241] M. Soleimani and M. Kezunovic, "Mitigating transformer loss of life and reducing the hazard of failure by the smart EV charging," *IEEE Trans. Ind. Appl.*, vol. 56, no. 5, pp. 5974–5983, Sep. 2020.
[242] P. Pradhan, I. Ahmad, D. Habibi, G. Kothapalli, and M. A. S. Masoum, "Reducing the impacts of electric vehicle charging on power distribution transformers," *IEEE Access*, vol. 8, pp. 210183–210193, 2020.
[243] S. Habib, M. Kamran, and U. Rashid, "Impact analysis of vehicle-to-grid technology and charging strategies of electric vehicles on distribution networks—A review," *J. Power Sources*, vol. 277, pp. 205–214, Mar. 2015.
[244] S. Rivera, J. Rojas, S. Kouro, P. W. Lehn, R. Lizana, H. Renaudineau, and T. Dragicevic, "Partial-power converter topology of type II for efficient electric vehicle fast charging," *IEEE J. Emerg. Sel. Topics Power Electron.*, early access, Oct. 4, 2021, doi: 10.1109/JESTPE.2021.3117910.
[245] V. M. Iyer, S. Gulur, G. Gohil, and S. Bhattacharya, "An approach towards extreme fast charging station power delivery for electric vehicles with partial power processing," *IEEE Trans. Ind. Electron.*, vol. 67, no. 10, pp. 8076–8087, Oct. 2020.
[246] J. Rojas, H. Renaudineau, S. Kouro, and S. Rivera, "Partial power DC–DC converter for electric vehicle fast charging stations," in *Proc. 43rd Annu. Conf. IEEE Ind. Electron. Soc. (IECON)*, Oct. 2017, pp. 5274–5279.
[247] A. Mahesh, B. Chokkalingam, and L. Mihet-Popa, "Inductive wireless power transfer charging for electric vehicles—A review," *IEEE Access*, vol. 9, pp. 137667–137713, 2021.
[248] P. Machura, V. De Santis, and Q. Li, "Driving range of electric vehicles charged by wireless power transfer," *IEEE Trans. Veh. Technol.*, vol. 69, no. 6, pp. 5968–5982, Jun. 2020.
[249] J. Y. Yong, V. K. Ramachandaramurthy, K. M. Tan, and N. Mithulananthan, "Bi-directional electric vehicle fast charging station with novel reactive power compensation for voltage regulation," *Int. J. Electr. Power Energy Syst.*, vol. 64, pp. 300–310, Jan. 2015.
[250] I. Vittorias, M. Metzger, D. Kunz, M. Gerlich, and G. Bachmaier, "A bidirectional battery charger for electric vehicles with V2G and V2H capability and active and reactive power control," in *Proc. IEEE Transp. Electrific. Conf. Expo (ITEC)*, Jun. 2014, pp. 1–6.
[251] D. Qin, Q. Sun, R. Wang, D. Ma, and M. Liu, "Adaptive bidirectional droop control for electric vehicles parking with vehicle-to-grid service in microgrid," *CSEE J. Power Energy Syst.*, vol. 6, no. 4, pp. 793–805, Dec. 2020.
[252] Y. Laba, A. Bruyère, F. Colas, X. Guillaud, and B. Silvestre, "Operating grid-forming control on automotive reversible battery charger," in *Proc. IEEE Vehicle Power Propuls. Conf. (VPPC)*, Oct. 2021, pp. 1–6.
[253] J. A. Suul, S. D'Arco, and G. Guidi, "Virtual synchronous machine-based control of a single-phase bi-directional battery charger for providing vehicle-to-grid services," *IEEE Trans. Ind. Appl.*, vol. 52, no. 4, pp. 3234–3244, Jul. 2016.
[254] M. Safayatullah, R. Rezaii, M. T. Elrais, and I. Batarseh, "Review of control methods in grid-connected PV and energy storage system," in *Proc. IEEE Energy Convers. Congr. Expo. (ECCE)*, Oct. 2021, pp. 951–958.
[255] H. Zhang, W. Xiang, W. Lin, and J. Wen, "Grid forming converters in renewable energy sources dominated power grid: Control strategy, stability, application, and challenges," *J. Mod. Power Syst. Clean Energy*, vol. 9, no. 6, pp. 1239–1256, 2021.
[256] A. Bindra, "Electric vehicle batteries eye solid-state technology: Prototypes promise lower cost, faster charging, and greater safety," *IEEE Power Electron. Mag.*, vol. 7, no. 1, pp. 16–19, Mar. 2020.
[257] P. Liu and J. Yu, "Identification of charging behavior characteristic for large-scale heterogeneous electric vehicle fleet," *J. Mod. Power Syst. Clean Energy*, vol. 6, no. 3, pp. 567–581, May 2018.
[258] K. S. Reddy, L. K. Panwar, R. Kumar, and B. K. Panigrahi, "Distributed resource scheduling in smart grid with electric vehicle deployment using fireworks algorithm," *J. Mod. Power Syst. Clean Energy*, vol. 4, no. 2, pp. 188–199, Apr. 2016.
[259] A. S. T. Tan, D. Ishak, R. Mohd-Mokhtar, S. S. Lee, and N. R. N. Idris, "Predictive control of plug-in electric vehicle chargers with photovoltaic integration," *J. Mod. Power Syst. Clean Energy*, vol. 6, no. 6, pp. 1264–1276, Nov. 2018.
[260] M. Ahmed, Y. Zheng, A. Amine, H. Fathiannasab, and Z. Chen, "The role of artificial intelligence in the mass adoption of electric vehicles," *Joule*, vol. 5, no. 9, pp. 2296–2322, Sep. 2021.
[261] X. Zhang, K. W. Chan, H. Li, H. Wang, J. Qiu, and G. Wang, "Deep-Learning-Based probabilistic forecasting of electric vehicle charging load with a novel queuing model," *IEEE Trans. Cybern.*, vol. 51, no. 6, pp. 3157–3170, Jun. 2021.
[262] C. Fang, H. Lu, Y. Hong, S. Liu, and J. Chang, "Dynamic pricing for electric vehicle extreme fast charging," *IEEE Trans. Intell. Transp. Syst.*, vol. 22, no. 1, pp. 531–541, Jan. 2021.
[263] J. Antoun, M. E. Kabir, B. Moussa, R. Atallah, and C. Assi, "A detailed security assessment of the EV charging ecosystem," *IEEE Netw.*, vol. 34, no. 3, pp. 200–207, May/Jun. 2020.

MD SAFAYATULLAH (Graduate Student Member, IEEE) received the B.Sc. degree in electrical and electronic engineering from the Bangladesh University of Engineering and Technology (BUET), in 2017. He is currently pursuing the Ph.D. degree in electrical engineering with the Florida Power Electronics Center, Department of Electrical and Computer Engineering (ECE), University of Central Florida, FL, USA.

He has been working as a Research Assistant and a Teaching Assistant with the ECE Department, University of Central Florida, since 2018. His research interests include the design, development, test validation of power electronic converters, multiport converters, their small signal modeling and advanced control algorithm for PV, energy storage, grid, and electric vehicle applications.

MOHAMED TAMASAS ELRAIS (Graduate Student Member, IEEE) received the B.Sc. and M.Sc. degrees in electrical and electronic engineering from the University of Benghazi, in 2007 and 2013, respectively. He is currently pursuing the Ph.D. degree with the Florida Power Electronics Center, Department of Electrical and Computer Engineering, University of Central Florida, FL, USA.

From 2009 to 2013, he was an Electrical Dispatcher Engineer with General Electrical Company of Libya (GECOL), Benghazi, Libya. From 2013 to 2019, he was a Faculty Member with the Electrical and Electronic Department, University of Benghazi, Benghazi. Since 2019, he has been a Research Assistant and a Teaching Assistant with the Department of Electrical and Computer Engineering, University of Central Florida. His research interests include the design, control, development of multiport multilevel power converters for photovoltaic and battery integration to the grid, multilevel power inverters, and electrical vehicles chargers based on GaN switches.

SUMANA GHOSH (Graduate Student Member, IEEE) received the bachelor's degree from the West Bengal University of Technology, West Bengal, India, in 2014, and the master's degree in electrical engineering from the National Institute of Technology, Durgapur, India, in 2018. She is currently pursuing the Ph.D. degree with the Florida Power Electronics Center, Department of Electrical and Computer Engineering, University of Central Florida.

Her research interests include the DC/DC resonant converters, advanced control methods, PV-battery topologies, and multi-port converters.

REZA REZAII (Graduate Student Member, IEEE) was born in Sari, Mazandaran, Iran, in 1991. He received the M.Sc. degree in electrical engineering from Tarbiat Modares University, Tehran, Iran, in 2015. He is currently pursuing the Ph.D. degree with the Department of Electrical and Computer Engineering, University of Central Florida, Orlando, FL, USA.

He has been working as a Research Assistant with the Florida Power Electronics Center (FPEC), University of Central Florida, since 2021. His current research interests include analysis, design, development of power electronic converters for photovoltaic and battery applications, high power and high gain power conversion, digital control in power electronics, soft-switching and resonant converters, electrical vehicles chargers, and multi-port converters.

ISSA BATARSEH (Fellow, IEEE) received the B.S.E.E. degree in electrical and computer engineering and the M.S. and Ph.D. degrees in electrical engineering from the University of Illinois at Chicago, Chicago, IL, USA, in 1983, 1985, and 1990, respectively.

He is currently a Pegasus Professor in electrical engineering with the Department of Electrical and Computer Engineering, University of Central Florida (UCF), Orlando, FL, USA. From 1989 to 1990, he was a Visiting Assistant Professor with Purdue University, Calumet, IN, USA, before joining UCF, in 1991. He has authored or coauthored more than 100 refereed journals and 350 conference papers in addition to 39 U.S. patents. He is also the author of a textbook titled *Power Electronics: Circuit Analysis and Design*, 2nd Edition, (Springer, 2017). His research interests include power electronics and high-frequency and smart grid-tied photovoltaic energy conversion systems. His team with the Florida Power Electronics Center has been leading the design, development, and commercialization of smart microinverters, and smart electric vehicle and industrial chargers. He is a member of the National Academy of Inventors and has been inducted into the Florida Inventors Hall of Fame. He has served as a Chairperson for the IEEE Power Electronics Specialists Conference 2007 and was the Chair of the IEEE Power Engineering Chapter and the IEEE Orlando Section. He is currently serving on the Global Steering Committee of the IEEE—Empower a Billion Lives (EBL) Global Competition. He is also a Registered Professional Engineer in the State of Florida and a Fellow Member of the American Association for the Advancement of Science.